INL/EXT-09-15446

Power Burst Facility: $U(18)O_2$-CaO-ZrO_2 Fuel Rods in Water

September 2009

The INL is a U.S. Department of Energy National Laboratory
operated by Battelle Energy Alliance

INL/EXT-09-15446

POWER BURST FACILITY: $U(18)O_2$-CaO-ZrO_2 FUEL RODS IN WATER

September 2009

Idaho National Laboratory
Idaho Falls, Idaho 83415

http://www.inl.gov

Prepared for the
U.S. Department of Energy
Office of Nuclear Energy
Under DOE Idaho Operations Office
Contract DE-AC07-05ID14517

NEA/NSC/DOC/(95)03/III
Volume III

IEU-COMP-THERM-009

POWER BURST FACILITY: $U(18)O_2$-CaO-ZrO_2 FUEL RODS IN WATER

Evaluators

Jose Ignacio Marquez Damian
Alexis Weir
Comision Nacional de Energia Atomica

Valerie L. Putman
Idaho National Laboratory

Internal Reviewer
John D. Bess
Idaho National Laboratory

Independent Reviewers

Richard Lell
Richard McKnight
Argonne National Laboratory

ACKNOWLEDGMENTS

This evaluation is mainly based on analysis and modeling work done by Valerie L. Putman at Idaho National Laboratory. The other two authors are grateful for her contribution to this evaluation. The authors also wish to thank David W. Nigg for his comments and help providing additional information to perform this evaluation, and to Christine White not only for providing the drawings that illustrate this evaluation but also for her help with details of the geometry.

IEU-COMP-THERM-009

POWER BURST FACILITY: $U(18)O_2$-CaO-ZrO_2 FUEL RODS IN WATER

IDENTIFICATION NUMBER: IEU-COMP-THERM-009 SPECTRA

KEY WORDS: acceptable, burst, calcia, inert matrix, intermediate enriched uranium, reactor, water moderated, water reflected, zirconia.

1.0 DETAILED DESCRIPTION

1.1 Overview of Experiment

The Power Burst Facility (PBF) reactor operated from 1972 to 1985 on the SPERT Area I of the Idaho National Laboratory, then known as the Nuclear Reactor Test Station. PBF was designed to provide experimental data to aid in defining the thresholds for and modes of failure under postulated accident conditions. In addition to the inherent value of the PBF startup experiment as an integral benchmark, the ternary ceramic form of the PBF fuel has some similarities to so-called "inert-matrix" fuels of interest to the international Generation IV advanced reactor program. As a result, the PBF benchmark also has relevance to current directions in reactor design.[a]

PBF reactor startup testing began in 1972. This evaluation focuses on two similar operational loading tests, differing only in the number of fuel rods and the position of the control rods, (chronologically numbered 1 and 2) published in a startup-test report in 1974 (Reference 1). The experiments are very similar and differ only in the number of fuel rods and the position of the control rods. It can be assumed the information in both cases is highly correlated and are included here to allow analysis of the parameters changed between experiments, but they should not be used as independent points in validations.

Data from these tests were used by one of the authors to validate an MCNP model for criticality safety purposes (Reference 1). Although specific references to original documents are kept in the text, all the reactor parameters and test specific data presented here were adapted from Reference 1.

The tests were performed with operational fuel loadings, a stainless steel in-pile tube (IPT) mockup, a neutron source, four pulse chambers, two fission chambers, and one ion chamber. The reactor's four transient rods (TRs) and eight control rods (CRs) were present but TR boron was completely withdrawn below the core and CR boron was partially withdrawn above the core. Test configurations differ primarily in the number of shim rods, and consequently the number of fuel rods included in the core. The critical condition was approached by incrementally and uniformly withdrawing CR boron from the core.

Based on the analysis of the experimental data and numerical calculations, both experiments are considered acceptable as criticality safety benchmarks.

[a] D. W. Nigg, personal communication, February 2009.

1.2 Description of Experimental Configuration

1.2.1 PBF Reactor Core, General – The reactor core (References 3 and 4) consisted of a square array of 121 square cells arranged according to the illustration given in Figure 1, each nominally 5.875 x 5.875 x 60 in. (14.9225 x 14.9225 x 152.4 cm).[a, b] Large components normally included 40 filler elements, 72 reactor assemblies, an IPT in a centrally located test space, four TRs in the active fuel region, and eight CRs in another part of the active fuel region. Core components and fuel rod loading patterns were designed to achieve a symmetrical, annular fuel region. Figure 1 is a transverse view of the reactor core, with instruments, source, fuel rods, and shim rods loaded in the pattern used for Operational Loading Test 2. This assembly and rod loading pattern was used during most of the reactor lifetime, with exception of the startup source that was moved into an assembly rod position after the subject startup tests. Figure 2 shows the reactor core component numbering system used in this evaluation.

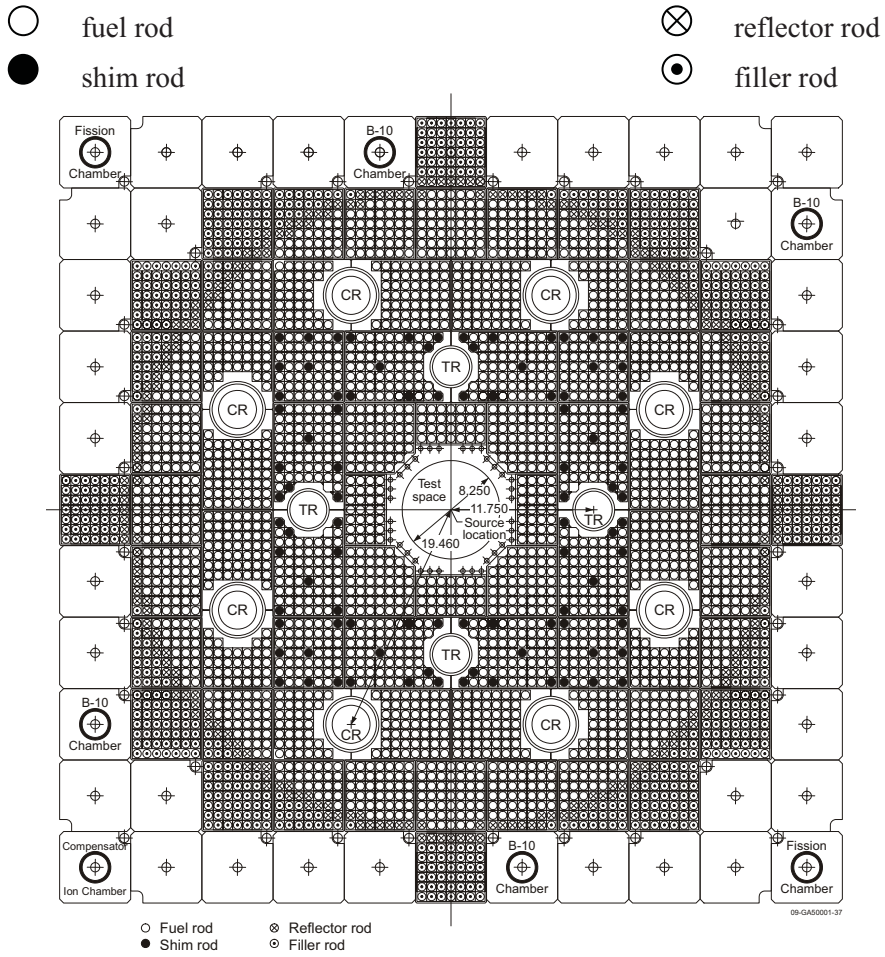

Figure 1. PBF Reactor Core, Operational Loading Test 2.

[a] Most dimensions were obtained from drawings and loading maps of PBF reactor, reactor components and details. A full list of drawings is available in Reference 2.
[b] Dimensions in the references are mostly in English units. Dimensions in parentheses were computed by the authors.

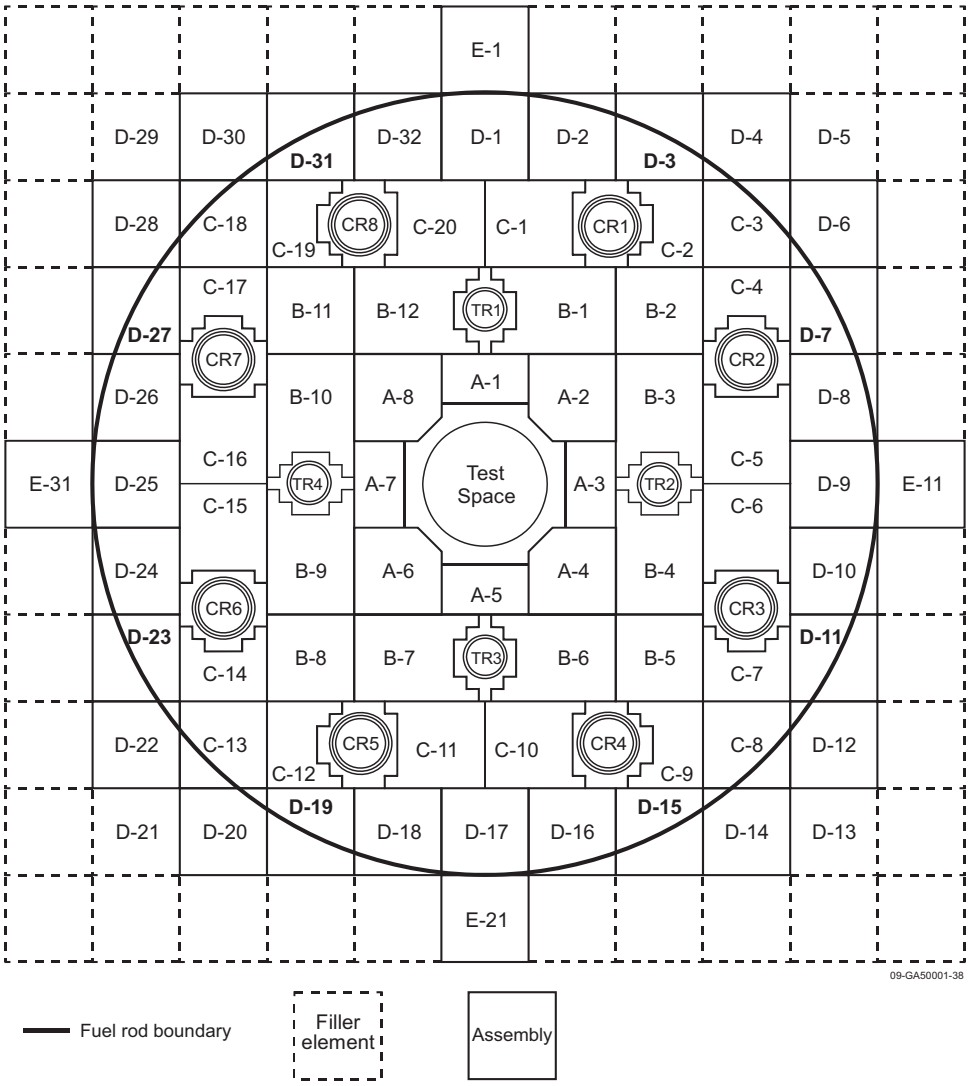

Figure 2. PBF Reactor Core Numbering System.

Filler elements were made of Type 6061 aluminum structural elements. As shown in Figure 3, these elements completed the core cell array outside the annular fuel region. A central cylindrical cavity in each filler element also provided a convenient location for reactor and test instrumentation.

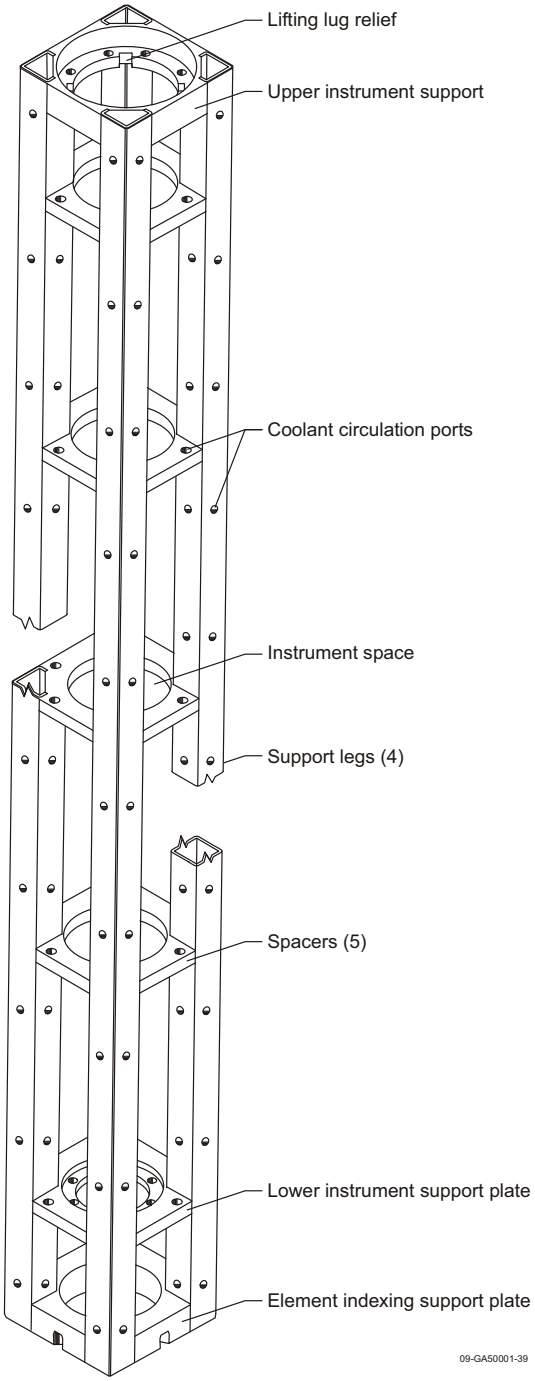

Figure 3. Core Filler Element.

PBF assemblies had several kinds of externally similar rods arrayed in canisters with miscellaneous structural items. Rods included fuel, reflector, shim (or absorber) and filler rods. Rods were arranged in a square-pitch near-rectangular array, typically 0.792 ± 0.005 in. (2.01168 ± 0.0127 cm) center-to-center, with seven rods along each side of each array.

Shown in Figure 4, a PBF fuel rod was a cylinder, nominally 47 1/2 in. (120.65 cm) long by 3/4 in. (1.905 cm) outer diameter.[a] Axially from the bottom, a fuel rod included a 1 5/32 in. (2.936875 cm) long Type 304L stainless steel bottom end cap, an active fuel region, a 4.625 in. (11.7475 cm) long Type 304L stainless steel bearing spool, a chromium-silicon alloy steel compression bearing spring, and a 1 15/32 in. (3.730625 cm) long Type 304L stainless steel top end cap with a cross pin for fuel rod handling. The bearing spool was cup shaped, located immediately above the fuel pellet stack, with a 0.469 in. (1.19126 cm) inner diameter, 0.5625 ± 0.0025 in. (1.42875 ± 0.00635 cm) outer diameter, and 4.312 ± 0.010 in. (10.95248 ± 0.0254 cm) interior length.

The active fuel region (Figure 4[b]) rested directly on the bottom end cap. In this region, a fuel rod was radially composed of concentric cylinders 36 in. (91.44 cm) long, 0.559 ± 0.001 in. (1.41986 ± 0.00254 cm) outer diameter, UO_2-CaO-ZrO_2 fuel pellet stack; 44 7/8 in. (113.9825 cm) long, 0.019 ± 0.0018 in. (0.04826 ± 0.004572 cm) thick helium gap; 38 1/2 $^{+1/32}/_{-1/4}$ in. (97.79 $^{+0.079375}/_{-0.635}$ cm) long, 0.048 ± 0.001 in. (0.12192 ± 0.00254 cm) thick, 0.6935 ± 0.0005 in. (1.76149 ± 0.00127 cm) outer diameter, CaO-ZrO_2 insulating sleeve stack; and 45 7/16 in. (115.41125 cm) long, 0.0285 ± 0.0015 in. (0.07239 ± 0.00381 cm) thick Type 304L stainless steel cladding. Fuel pellets and insulating sleeve pieces were respectively 0.600 ± 0.040 in. (1.524 ± 0.1016 cm) and 1.0 to 3.0 in. (2.54 to 7.62 cm) long.

Fuel rod interiors were filled with helium to provide a chemically inert atmosphere. Some stainless steel surfaces were also coated with a very thin zirconia (ZrO_2) film or layer to minimize any potential for undesirable oxidation or other chemical reactions.

PBF also had other in-pile rod types: Type 304L stainless steel reflector, Type 304L stainless steel shim, and Type 6061 aluminum filler rods. These rods had the same external dimensions as fuel rods and were visually similar. Each non-fuel rod was a solid metal cylinder except at its ends. In an assembly these rods were dimensionally interchangeable with each other and with fuel rods.

[a] PBF Fuel Specification F-11-PBF, Purchase Order C-286-A. Includes variously authored, numbered, and dated documents approved and filed by Idaho Nuclear Corporation: Idaho Falls, Idaho (1969-1970).
[b] Figure 4 and others available in the references show the fuel pellet diameter rounded to two significant digits. The value accepted in this evaluation is 0.559 in.

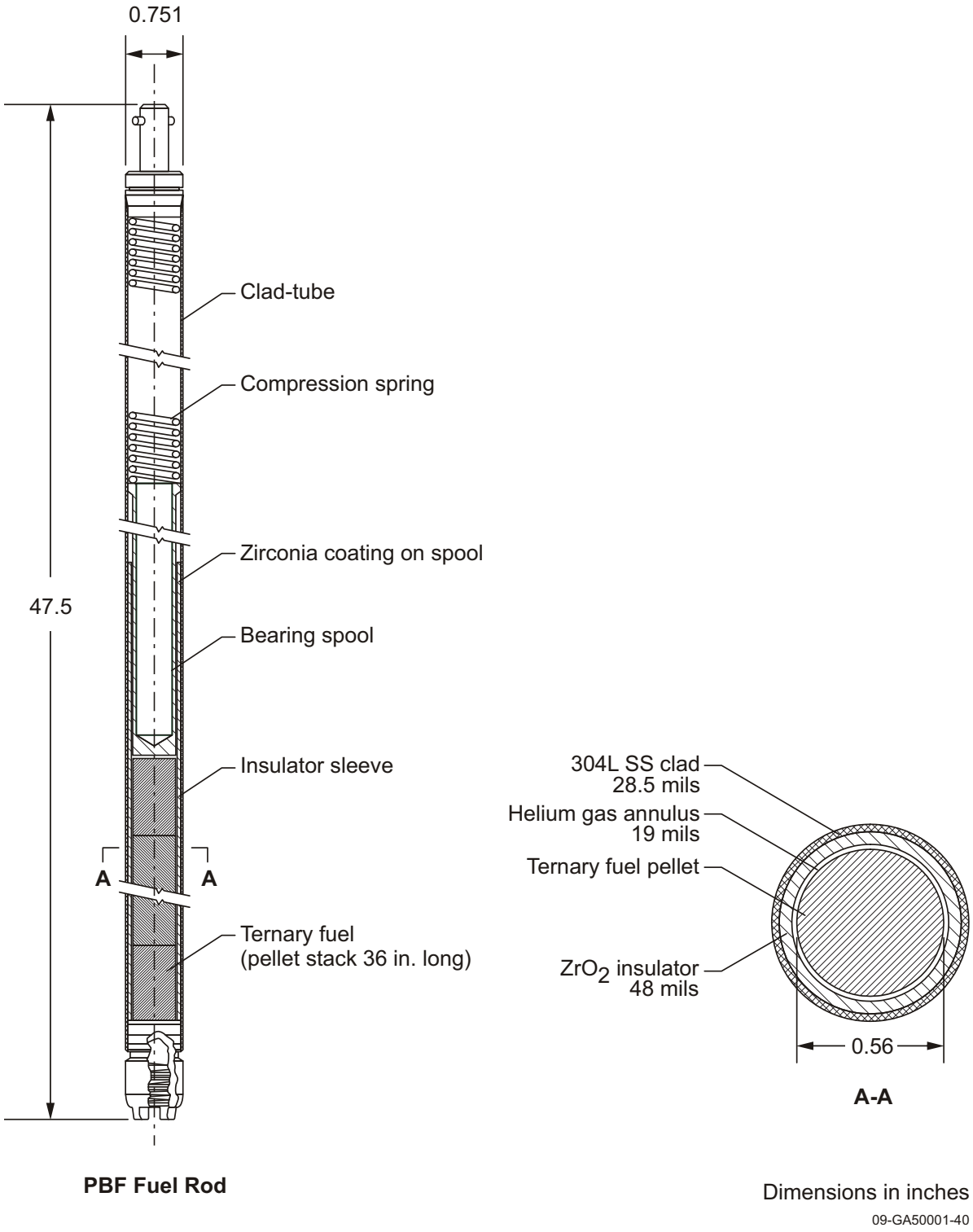

Figure 4. PBF Fuel Rod.
(Note fuel pellet diameter is rounded to two significant digits in the original document.)

Figure 5 illustrates six cross sections for 28-, 34-, 46-, 49-, 51- and 62-rod assemblies. The most common assemblies had 49 rods in a 7 x 7 array. Some drawings indicate these assemblies had a square cross-section with a 5.848 in. (14.85392 cm) outside width, but most drawings and graphics indicate a 5.875 ± 0.004 in. (14.9225 ± 0.01016 cm) outside width. Most 49-rod assemblies had 0.147 in. (0.37338 cm) thick Type 5454 aluminum walls, but at least one drawing indicates a few 49-rod assemblies could have had 0.166 in. (0.42164 cm) thick walls. Other assemblies had 0.147 in. (0.37338 cm) thick walls and departed from this square design only as needed to accommodate PBF reactor core features. The 28- and 46-rod assemblies were designed to fit around a test space as shown in Figure 1, with a 0.027 in. (0.06858 cm) water gap between assemblies and the test space filler piece. The 34- and 51-rod assemblies surrounded each CR as shown in Figure 1, with a 0.050 in. (0.127 cm) water gap between assemblies and the CR air shroud. The 62-rod assemblies nearly surrounded each TR as shown in Figure 1, with a 0.065 in. (0.1651 cm) water gap between assemblies and the TR air shroud.

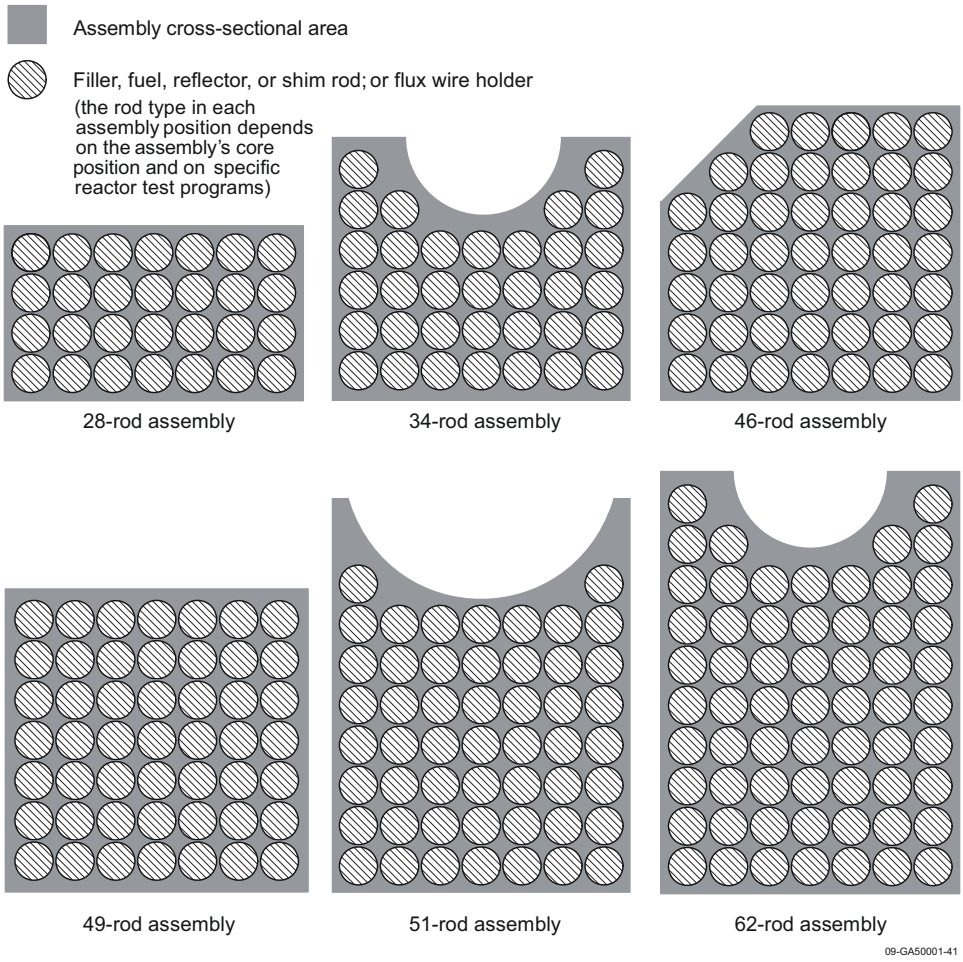

Figure 5. PBF Fuel Assembly Cross Sections.

Figure 6 shows a typical reactor assembly viewed from a seven-rod-wide side. Assemblies were 60.000 ± 0.010 in. (152.400 ± 0.0254 cm) long. Each rod was held in place by a 17-4 PH stainless steel hold-down screw (or rod restraining bolt) bolted into the rod bottom cap through a ¾ to 1 3/8 in. (1.905 to 3.4925 cm) wide, 3/8 in. (0.9525 cm) thick Type 304 stainless steel or 17-4 PH stainless steel captive strip. Just above the captive strip, rods passed through a perforated, Type 6061 aluminum 2 7/32 in. (5.635625 cm) thick mounting (or hold down) plate. This mounting plate was nominally 7.0 in. (17.78 cm) above the assembly bottom. Rod spacing was established with 0.375 in. (0.9525 cm) diameter holes in the mounting plate; 0.438 in. (1.11252 cm) diameter holes, located diagonally between the other holes, permitted water flow through assemblies. Rod spacing was also maintained by spacer- and locking-blade structures, often called egg-crates (Figure 7), located about 12 in. (30.48 cm) apart at two elevations in the assembly. Individual Type 7075 aluminum spacer blades measured 1.250 in. (3.175 cm) high by 0.042 in. (0.10668 cm) thick. Individual locking blades at the outside edges of the egg-crates, were made of either Type 7075 or 6061 aluminum, and were about half the spacer blade height. Rods were axially positioned with bottoms and tops at the same elevation and, for fuel rods, with the active fuel region typically ending 9.0 in. (22.86 cm) above the assembly bottom.

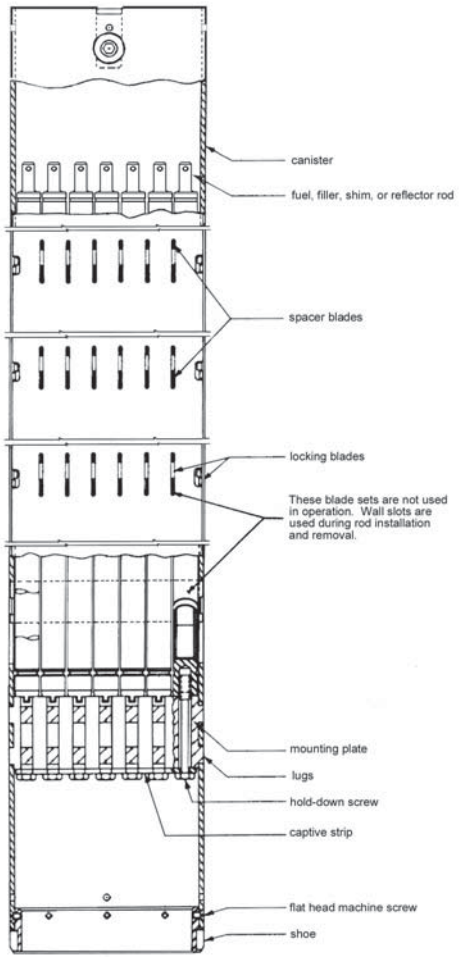

Figure 6. Typical PBF Reactor Assembly.

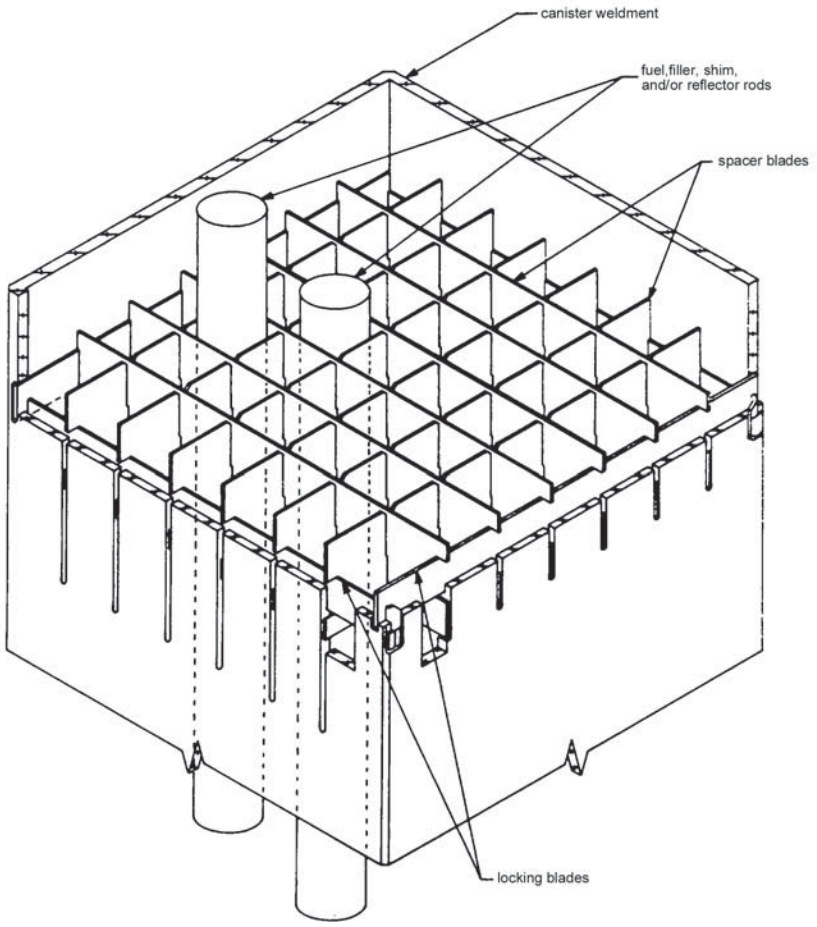

Figure 7. Spacer Blade Egg-Crate.

The reactor core had a large central test space, with a nominally 0.027 in. (0.06858 cm) water gap between the test space central filler piece and adjacent assemblies. This Type 6061 aluminum filler piece had a somewhat octagonal external cross section measuring $10.600\ ^{+0.000}/_{-0.005}$ in. ($26.924\ ^{+0.000}/_{-0.0127}$ cm) across its flat outer surfaces and $10.750\ ^{+0.000}/_{-0.005}$ in. ($27.305\ ^{+0.000}/_{-0.013}$ cm) across its angled outer surfaces. The filler piece had a central cylindrical cavity, nominal 8.250 in. (20.955 cm) diameter, designed to position the PBF IPT. The IPT provided an environment similar to a pressurized water reactor for fueled test specimens. This IPT is not described further here because the subject startup test used a stainless steel mockup instead of the inconel IPT.

Four TRs were distributed around an 11.750 in. (29.845 cm) radius concentric with the core center. Figure 8 shows a TR axial cross section. Table 1 lists component materials and dimensions. When the transient rods were withdrawn, TR tie rods and air shrouds were in-core but TR boron was below the core. TR tie rod bottom and top cross sections were of such lengths that the top section was always above the core.

In their withdrawn position, the upper end of TR B_4C was at least 9 in. (22.86 cm) below the active core. TRs were pulled through the core by drives that increased rod internal elevation. At their highest position (equivalent to 0.00 in. TR position), the lower end of TR B_4C was even with the bottom of the core's fueled region. TRs are not described further here because TRs were in their withdrawn positions during subject tests.

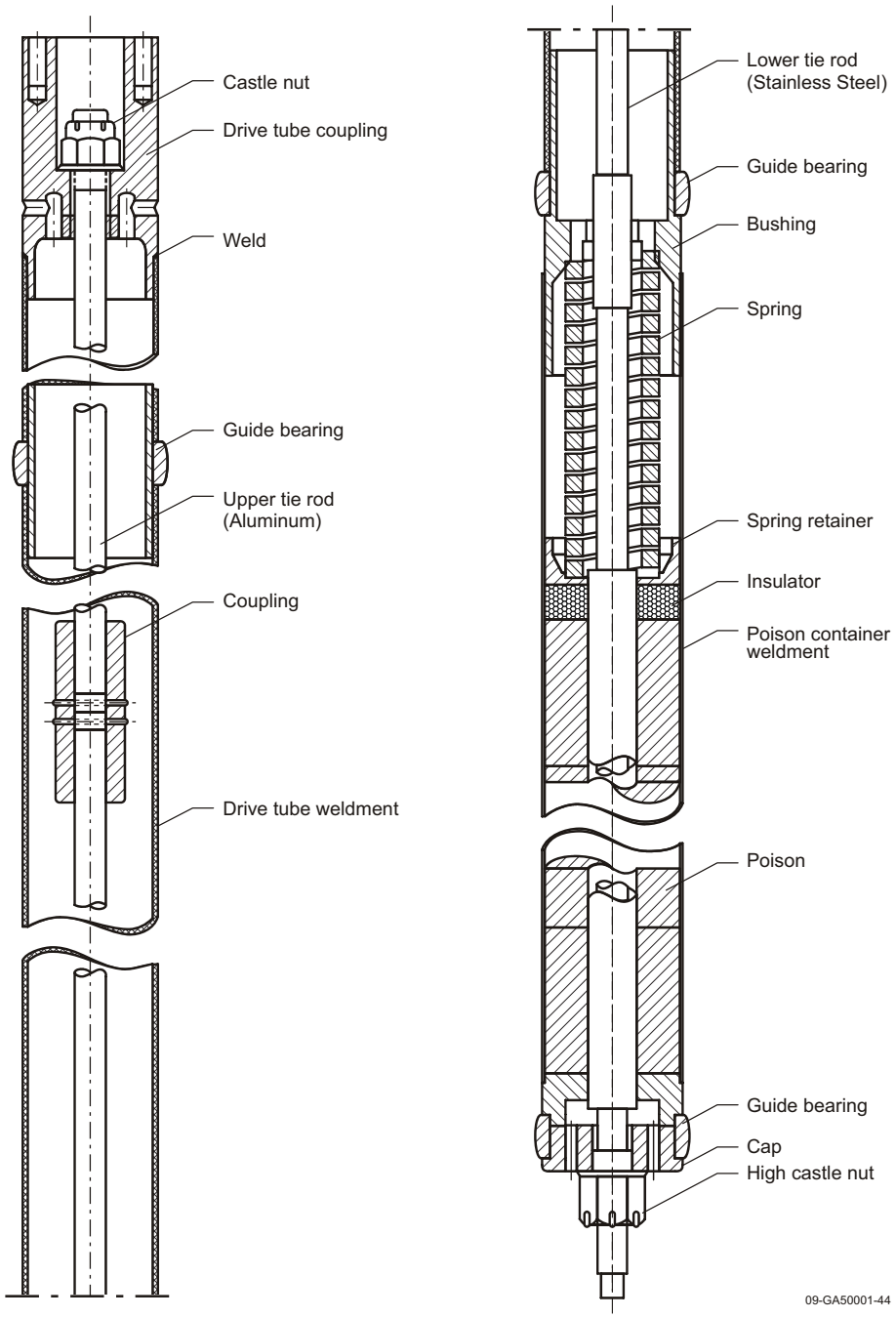

Figure 8. PBF Transient Rod, Axial View.

Eight control rods were distributed around a 19.461 in. (49.43094 cm) radius concentric with the core center. Figure 9 shows a CR axial cross section. Table 1 lists CR component materials and dimensions. When the control rods were fully withdrawn, CR shrouds were in-core but CR boron was above the core. CR tie rod bottom and top sections were of such lengths that the top section was always above the core.

At its reference, inserted position (equivalent to 0.00 in. CR position), the lower end of CR B_4C was even with the bottom of the core's fueled region. CRs were withdrawn by drives that increased internal rod elevation. In their fully withdrawn position, CR B_4C was above or even with the top of the core's fueled region. CR drives were designed to operate in unison such that all CRs would be at the same position at any given time. Like TR positions, CR positions were individually displayed on the reactor control console by four-digit, digital voltmeters. Input signals were scaled so meters read directly in inches with a 0.01 in. (0.0254 cm) resolution.

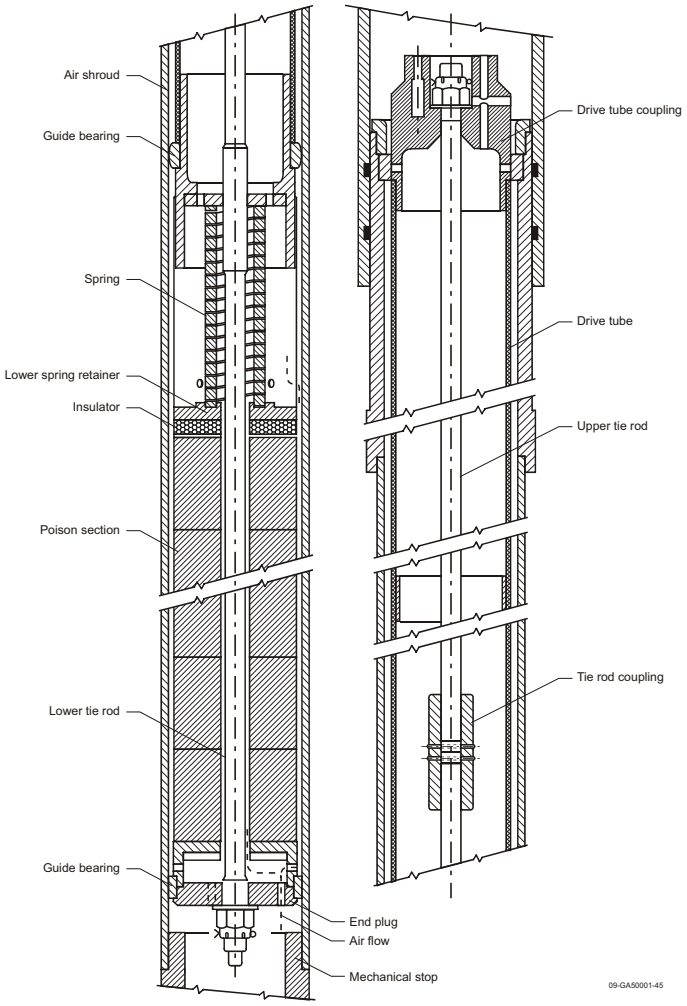

Figure 9. PBF Control Rod, Axial View.

Table 1. Control and Transient Rod Components.

	Control Rod	Transient Rod
Type 6061 Aluminum Air-Shroud Tube		
Overall length	34 ft 3.44 in. (1045.0576 cm) from CR drive to blind end of shroud at manhole cover	33 ft 6.625 in. (1022.6675 cm) from bridge to blind end of shroud at manhole cover
Main stem diameter[(a)]	4.25 in. (10.795 cm) ID 4.75 in. (12.065 cm) OD standard 5.25 in. (13.335 cm) OD top 18 in. (45.72 cm)	3.125 in. (7.9375 cm) ID 3.5 in. (8.89 cm) OD 4.0 in. (10.16 cm) top 18.5 in. (46.99 cm)
Radial location of shroud 6 with respect to core 6	19.461 in. (49.43094 cm)	11.750 in. (29.845 cm)
Center-to-center chord spacing of shrouds	"Alternates diagonal sets 13.257 in. (33.67278 cm) 0^0-90^0-180^0-270^0 sets 16.502 in. (41.91508 cm)"	16.618 in. (42.20972 cm)
Type 6061 Aluminum Drive Tube		
Overall length	15 ft 8.75 in. (479.425 cm)	18 ft 10.875 in. (576.2625 cm)
Diameter	3.51 in. (8.9154 cm) ID 3.75 in. (9.525 cm) OD	2.50 in. (6.35 cm) ID 2.75 in. (6.985 cm) OD
Tie Rod		
Top section	7075 Al 121 ½ ± 1/16 in. (308.61 ± 0.15875 cm) long	7075 Al
Bottom Section	SS304 121 ¾ ± 1/16 in. (309.245 ± 0.15875 cm) long	SS304
Overall length	20 ft 3.250 in. (617.855 cm)	23 ft 9.375 in. (724.8525 cm)
Diameter, central portion	0.665 in. (1.6891 cm)	0.625 in. (1.5875 cm)
Cooling Air Annuli		
Inner	0.102 in. (0.25908 cm) radial annulus	0.123 in. (0.31242 cm) radial annulus
Outer	0.125 in. (0.3175 cm) radial annulus	0.125 in. (0.3175 cm) radial annulus
B_4C Section		
Pellet Shape	Cylindrical annulus	Cylindrical annulus
Pellet	3.870 in. (9.8298 cm) OD 1.030 in. (2.6162 cm) ID 3 to 12 in. (7.62 to 30.48 cm) L	2.71 in. (6.8834 cm) OD 1.031 in. (2.61874 cm) ID 3 to 12 in. (7.62 to 30.48 cm) L
Pellet stack L	$36^{-0.000}_{+0.125}$ in. ($91.440^{-0.000}_{+0.3175}$ cm)	$42^{-0.000}_{+0.125}$ in. ($106.680^{-0.000}_{+0.3175}$ cm)
Axial spacing	0.015 in. (0.0381 cm) max	0.015 in. (0.0381 cm) max
Axial insulators	0.5 in. (1.27 cm) supermica 620	0.625 in. (1.5875 cm) supermica 620
B4C Container / Canister		
SS304 inner tube	1.000 in. (2.54 cm) OD x 0.065 in. (0.1651 cm) wall	1.000 in. (2.54 cm) OD x 0.065 in. (0.1651 cm) wall
SS304 outer tube	4.000 in. (10.160 cm) OD x 0.049 in. (0.12446 cm) wall	2.875 in. (7.3025 cm) OD x 0.065 in. (0.1651 cm) wall
closure plate thickness	0.375 in. (0.9525 cm) SS304 bottom 0.105 in. (0.2667 cm) SS304 top 0.500 in. (1.270 cm) supermica 620 insulator 0.375 in. (0.9525 cm) SS 304 spring retainer	0.375 in. (0.9525 cm) SS304 bottom 0.062 in. (0.15748 cm) SS304 top 0.675 in. (1.7145 cm) supermica 620 insulator 0.188 in. (0.47752 cm) SS 304 spring retainer

(a) This component is not clearly defined in the references.

1.2.2 Reactor Core, Test Specific – As previously mentioned, Operational Loading Tests 1 and 2 differed by control rod positions and the number of shim rods (Reference 1). A full complement of 104 shim rods was used in the first test with an excess reactivity of 3.50 $. However, PBF's long range program required an excess reactivity of more than 4.00 $. Therefore, twelve shim rods were replaced with fuel rods and a second test was conducted. Rod loading patterns are shown in Figure 10 and Figure 11. These figures respectively show only one quadrant of each test core because loading patterns are symmetric about the indicated centerlines. Table 2 lists control and transient rod vertical positions. In the fully inserted position (equivalent to 0.00 in. CR position), the lower end of CR B_4C was even with the bottom of the core's fueled region

Table 2. Operational Loading Test CR and TR Positions.

Test Number	Number of Shim Rods	Control Rod Position (0.0 in. = fully inserted)	Transient Rod Position
1	104	22.05 in. (56.007 cm)	fully withdrawn
2	92	20.26 in. (51.4604 cm)	fully withdrawn

These tests were otherwise physically identical. Figure 1 shows the locations and types of test instrumentation. Instrumentation consisted of a neutron source in the test space and four ^{10}B-lined pulse chambers, two dual-range fission chambers, and one compensated ion chamber in filler elements. Locations were selected to avoid affecting flux profiles, component reactivity worths, and core symmetry. Readily available test documents (Reference 1) provide functional, but not physical, descriptions of this instrumentation.

The source used during the tests was the 4.5 x 10^7 nps reactor startup source. During the test it was positioned near the axial center of the fuel region as well as at the radial core center. This neutron source was a 19 Ci (703 GBq) ^{238}PuBe source doubly encapsulated in stainless steel. It was further contained in a 47.50 in. (120.65 cm) long rod composed of steel bottom and top caps and a 45.438 ± 0.016 in. (115.41252 ± 0.04064 cm) long, ¾ in. (1.905 cm) outer diameter with 0.028 in. (0.07112 cm) thick wall, Type 304L stainless steel tube. Inside the rod tube the 7 ± 3 in. (17.78 ± 7.62 cm) long source was positioned between two solid, 0.670 ± 0.005 in. (1.7018 ± 0.0127 cm) outer diameter, 18-8 stainless steel spacer rods, held in place from above by a compression spring. The lower and upper spacer rods were respectively 15.90 ± 0.03 in. (40.386 ± 0.0762 cm) and 19.62 ± 0.03 in. (49.8348 ± 0.0762 cm) long. Dimensionally this source rod was completely interchangeable with any PBF fuel, shim, reflector, or filler rod in an assembly.

An IPT mockup was installed in the test space during subject tests. The test report describes this mockup as an open-ended stainless steel tube having a reactivity worth of -0.89 $, compared to the inconel IPT with a reactivity worth of -0.93 $. Dimensions and stainless steel alloys are not identified.

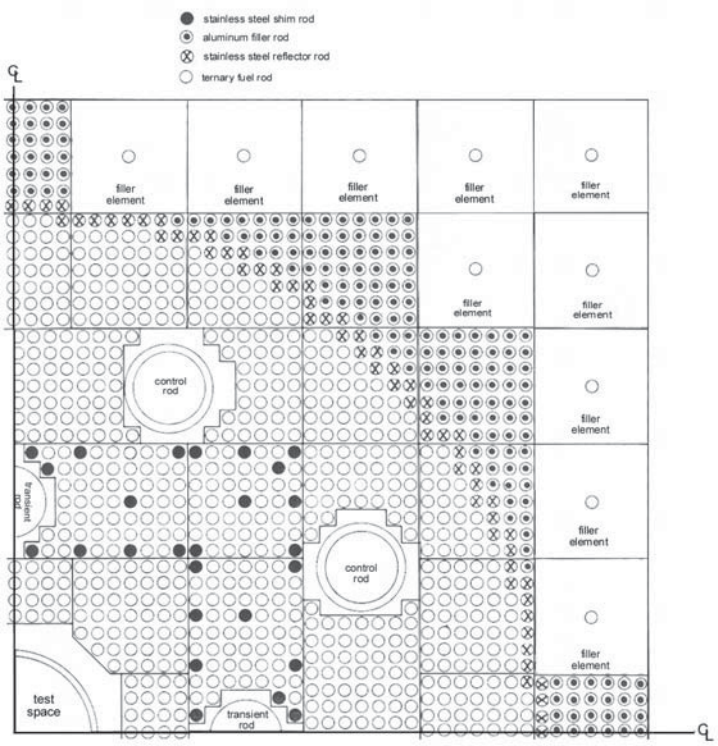

Figure 10. Operational Loading Test 1 Core Loading Pattern.

Figure 11. Operational Loading Test 2 Core Loading Pattern.

1.2.3 Other Components in Reactor Vessel (References 3 and 4) – Figure 12 shows the reactor vessel location and dimensions. The vessel was an open top Type 304 stainless steel cylindrical tank 28 ft 9 in. (876.3 cm) deep, with a 15 ft (457.2 cm) inner diameter. The operational water level was about 1 ft (30.48 cm) below the vessel rim. Therefore, during operations the surrounding water extended about 10 ft (304.8 cm) below, 14 ½ ft (441.96 cm) above, and 5 ft (152.4 cm) around the core. Figures 13 and 14 show dimensions and locations of major components in the vessel.

The PBF reactor core was located in a Type 304 stainless steel core container as shown in Figure 14. This container was radially centered in a relatively large, water flooded reactor vessel. The container consisted of an open-bottomed square box inside circular ribs. The box had a square section with a $64.642\ ^{+0.004}/_{-0.000}$ in. ($164.19068\ ^{+0.01016}/_{-0.000}$ cm) inner side width and nominal ¼ in. (0.635 cm) thick Type 304 stainless steel walls. Drawings[a] indicate a "60.520 Ref." box height.

Aforementioned ribs surrounded the core container box at five elevations. They were maintained at their elevations with vertical, ¼ in. (0.635 cm) thick Type 304 stainless steel plates. The ribs were made of 0.375 in. (0.9525 cm) thick Type 304 stainless steel plate inside hoops made of 2.5 in. (6.35 cm) wide, 1.0 in. (2.54 cm) thick Type 304 stainless steel. These ribs gave the container an overall 97.5 in. (247.65 cm) diameter, cylindrical cross section.

The core and container rested directly on a Type 7075 aluminum core support grid (or plate), directly above Type 7075 aluminum orifice plates. The 74.750 ± 0.005 in. (189.865 ± 0.0127 cm) square, 1.125 ± 0.005 in. (2.8575 ± 0.0127 cm) thick, core support grid had relatively large holes to position core components and to permit water flow through the core. The 1/8 in. (0.3175 cm) thick orifice plates were perforated in various locations and with various hole sizes to control water flow. These orifice plates were located below all fuel assemblies during most or all of the reactor life. However, the core design permitted these or similar orifice plates to be located above assemblies inside the core container, a design that is inconsistent with the above-quoted core container height.

As shown in Figure 14, the core, core container, and core support grid were held vertically between Type 304 stainless steel structures composed of steel beams or bars. The hold down structure, above the core, was primarily composed of steel beams or bars. Overall, the hold down structure was significantly taller near core center than near core edges. The core support structure, below the core, was apparently composed of a variety of 3 to 7 in. (7.62 to 17.78 cm) high beams and bars, with 14 in. (35.56 cm) high beams at the structure's outer edges.

[a] A full list of drawings is available in Reference 2.

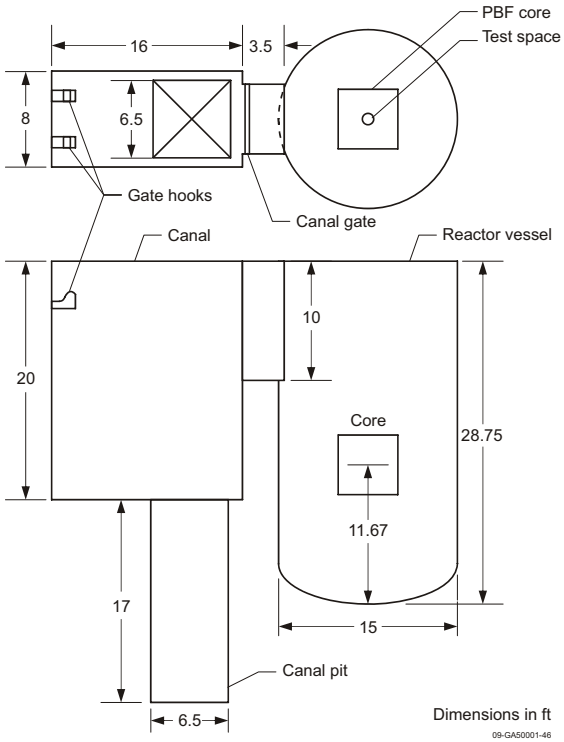

Figure 12. PBF Reactor Vessel Dimensions and Location.

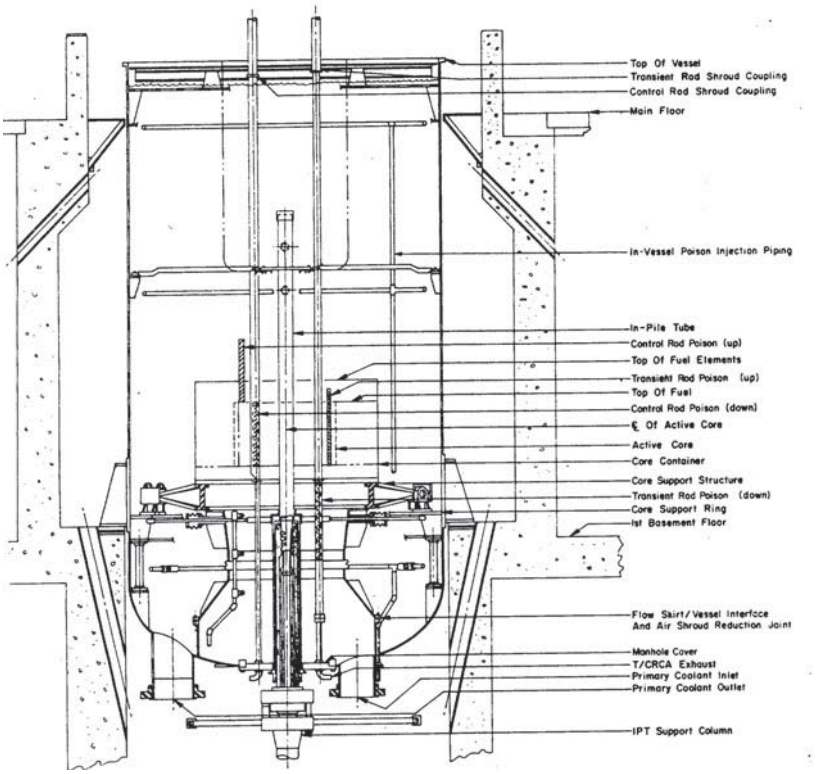

Figure 13. PBF Reactor Vessel and Contents.

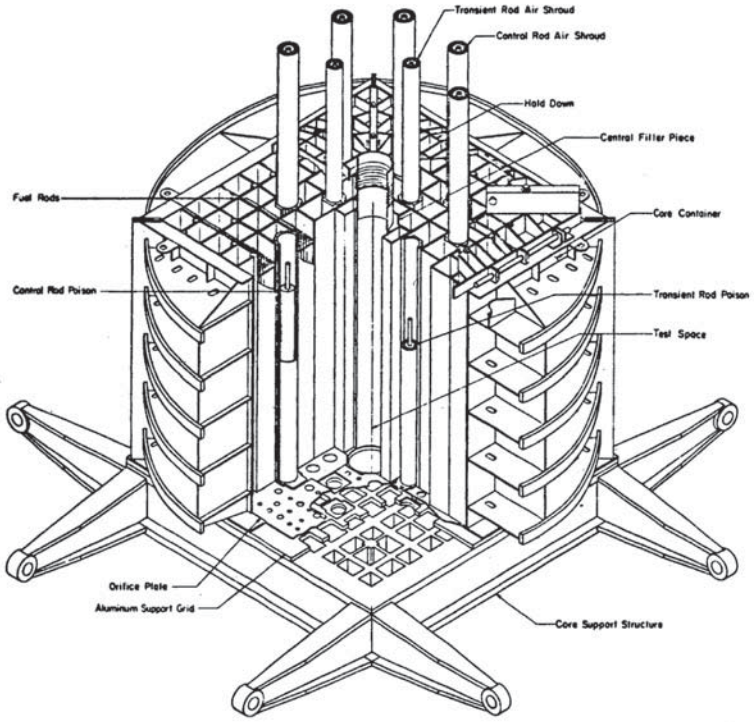

Figure 14. PBF Reactor Core Cut-Away View.

1.2.4 Other Information – Most subject drawings indicate that, unless otherwise specified, dimension tolerances are ± 1/64 in. (0.0396875 cm) when expressed in fractions and ± 0.005 in. (0.0127 cm) when expressed in decimals.

Additional information about differential control worths and excess reactivities are included in the following subsection.

1.2.5 Measurement Method and Uncertainty – The loading experiment was performed (Reference 1) with the IPT replaced by a stainless steel mockup and the transient rod poison withdrawn from the core. A plutonium-beryllium neutron source having a strength of 4.5 x 10^7 n/s was located in the test space at the center of the core. The operational instrumentation consisted of four boron-10-lined pulse chambers, two dual-range fission chambers, and one compensated ion chamber. The chambers were located near the periphery of the core as shown in Figure 1.

The loading experiment was performed by increasing the reactivity worth of the subcritical core in incremental steps using the change in counting rate to predict criticality and determine the reactivity worth of the configuration for each step. The quantity 1/m, referred to as "inverse multiplication" and defined as the initial counting rate divided by the counting rate for the current configuration, was plotted as a function of the incremental core configuration. Extrapolations of this curve to 1/m = 0 were made to predict criticality. The reactivity worth of the configuration at each time was determined from the equation:

$$R(\$) = \frac{1/m}{(1-1/m)\beta}$$

where

β = delayed neutron fraction
$1 / m = C_0 / C$
C_0 = initial counting rate
C = counting rate for the current configuration

The loading experiment was initiated and preceded by manually placing preassembled fuel assemblies in the core grid lattice: first around the test space and progressing outward in such manner that a generally cylindrical configuration was maintained. Following each loading of a predetermined number of fuel assemblies, the criticality state of the core was determined by stepwise withdrawal of the control rods, and for the configurations of control rod poison inserted and withdrawn, an estimate of the number of fuel assemblies that could be safely added in the next loading step and the shutdown reactivity worths were determined.

Problems to ensure a required measured shutdown reactivity of 3.0 $ with this method due to uncertainties in core parameters and geometry effects of the chambers resulted in a change of approach to the loading experiment. The change consisted of inserting boron containing aluminum wires in each fuel assembly before loading the assembly in the core. The poison wires were uniformly distributed and sufficient in number so that all the fuel assemblies could be loaded in the core and still result in a subcritical reactor with the control rod poison withdrawn. Each wire was 0.125 in. (0.3175 cm) in diameter and extended along the full active length of the fuel. The boron content of the wires was 3.3 wt.% natural boron. The total complement consisted of 1064 wires, which inserted a total of 640 g of boron and displaced 7720 cm^3 of water volume in the active region of the core.[a] The fuel assemblies containing poison wires were loaded manually in predetermined steps into the core lattice; first around the experimental test space and progressing outward in such a manner that a generally cylindrical configuration was maintained. After the fueled assemblies were loaded, the filler and reflector assemblies were placed in their respective lattice positions – thus completing the loading of the poison wire-shimmed core. Following each loading of a predetermined number of assemblies, the criticality state of the core and the reactivity worth for the control rod poison inserted and withdrawn was determined. For the fully loaded, poison wire-shimmed core, the reactivity worths for the control rod poison inserted and withdrawn were -20.8 $ and 10.3 $, respectively.

The critical experiment proceeded by withdrawing increments of poison wires (not exceeding about 1.0 $ in reactivity worth) from the core until criticality was reached. After each withdrawal of an increment of wires, the criticality state of the core and the reactivity worth for control rod poison inserted and withdrawn were determined using the inverse multiplication. From the criticality state determined for each step, a prediction of the number of wires remaining in the core and the number of wires to be withdrawn in the next increment was determined. The reactor became supercritical with the control rod poison fully withdrawn, with 264 poison wires remaining in the core.

The Operational Loading Test 1 analyzed in the evaluation consisted of removing the 264 poison wires which remained inserted in the core for the just-critical configuration. The wires were removed in increments to generate the differential reactivity worth of the control rods and produce data to allow a stepwise prediction of the critical position of the control rods for the core with the poison wires removed. After the removal of each increment of wires, the critical position of the control rods was determined. From each new critical position, control rod bumps were made generating positive power excursions in the period range 20 to 80 sec. From the periods of the power excursion, the reactivity worths of the bumps were obtained, allowing the differential reactivity worth of the control rods at the midpoint of the

[a] 7720 cm^3 is the volume as reported in Reference 2. With an active length of 36 in (91.44 cm) the computed wire volume is 7703 cm^3.

bump to be determined. The differential reactivity worth for each incremental wire removal was plotted as a function of the respective control rod position, and the resultant curve was integrated over the range to the fully withdrawn control rods to determine the accumulated excess reactivity. The incremental poison wire removal and the simultaneous determination of the differential and integral reactivity worths continued until all the poison wires were removed from the core. The critical position of the control rods with the poison wires removed was 22.05 in. (56.007 cm), and the differential reactivity worth was 0.456 $/in. (0.180 $/cm). The excess reactivity determined by integration of the differential reactivity data was 3.50 $. Figures 15 and 16 show the differential and integral reactivity versus the control rod position, respectively.

In order to obtain a required excess reactivity over 4.00 $ 12 stainless steel shim rods, 1 from each shimmed assembly, were replaced in the core with the standard fuel rods. The replacement of the 12 shim rods with fuel rods resulted in an increase of excess reactivity of 0.84 $. The resultant operational core (Operational Test 2) had a control rod critical position at 20.26 in. (51.4604 cm) and a total excess reactivity of 4.30 $ with a differential control rod worth of 0.478 $/in. (0.188 $/cm) at the critical position. The resultant changes in excess and differential reactivity worths were plotted as extensions of the data shown in Figures 15 and 16.

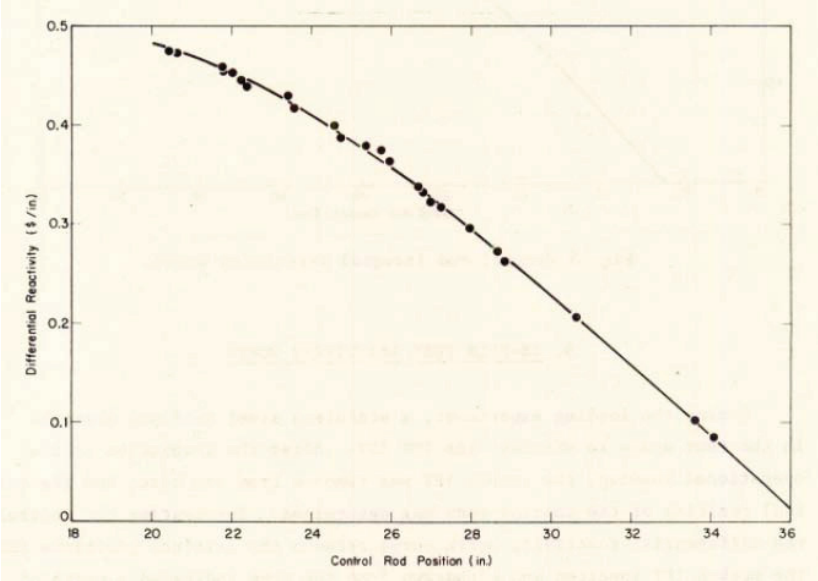

Figure 15. Control Rod Differential Reactivity Worth.

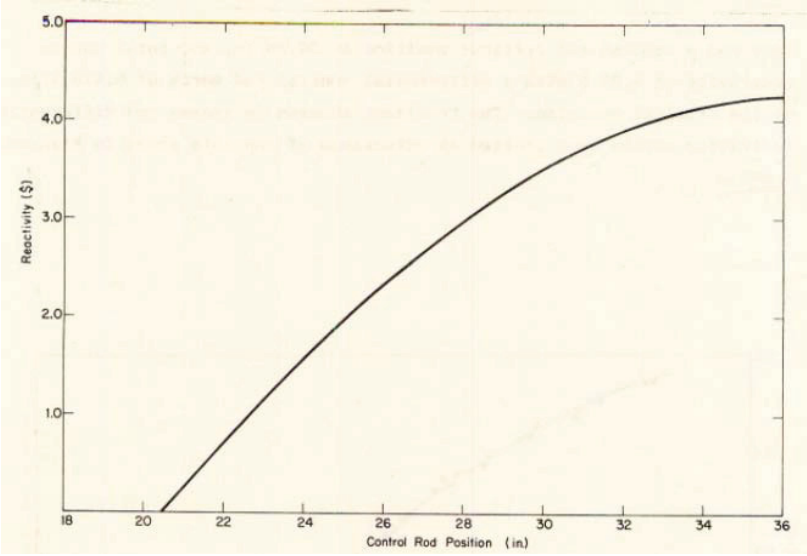

Figure 16. Control Rod Integral Reactivity Worth.

1.3 Description of Material Data

1.3.1 Fuel Matrix – The PBF fuel matrix was a unique $U(18)O_2$-CaO-ZrO_2 ternary ceramic.[a] Table 3 lists as-manufactured fuel pellet characteristics. Table 4 lists maximum values of permitted fuel impurities

Table 3. PBF BOL Fuel Matrix Description.

	PBF Fuel Specifications[(a)]	Wahnschaffe INEL-96/301 (Ref. 4)
Pellet Diameter	0.559 ± 0.001 in. (1.41986 ± 0.00254 cm)	1.4199 ± 0.025 cm
Pellet Length	0.600 ± 0.040 in. (1.524 ± 0.1016 cm)	
Pellet Stack Length[(b)]		91.4 cm
UO_2 (wt.%)	30.6 ± 0.4	30.6
ZrO_2 (wt.%)	61.8 ± 0.7	61.8
CaO (wt.%)	7.6 ± 0.7, or 6.94 to 8.33, or 10-12 wt.% in zirconia feed	7.6
CaO + ZrO_2 (wt.%)	69.4 ± 0.4	
Enrichment (^{235}U)	18.31 ± 0.2 wt.%	18.5 at.% in feed
Uranium (atoms/cm^3)		4.21×10^{21}
^{235}U		7.6×10^{20}
^{238}U		3.4×10^{21}
Bulk Density (g/cm^3)	5.97 ± 0.06	5.97 ± 0.09
Crystal Structure	FCC (100%)	

(a) PBF Fuel Specification F-11-PBF, Purchase Order C-286-A. Includes variously authored, numbered, and dated documents approved and filed by Idaho Nuclear Corporation: Idaho Falls, Idaho (1969-1970).
(b) Drawing 088743 (see footnote in page 2) indicates stack height of 36.000 ± 0.036 in. (91.44 ± 0.091 cm).

Table 4. Maximum Limits of Fuel Matrix Impurities.

Element	ppm
Carbon	100
Fluorine	50
Nitrogen	500
Hafnium	100
Titanium	100
Total[(a)]	2500

(a) Includes Ag, Al, B, Be, Cd, Co, Cr, Cu, Dy, Eu, Mg, Mn, Ni, Pb, Si, Sm, and Sn as well as previously listed elements. The accumulated total of impurities was also limited to a maximum thermal macroscopic cross section of 10^{-3} cm^{-1}.

[a] PBF Fuel Specification F-11-PBF, Purchase Order C-286-A. Includes variously authored, numbered, and dated documents approved and filed by Idaho Nuclear Corporation: Idaho Falls, Idaho (1969-1970).

1.3.2 Fuel Insulator – Sintered calcia-stabilized zirconia (ZrO_2-CaO) was used as fuel insulation because of its relatively high heat capacity, high melting point, and low thermal conductivity.[a] This material's nominal bulk density was either 4.47 g/cm^3 or 4.7 g/cm^3 (references are in conflict: 4.47 g/cm^3 in one report, 4.7 g/cm^3 in most reports) (Reference 2). During manufacture CaO comprised 10 to 12 wt.% of the zirconia feed.

1.3.3 Helium – PBF fuel rods were filled with helium to provide a chemically inert atmosphere.

1.3.4 Boron Carbide – The neutron absorber in CRs and TRs was boron carbide, B_4C. The FSAR (Reference 3) indicates this B_4C has a 2.50 to 2.51 g/cm^3 bulk density and was 76.5 wt.% B with a minimum 19.6 at.% ^{10}B in the boron.

1.3.5 Air – Air outside the building was compressed, filtered, and pumped into CR and TR air shrouds. It passed through the reactor once and was then filtered and exhausted to the outside. The air cooled CRs and TRs heated by radiation absorption. The air also provided a better medium than water in which to control CR and TR velocities.

1.3.6 Water – Demineralized coolant water also functioned as moderator and reflector. The FSAR (Reference 3) indicates, under operating conditions, that the water was saturated in oxygen and CO_2, having a maximum 0.15 ppm chlorides and 1.0 ppm suspended solids.

1.3.7 Aluminum Alloys – Aluminum alloys with various heat treatments were used for many reactor structural components to minimize neutron absorption and reflection. Many components were made of Type 6061 aluminum, some components were made of Type 7075 aluminum, and assembly walls were made of 5454 aluminum.

1.3.8 Steels – Stainless steels were used for some reactor and fuel rod structural components where aluminum alloy was inappropriate for the structural task. Most steel components were made of Type 304 stainless steel. However, fuel cladding was Type 304L stainless steel. Various comparatively small components were made of other steels. For example, rod restraining bolts were made of 17-4 PH stainless steel and fuel rod compression springs were made of a chromium-silicon alloy steel per temporary standard ASTM-A401-63T.

1.3.9 Temperature

Water temperatures from 69 to 100°F (20.5 to 37.7 °C) were used in the startup series, but temperatures for subject tests were not identified. The FSAR (Reference 3) indicates the initial fill temperature was normally 60°F (15.5°C). However the water inlet temperature was required to be 86 °F (30 °C) for normal reactor startup and for burst operation, and 97 to 136 °F (36.1 to 57.8 °C) for steady-state operation. Warming water from initial fill to startup temperatures could be accomplished by operating the coolant pumps alone.

1.4 Supplemental Experimental Measurements

The startup report (Reference 1) includes experimental data regarding control and transient rod worth, shim rod worth, various reactivity effects (void coefficients, temperature coefficients, and flow effects), flux profiles and instrumentation calibration. They are included in Appendix B.

[a] PBF Fuel Specification F-11-PBF, Purchase Order C-286-A. Includes variously authored, numbered, and dated documents approved and filed by Idaho Nuclear Corporation: Idaho Falls, Idaho (1969-1970).

2.0 EVALUATION OF EXPERIMENTAL DATA

2.1 Analysis of Experimental Parameters

2.1.1 Currently Missing Information -

- **As-built drawings:** Most readily available drawings appear to be design, rather than verified as-built, drawings. Most drawing information is dated between 1968 and 1970, before or soon after reactor construction began. One document revision was incorporated in most drawings after construction, but it is annotated, "add DCCS [document change control system] code."

  However, there is little or no reason to suspect these drawings are inaccurate. First, some drawings might be as-built because many components were manufactured before reactor construction began. Second, experimenter-calculated predictions were within expected uncertainties, which would not be true if the drawings these experimenters used included significant inaccuracies. Still, subtle discrepancies between drawings and as-built structures are not ruled-out by this evidence.

- **IPT mockup description:** The IPT mockup is described only as an open-ended stainless-steel tube having a reactivity worth of -0.89 $, compared to the inconel IPT with a reactivity worth of -0.93 $. Using this information the IPT can be replaced by reflector water, and the reactivity bias for this modification is +0.89 β_{eff}. β_{eff} was computed for both critical configurations using the prompt method,[a] resulting in a value of 742 pcm for Test 1, and 730 pcm for Test 2. IPT mockup removal therefore requires a 660 ± 35 pcm correction in multiplication factor of Test 1, and a 650 ± 35 pcm correction in Test 2. The uncertainty in the correction includes a 5% assigned to the delayed neutron fraction in the cross section libraries.

- **Test / start-up source:** Readily available information about the neutron source used in these tests does not include material density, dimension, and detailed nuclide compositions, and does not include encapsulation stainless steel type and dimension. Other typical used information is discrepant. For example, the source is about 4 or 7 in. long. As another example, the ^{238}Pu (or PuBe) mass is about 1.3 to 1.6 g. The source is neglected here, and a 40 pcm uncertainty is considered to take into account its effect.[b]

- **Other test instruments:** Readily available test documents provide functional, but not physical, descriptions of other test instrumentation (four ^{10}B-lined pulse chambers, two dual-range fission chambers, and one compensated ion chamber). However, these instruments were located in filler elements, separated from the active core by at least several inches of water and two rows of reflector rods. (Instrument locations were selected to avoid affecting flux profiles, component reactivity worths, and core symmetry). Any effect these instruments had on core k_{eff} is negligible.

2.1.2 Rod Dimensions – Fuel rod dimensions as expressed in Section 1.2 are inconsistent: partial dimensions do not add up to the outer clad diameter. Several sources[c] report fuel pellet diameter as 0.559 in. (1.41986 cm), although some drawings (like the one reproduced in Figure 4) show this value rounded to 0.56 in. (1.4224 cm).

---

[a] S. C. van der Merck, R. K. Meulekamp, "Calculating the effective delayed neutron fraction using Monte Carlo techniques", Proceedings of PHYSOR 2004, 2004.
[b] A 40 pcm bias was computed for a similar experiment, IEU-COMP-THERM-003.
[c] See references in Table 3, and also: D. W. Nigg, and A. J. Scott, "Computed Reactivity Requirement and Control Rod Worth for 30 MWth, 2-day Operation of PBF with a Large Reactive Experiment", TREE-NUREG-1024, 1976.

Assuming outer diameters (fuel pellet OD, clad OD, insulator OD) and thicknesses (insulator thickness, clad thickness) reported in Section 1.2 are valid, the resulting thickness for the He gap is 19.25 mil (0.048895 cm), and an additional 0.25 mil (0.000635 cm) gap has to be added between the ceramic insulator and the cladding.

2.1.3 ^{234}U and ^{236}U Content – ^{234}U and ^{236}U were not reported. According to similar evaluated experiments, the uranium composition should include 0.15 ± 0.05 wt.% ^{234}U. Assuming the uranium used in the fuel is fresh, no ^{236}U should be expected. Considering these factors, and assuming the enrichment is correct, the ^{238}U content is 81.54 wt.%. Uranium Compositions are given in Table 5.

Table 5. Uranium Composition.

Nuclide	wt.%
^{234}U	0.15 ± 0.05
^{235}U	18.31 ± 0.20
^{236}U	-
^{238}U	81.54 (Balance)

2.1.4 Fuel Impurities – Fuel specification includes maximum values for several elements in the fuel matrix (Section 1.3.1) and limits the thermal absorption cross section of the impurities to 10^{-3} cm^{-1}. To include the absorption effect of the impurities 1.1287 x 10^{-6} 1/(b cm) of ^{10}B (equivalent to 5 x 10^{-4} cm^{-1}) is included in the composition of the fuel, and ±1.1287 x 10^{-6} 1/(b cm) of ^{10}B is considered to be a bounding value for the uncertainty in the impurity content.

2.1.5 Water Density – Water's bulk density is 1.0 g/cm^3 at temperatures of concern here. However, a more precise value is often desired, although there is some disagreement over specific values chosen. Water density is assumed to be 0.99566 g/cm^3 at operation temperature (30 ^{o}C), based on values listed in Table 6.

Table 6. Water Mass Densities [g/cm^3].

Temperature [ºC]	Perry and Chilton[(a)]	Lide[(b)]	Green[(c)]
0	0.99987	0.99984	0.999839
10	0.99973	0.99970	0.999699
20	0.99823	0.99821	0.998204
30	0.99568	0.99565	0.995647
40	0.99225	0.99222	0.992215
50	0.98807	0.98803	0.988037

(a) R. H. Perry, and C. H. Chilton, "Chemical Engineers' Handbook", 5th ed., New York, New York, McGraw-Hill Book Company, 1973.
(b) D. R. Lide, chief editor, "CRC Handbook of Chemistry and Physics", 77th ed. Boca Raton, Florida, CRC Press, 1996.
(c) D. W. Green, editor, "Perry's Chemical Engineers' Handbook", 7th ed., New York, New York, McGraw-Hill, 1997.

2.1.6 Aluminum Alloys – Aluminum alloys with various heat treatments were used for many reactor structural components to minimize neutron absorption and reflection. Many components were made of Type 6061 aluminum, some components were made of Type 7075 aluminum, and assembly walls were made of 5454 aluminum. Table 7 lists bulk densities and chemical compositions of these alloys. For comparison convenience Table 7 includes values used in the final experiment models.

Table 7. Aluminum Alloy Characteristics.

	Type 5454 Al		Type 6061 Al		Type 7075 Al	
	Reference	Modeled	Reference	Modeled	Reference	Modeled
Bulk Density (ASM 1990, Vol. 2) [g/cm^3][(a)]						
	2.68	2.69	2.70	2.69	2.80	2.795
Nuclide wt.% (ASTM B 209-96[(b)]; ASM 1990, Vol. 2)						
Al	Balance	95.825	Balance	97.365	Balance	89.37
Mg	2.4 – 3.0	2.7	0.8 – 1.2	1.0	2.1 – 2.9	2.5
Ti	< 0.2	0.1	< 0.07	0.035	< 0.2	0.1
Cr	0.05 – 0.20	0.125	0.04 – 0.35	0.20	0.18 – 0.28	0.23
Mn	0.5 – 1.0	0.75	< 0.15	0.075	< 0.3	0.15
Fe	< 0.4	0.2	< 0.7	0.35	< 0.5	0.25
Cu	< 0.10	0.05	0.15 – 0.40	0.25	1.2 – 2.0	1.6
Zn	< 0.25	0.125	< 0.25	0.125	5.1 – 6.1	5.6
Si	< 0.25	0.125	0.4 – 0.8	0.6	< 0.4	0.2

(a) ASM, "Metals Handbook", Vol, 1 and 2, 10th ed., Metal Parks, Ohio, ASM, 1990
(b) ASTM B 209-96, "Standard Specification for Aluminum and Aluminum-Alloy Sheet and Plate", ASTM, approved August 10 1996.

2.1.7 Steels - Stainless steels were used for some reactor and fuel rod structural components where aluminum alloy was inappropriate for the structural task. Most steel components were made of Type 304 stainless steel. However, the fuel cladding is Type 304L stainless steel. Tables 8 and 9 respectively list standard chemical compositions and the values used in the final experiment models.

Table 8. Type 304 Stainless Steel Characteristics.

	Standard Composition[(a)]	**Used in Model**
Density [g/cm^3]	8.0	8.0
wt.%		
Fe	Balance	70.1725
C	< 0.08	0.04
Cr	18.0 – 20.0	19.00
Mn	< 2.00	1.00
Ni	8.0 – 10.5	9.25
P	< 0.045	0.0225
Si	< 1.00	0.50
S	< 0.03	0.015

(a) ASM, "Metals Handbook", Vol, 1 and 2, 10th ed., Metal Parks, Ohio, ASM, 1990.

Table 9. Type 304L Stainless Steel Characteristics.

	Standard Composition[(a)]	**Used in Model**
Density [g/cm^3]	8.0	8.0
wt.%		
Fe	Balance	69.4475
C	< 0.03	0.015
Cr	18 - 20	19.00
Mn	< 2.00	1.00
Ni	8 – 12	10.00
P	< 0.045	0.0225
Si	< 1.00	0.50
S	< 0.03	0.015

(a) ASM, "Metals Handbook", Vol, 1 and 2, 10th ed., Metal Parks, Ohio, ASM, 1990

2.1.8 Homogenized Materials – Some non-continuous items (bar grids, perforated items) are not explicitly represented in Reference 1. The reference includes homogenized material descriptions to represent these components, computed from the geometry reported in the specification drawings. These homogenized materials include a 58.36 / 41.64 mixture of Type 6061 aluminum and water for the mounting plates in the assemblies, a 50 / 50 mixture of Type 7075 aluminum and water for the core support grids and orifice plates, and a 25 / 75 mixture of Type 304 stainless steel and water for various items above and below the core container.

2.1.9 Components Surrounding the Reactor Core – The reactor vessel, reactor hall and its equipment, and any other component and materials outside the reactor vessel are neglected. These items are separated from the active core by more than 60 cm of water. Therefore, such items are considered to have no appreciable effect on the core's calculated k_{eff}.

2.1.10 Control and Transient Rod Positions – Readily available documents provide discrepant information regarding CR and TR relaxed (down) axial positions. In the fully-relaxed CR position, the lower edge of CR B_4C is either even with the bottom of the active core, or 8.0 in. (20.32 cm) below the active core. However, all documents apparently agree that rod positions are measured from a reference 0.00 position at which the lower edge of CR B_4C is even with the lower edge of the active core. The CR fully relaxed position discrepancy therefore will not affect these experiments models.

There is some discrepancy between control rod centerline position as reported in the references and outer dimensions of the fuel assemblies. Control rods are reported to be located at 19.461 in. (49.43094 cm) from the center of the test space, with control rod center to center distances of 13.257 in. (33.67278 cm) and 16.502 in. (41.91508 cm) (Table 1). But, using these dimensions the control rods interfere with assemblies with nominal dimensions in a 5.875 x 5.875 in. (14.9225 x 14.9225 cm) spaced grid. This might have been caused by the use of nominal dimensions to model fuel assemblies, instead of specific measured dimensions for each assembly that are not currently available. Therefore, the position of control rods was adjusted to fit the core lattice. The reactivity effect of these adjustments was computed and is less than 10 pcm and neglected. Control and transient rods positions are listed in Table 10.

Table 10. Absorber Rod Model Coordinates[(a)] [cm].
(x = 0, y = 0 is the center of the test space. z = 0 is the midpoint of the active region of fuel)

Absorber Rod Identifier	Tie Rod Center Coord.		B_4C Elevation (Test 1)		B_4C Elevation (Test 2)	
	X	Y	Bottom	Top	Bottom	Top
CR1	21.07	44.7675	10.287	101.727	5.7404	97.1804
CR2	44.7675	21.07	10.287	101.727	5.7404	97.1804
CR3	44.7675	-21.07	10.287	101.727	5.7404	97.1804
CR4	21.07	-44.7675	10.287	101.727	5.7404	97.1804
CR5	-21.07	-44.7675	10.287	101.727	5.7404	97.1804
CR6	-44.7675	-21.07	10.287	101.727	5.7404	97.1804
CR7	-44.7675	21.07	10.287	101.727	5.7404	97.1804
CR8	-21.07	44.7675	10.287	101.727	5.7404	97.1804
TR1	0	29.845	-175.26	-68.58	-175.26	-68.58
TR2	29.845	0	-175.26	-68.58	-175.26	-68.58
TR3	0	-29.845	-175.26	-68.58	-175.26	-68.58
TR4	-29.845	0	-175.26	-68.58	-175.26	-68.58

(a) Computed from dimensions in inches.

2.1.11 Transient and Control Rod Insulator Material – Between the absorber region and the upper end cap (Figures 8 and 9) of the control and transient rods there is an insulator specified as "supermica 620" (Table 1). The composition of this material is not given in the references. In the case of control rods this insulator is well above the core and might be neglected, but in the transient rods this insulator material is close to the active region of the core. To model this component a generic muscovite mica is used in the model. The composition for this material is listed in Table 11.

Table 11. Muscovite Mica Composition (Density = 2.83 g/cm^3).[(a)]

Component	wt.%
SiO_2	45.26
Al_2O_3	38.40
K_2O	11.82
H_2O	4.52

(a) Muscovite Datasheet, from the "Handbook of Mineralogy", Mineral Data Publishing, 2001.

2.1.12 Boron Carbide Composition – The values given in the FSAR for the boron isotopic vector (19.6 at.% ^{10}B) and the boron weight percent (76.5 wt.% B) in the B_4C contained in the control and transient rods are likely to be minimum values. In the absence of any measured values the isotopic composition recommended by IUPAC[a] (19.9 ± 0.7 at.% ^{10}B) and the stoichiometric composition of B_4C (78.26 wt.% B) are assumed for the models.

2.2 Sensitivity Analysis

The variables chosen for sensitivity analysis were the following:

- Fuel assembly dimensions;
- Fuel, shim, reflector and filler rods dimensions and compositions;
- Control and transient rods dimensions and compositions;
- Water density; and
- Structural alloys composition.

For each of the variables in each experiment, a model was run for $\pm \delta x_i$, and the results were used to calculate the effect of the uncertainty in the variable using:

$$\sigma_i(keff) = \left| \frac{k_{\delta x} - k_{ref}}{\delta x_i} \right| \sigma(x_i)$$

MCNP5[b] with ENDF/B-VI.6 cross sections was used to compute the multiplication factor for all of the perturbed variables, which was compared to a one-quarter core model with nominal values.

A brief analysis of the uncertainties in each variable follows.

2.2.1 Fuel Assemblies – Most assembly drawings and descriptions indicate assemblies have a 14.9225 ± 0.01016 cm outside width along the seven-rod-wide side. However, most reactor core drawings identify this same width for assembly positions, either identifying a 14.85392 cm assembly outside width or not identifying assembly dimensions. The 14.85392 cm assembly width allows a 0.06858 cm water gap between assemblies. The 14.9225 cm assembly does not allow a water gap between assemblies

[a] T. B. Coplen, et al. *Isotope-Abundance Variations of Selected Elements*, Pure Appl. Chem., Vol. 74, No. 10, pp. 1987 - 2017, 2002.
[b] X-5 Monte Carlo Team. "MCNP – A General Monte Carlo N-Particle Transport Code, Version 5". LA-UR-03-1987. Los Alamos National Laboratory, 2003.

although it does allow more water between outer rods and assembly walls. This discrepancy would have negligible effect on subject calculations because only wall placement is affected in this thermal reactor (distance, material compositions, and material thicknesses between rods in adjacent assemblies are not affected). The uncertainty information provided in the references comes from design tolerances, which are treated here as Type B uncertainties with a uniform probability distribution, and divided by $\sqrt{3}$ to obtain one standard deviation. Therefore, assembly and assembly-position widths are respectively assumed to be 14.85392 ± 0.00587 cm and 14.9225 ± 0.00587 cm.

With one exception, descriptions indicate assemblies have 0.37338 cm thick walls. The exception is one 49-rod assembly drawing[a] in which component dimensions sum to a value indicating canister walls are 0.42164 cm thick. However, this 0.42164 cm wall thickness seems unlikely because it does not leave sufficient space for seven rods at nominal pitch, even with a 14.9225 assembly outside width. Noting drawing-specified standard tolerances and considering them to be uniformly distributed, assembly wall thicknesses are concluded to be 0.37338 ± 0.00733 cm.

The calculation using MCNP models resulted in an effect of assembly width uncertainty of 107 ± 20 pcm. The effect of assembly wall thickness was computed to be 31 ± 19 pcm.

2.2.2 Fuel, Shim, Reflector, and Filler Rods – Rod tolerances have negligible to minor effects on calculated k_{eff}'s. Radial tolerances within the active core regions have significantly more effect than axial tolerances affecting items above and below the active core. Radial tolerance effects and some items affecting active core height are therefore addressed here, but most axial tolerance effects are negligible and not specifically addressed. The uncertainties in these fuel-fabrication parameters consist of a component due to deviations in process parameters during the fabrication process which affect individual fuel rods randomly, and a component due to systematic deviations from specifications which affect all fuel rods in the same way. The systematic component is considered to be 10% of the total uncertainty, and the random component accounts for the remaining 90% of the uncertainty. The total effect of these uncertainties in the multiplication factor is computed using:

$$\delta k_{eff}{}^{x} = 0.9 \cdot \Delta k_{eff}{}^{x} / \sqrt{N} + 0.1 \cdot \Delta k_{eff}{}^{x}$$

where $\Delta k_{eff}{}^{x}$ is the effect in the multiplication caused by perturbing the quantity in all the fuel rods, and $N = 2380$ is the number of fuel rods during the first test.

Fuel, shim, reflector, and filler rods are described as having 120.65 ± 0.0396875 cm length, 1.90754 ± 0.01016 cm OD, and 2.01168 ± 0.0127 cm square pitch. The uncertainties given for these values are tolerances and can be treated as Type B uncertainties with uniform distributions of probability. The computed effect of rod pitch uncertainty, considered as systematic, is 57 ± 38 pcm. Considering the outer diameter uncertainty is systematic, the effect on the multiplication factor is 291 ± 20 pcm. If we assume the uncertainty is 90% random, 10% systematic, the effect on k_{eff} caused by pitch uncertainty is 7± 2 pcm, and the effect caused by the outer diameter is 34 ± 2 pcm.

In the active fuel region, fuel rods are composed of concentric cylinders of fuel matrix (1.41986 ± 0.00254 cm OD), helium gas gap (0.048895 ± 0.004572 cm thick), calcia stabilized zirconia insulator (0.12192 ± 0.00254 cm thick), outer helium gap (0.000635 cm thick) and stainless steel cladding (0.07239 ± 0.00381 cm thick, 1.90754 cm OD).

[a] A full list of drawings is available in Reference 2.

Assuming tolerances to be Type B uncertainties and using a uniform probability distribution, 1-sigma uncertainty for clad thickness is ± 0.00220 cm. Considering the cladding wall thickness effect to be completely systematic, the effect in k_{eff} is 286 ± 20 pcm. If we assume the uncertainty is 90% random, 10% systematic, the effect in k_{eff} is 25 ± 2 pcm.

2.2.3 Fuel and Insulator Composition – Quantity and distribution of ^{235}U in a fuel rod is a function of enrichment (18.31 ± 0.20 wt.%), UO_2 in the fuel matrix (30.6 ± 0.4 wt.%), fuel matrix density (5.97 ± 0.09 g/cm^3), fuel pellet diameter (1.41986 ± 0.00254 cm), fuel pellet stack height (91.44 ± 0.09144 cm), and vertical gap lengths between fuel pellets in fuel stack (not specified). Vertical gaps between fuel pellets are typically very small and are assumed here to be enveloped by fuel density and fuel stack height effects. Assuming the enrichment is a measured value, and all the other variables to be uniformly distributed within their respective tolerances, the uncertainty effect of enrichment is 258 ± 33 pcm, the effect of UO_2 wt.% is 123 ± 19 pcm, the effect of pellet OD is 61 ± 20 pcm, the effect of matrix density is 63 ± 20 pcm, and the effect of stack height is 33 ± 18 pcm.

Assuming a 0.05 wt.% standard deviation in the ^{234}U content (Section 2.1.3), the effect of this uncertainty in the multiplication factor is 91 ± 33 pcm.

Fuel impurities are considered to have a thermal absorption cross section uniformly distributed in the range 0 – 10^{-3} 1/cm. The effect was modeled by adding 1.1287 x 10^{-6} 1/(b cm) of ^{10}B as an average impurity value and considering a 1-sigma uncertainty of 6.5164 x 10^{-7} 1/(b cm) of ^{10}B. The effect of the uncertainty in the impurities was computed to be 373 ± 13 pcm.

Calcium quantity and distribution in a fuel rod is a function of CaO in the fuel matrix (7.6 ± 0.7 wt.%), fuel matrix density (addressed in previous paragraph), fuel matrix dimensions (addressed in previous paragraph), CaO in insulator feed (10 to 12 wt.%), insulator density (4.47 g/cm^3 in one report, 4.7 g/cm^3 in most reports, tolerance not specified),[a] insulator OD (1.761 ± 0.001 cm) insulator wall thickness (0.12192 ± 0.00254 cm), insulator-sleeve-piece lengths (2.54 to 7.62 cm), insulator-sleeve-stack length (97.79 ± 0.0127 cm),[b] and distances between pieces in insulator sleeve stack (not specified). Sleeve piece length and stack length are not considered here because they have negligible effect on calculated k_{eff}'s since associated calcium changes occur above the active core. Distances between pieces within a stack are typically extremely small and are therefore assumed to be enveloped by sleeve density effects. Assuming uniform probability distributions in CaO wt.% and insulator wall thickness, and assigning a 1-sigma uncertainty of 0.23 g/cm^3 to insulator density (based on discrepancy found in the different available values), the uncertainty effects in k_{eff} are 44 ± 19 pcm for CaO in the fuel matrix and insulator, and 55 ± 26 pcm for insulator density. The effect of the uncertainty in wall thickness is below calculation error and is considered to be bound by 20 pcm.

Zirconia quantity and distribution effects are addressed as part of the previously summarized sensitivity calculations. Important zirconia values were adjusted in conjunction with the ^{235}U and calcia values. Helium gap thickness effect is considered in conjunction with the clad thickness.

2.2.4 Control and Transient Rods – In the fully-relaxed TR position, various drawings and graphics show the top edge of TR B_4C to be somewhere between 22.86 and 49.2125 cm below the active core. Experiment models use the highest indicated position. Comparing results modeling TRs with and without B_4C enveloped TR position uncertainty, which was then divided by $\sqrt{3}$ to estimate a 1-sigma uncertainty value. The effect of this uncertainty in k_{eff} is 31 ± 20 pcm.

[a] Typical nuclear tolerances, ± 0.01 wt.% or less, are well within the range created by value discrepancy.
[b] Based on drawing-specified standard tolerances.

Absorber-rod drive tube, guide tube, shroud tubes, and B_4C container outer tube data are also somewhat discrepant. The combined-tube's thickness uncertainty is assumed to be ± 10%.[a] The effect of this uncertainty in k_{eff} is 48 ± 34 pcm.

Boron quantity and distribution in the active core is affected by various CR and TR characteristics. Characteristics for which uncertainty effects are not necessarily negligible include rod positions (CRs at 56.007 ± 0.0254 and 51.4604 ± 0.0254 cm respectively for Test 1 and 2),[b] B_4C pellet ID (2.6162 ± 0.0127 cm),[c] and B_4C pellet OD (9.8298 ± 0.0127 cm),[d] B_4C density (2.50 to 2.51 g/cm^3), and boron isotopic composition (19.9 ± 0.7 at.% ^{10}B).[e] In the case of rod positions, assuming the resolution of the position meters can be considered 1-sigma uncertainty, the calculated effect of CR position in k_{eff} is 33 ± 20 pcm for Case 1, and 31 ± 20 pcm for Case 2. Assuming tolerances in dimensions define Type B errors, the computed effect of the internal diameter uncertainty is 25 ± 20 pcm, and the effect of the external diameter of the rods in k_{eff} is below computational uncertainty and considered to be bound by 20 pcm. The effects of B_4C density and boron isotopic composition were found to be below computational uncertainty and each one is considered to be bound by 20 pcm.

Gaps between pellets in the B_4C pellet stack are very small and, therefore, resultant effects are assumed to be well enveloped by B_4C and ^{10}B density uncertainties. CR characteristics affecting B_4C stack height are not considered here because resultant boron changes are well above the active core.

Similar TR uncertainties involving boron are negligible because this boron is well below active core.

2.2.5 Water – Water temperatures from 69 to 100°F (20.5 to 37.7 °C) were used in the startup series, but temperatures for subject tests were not identified. For the purpose of this evaluation, operational water temperature is considered to be 30°C, which was usually achieved by the sole operation of the coolant pumps.[f] A 1-sigma uncertainty of 6°C is assigned to the temperature, which results in an uncertainty of 81 ± 29 pcm in k_{eff}.

Water impurities are not completely defined in the references. To check the effect of the impurities, 0.15 ppm of chlorine were added to the water composition. The effect was found to be below computational uncertainty and is considered to be bound by 20 pcm.

2.2.6 Alloy Compositions – To estimate the effect of the uncertainty in stainless steel composition the effect of uncertainty in the weight percentage of Manganese and Nickel (the alloying elements with highest contribution to the thermal absorption cross section of stainless steel) was considered separately, and then the effects were added in quadrature.

For each of the alloying elements two cases were considered: one with the element at its maximum value, and the other with the element at its minimum value. These two extreme cases are considered to include all intermediate compositions with equal probability, then the result is divided by $2\sqrt{3}$ to compute the effect in k_{eff}.

[a] A ± 10% thickness uncertainty is typical of non-fuel nuclear manufacturing precision. It is less precise than a ± 5 to 8% typical for nuclear fuel applications and more precise than the ± 12.5 % typical for non-nuclear applications.
[b] Based on CR and TR position output resolutions described in section 1.2.1.
[c] Assumed tolerance based on other CR tolerances and on drawing-specified standard tolerances.
[d] Assumed tolerance based on other CR tolerances and on drawing-specified standard tolerances.
[e] T. B. Coplen, et al. *Isotope-Abundance Variations of Selected Elements*, Pure Appl. Chem., Vol. 74, No. 10, pp. 1987 - 2017, 2002.
[f] D. W. Nigg, personal communication, February 2009.

With this methodology, the effect of SS 304L composition uncertainty in k_{eff} is 268 ± 23 pcm and the effect of uncertainty in SS 304 composition is 94 ± 23 pcm.

Nominal values are used for the densities of stainless steel. A ± 0.05 g/cm^3 uncertainty is considered for these values. The computed effect of uncertainty in Type 304L stainless steel density is 77 ± 23 pcm. The effect of uncertainty in Type 304 stainless steel density is below computational uncertainty and is considered to be bound by 20 pcm.

2.2.7 Other Reactor Components – Documents provide discrepant information that affects the core container height. In addition, the core container top is most probably not a solid piece of metal with penetrations only for CRs, TRs and the test space. However, these discrepancies have negligible effect on calculated k_{eff} because the core container top is approximately 60 cm above the active core.

2.2.8 Experiment k_{eff} Uncertainty – These operation loading tests were critical (k_{eff} = 1.000) within the reactor's measurement precision. However, in this experiment k_{eff} uncertainty also incorporates the precision to which subject conditions are described.

Table 12 summarizes calculated uncertainty effects for each of these parameters. Combining the uncertainty for each source, total uncertainties in k_{eff} for Test 1 of 602 pcm, and of 602 pcm for Test 2 are computed. The experiment k_{eff}'s are therefore determined to be 1.0000 ± 0.0060 for Test 1, and 1.0000 ± 0.0060 for Test 2.

Based on the previous analysis, both experiments are considered acceptable as criticality safety benchmarks.

Table 12. Uncertainty Summary for Test 1 and Test 2.

Variable	Nominal Value	1-σ uncertainty	Uncertainty Effect [pcm]	
			Test 1	Test 2
Startup Source	-	-	40	
Assembly width [cm]	14.9225	0.00587	107 ± 20	
Assembly walls [cm]	0.37338	0.00733	31 ± 20	
Rod pitch [cm]	2.01168	0.00733	57 ± 38	
Rod OD [cm]	1.90754	0.00587	34 ± 2	
Cladding wall thickness [cm]	0.07239	0.00220	25 ± 2	
Enrichment [wt.%]	18.31	0.20	258 ± 33	
UO_2 [wt.%]	30.6	0.23	123 ± 19	
^{234}U [wt.%]	0.15	0.05	92 ± 33	
Pellet OD [cm]	1.41986	0.00147	61 ± 20	
Fuel matrix density [g/cm^3]	5.97	0.05	63 ± 20	
Stack height [cm]	91.44	0.05	33 ± 18	
CaO effect in fuel and insulator	-	-	44 ± 19	
Fuel impurities [at ^{10}B/(cm b)]	1.1287×10^{-6}	6.5164×10^{-7}	373 ± 13	
Insulator density [g/cm^3]	4.7	0.23	55 ± 26	
Insulator wall thickness [cm]	0.12192	0.00147	< 20	
TR position	-	-	31 ± 20	
CR & TR design	-	-	48 ± 34	
CR position	56.007 | 51.4604	0.0254 | 0.0254	33 ± 20	31 ± 20
CR absorber inner diameter [cm]	2.6162	0.00733	25 ± 20	
CR absorber outer diameter [cm]	9.8298	0.00733	< 20	
B_4C density [g/cm^3]	2.505	0.05	< 20	
B isotopic vector [at.% ^{10}B]	19.9	0.7	< 20	
Water temperature [ºC]	30	6	81 ± 29	
Water impurities	-	-	< 20	
SS 304L composition	-	-	268 ± 23	
SS 304L density [g/cm^3]	8.03	0.05	77 ± 23	
SS 304 composition	-	-	94 ± 23	
SS 304 density	7.92	0.05	< 20	
		Combined uncertainty:	602 ± 119	602 ± 119

3.0 BENCHMARK SPECIFICATIONS

3.1 Description of Model

A detailed full core model was developed for each subject configuration. For convenience positions within models are relative to the center of the test space, and elevations are relative to the midpoint of the active length of the fuel. Figures 17 and 18 respectively show transversal and axial views of the reactor model. Figure 19 shows a full-core transverse view of the Test 1 model, expanded to show the positive quadrant in Figure 20. A similar, positive quadrant view of Test 2 model is shown in Figure 21.

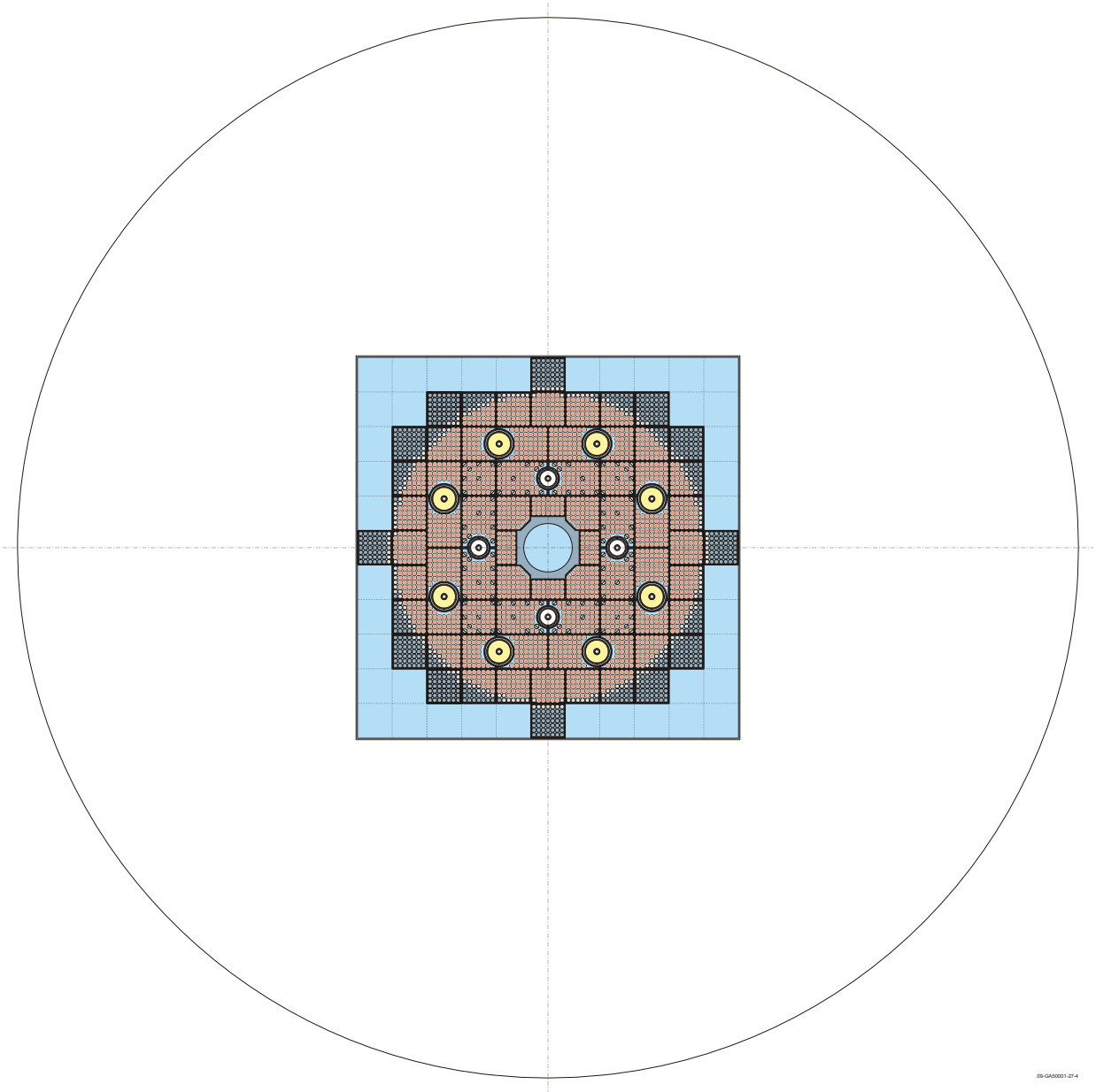

Figure 17. PBF Reactor Model, Radial View, 15 cm Elevation.

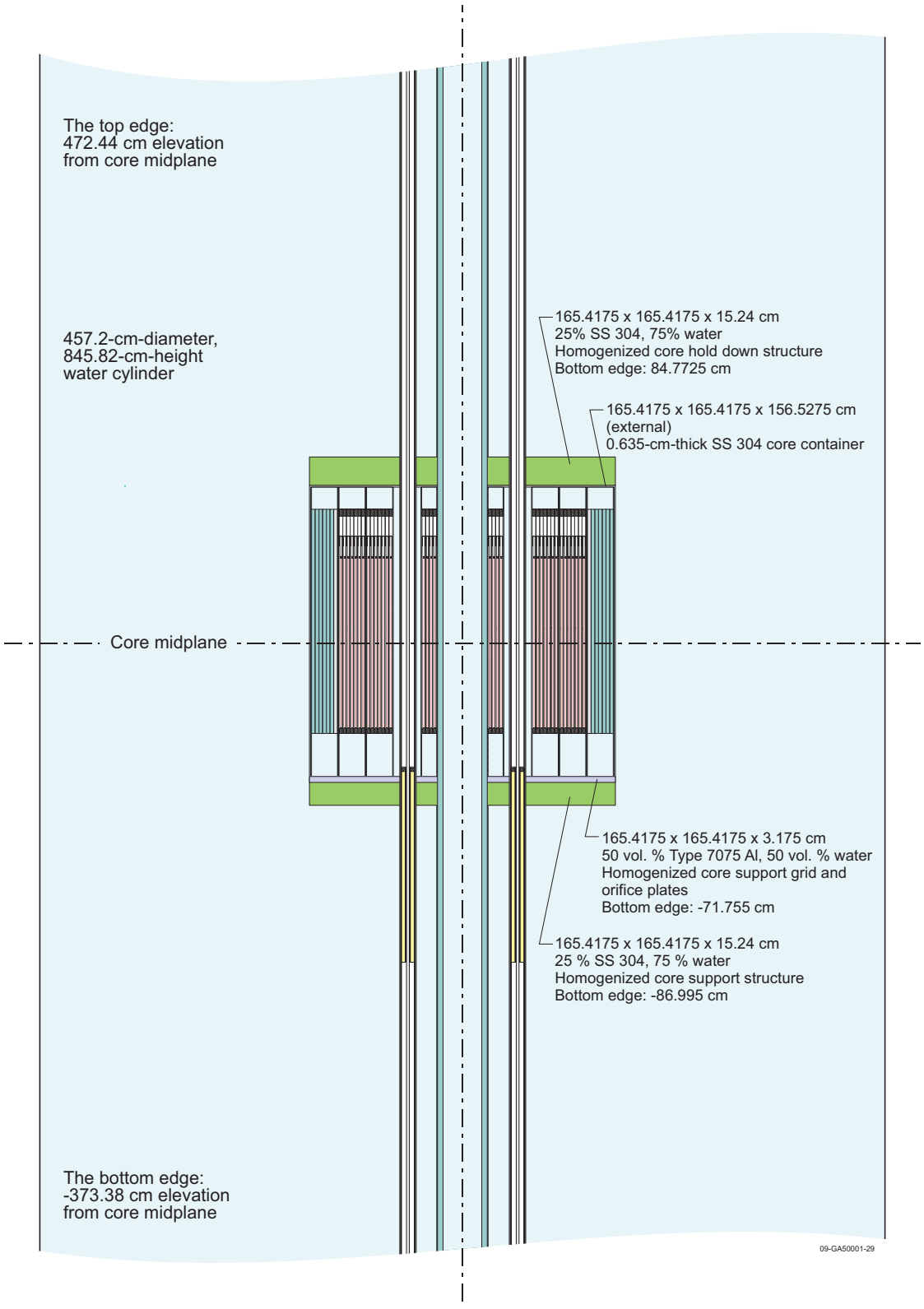

Figure 18. PBF Reactor Model, Axial View, x = 0.00 cm.

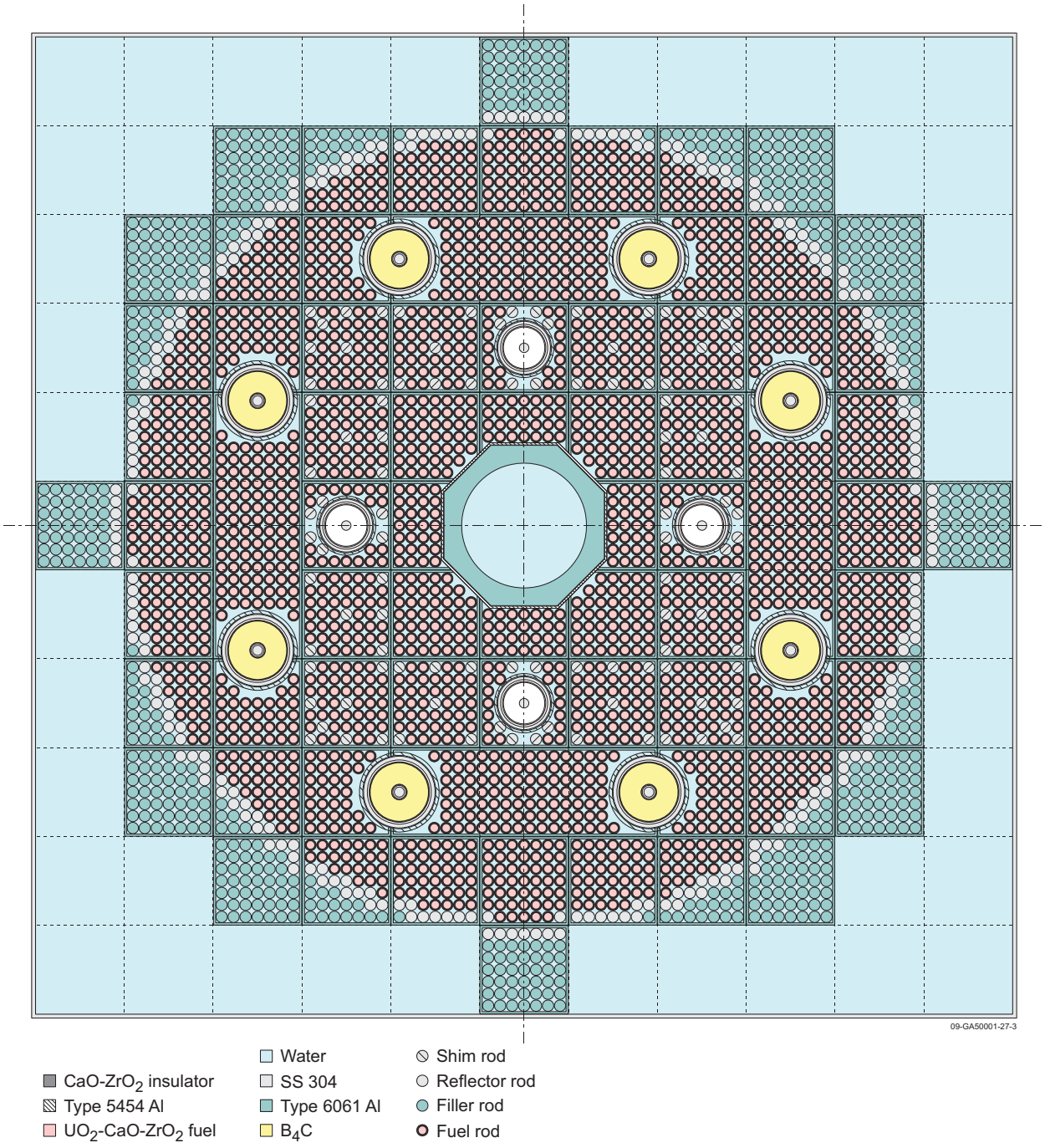

Figure 19. Radial View of Test 1 Core Model, 15 cm Elevation.

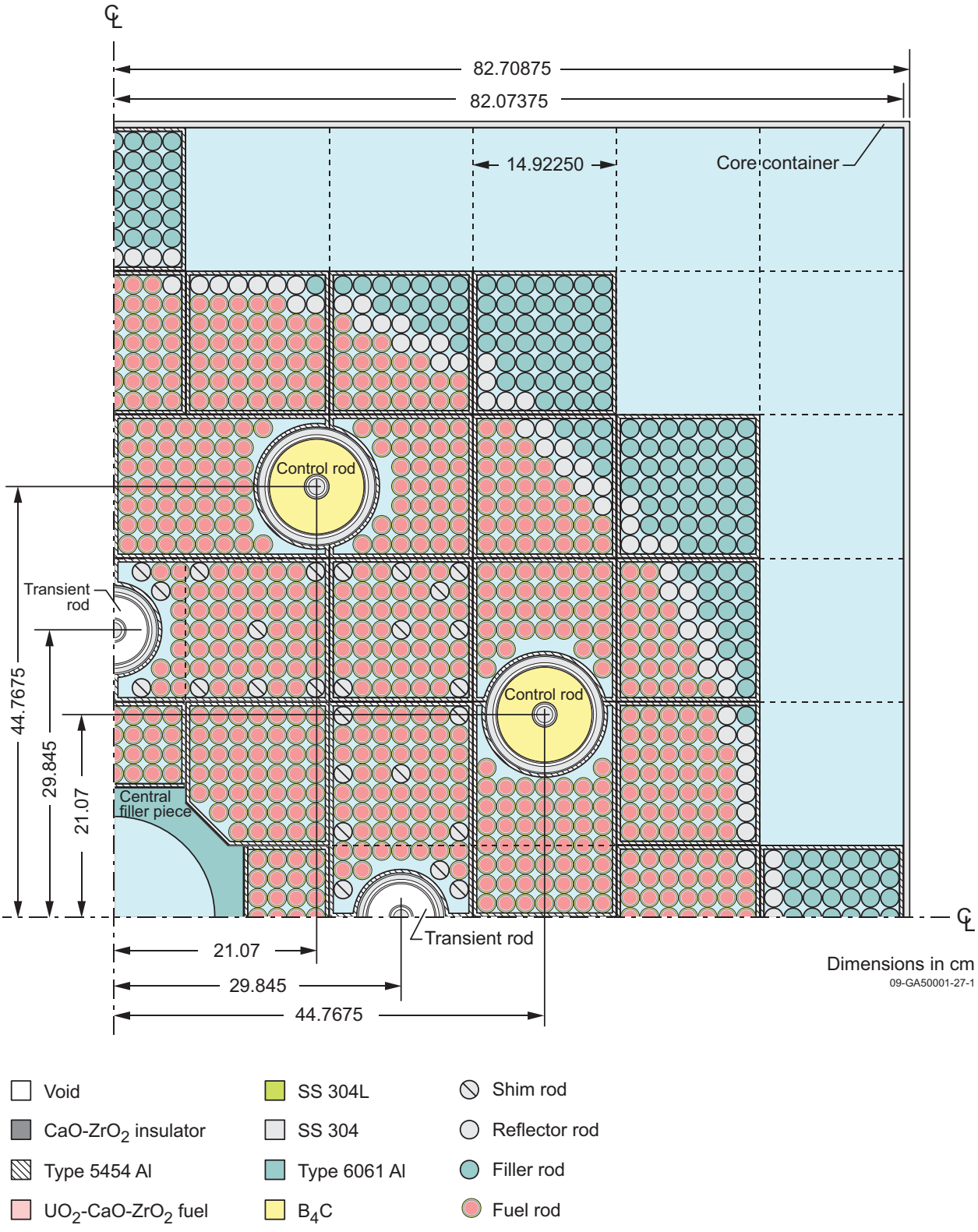

Figure 20. Positive Quadrant of Test 1 Model, Radial View, 15 cm Elevation.

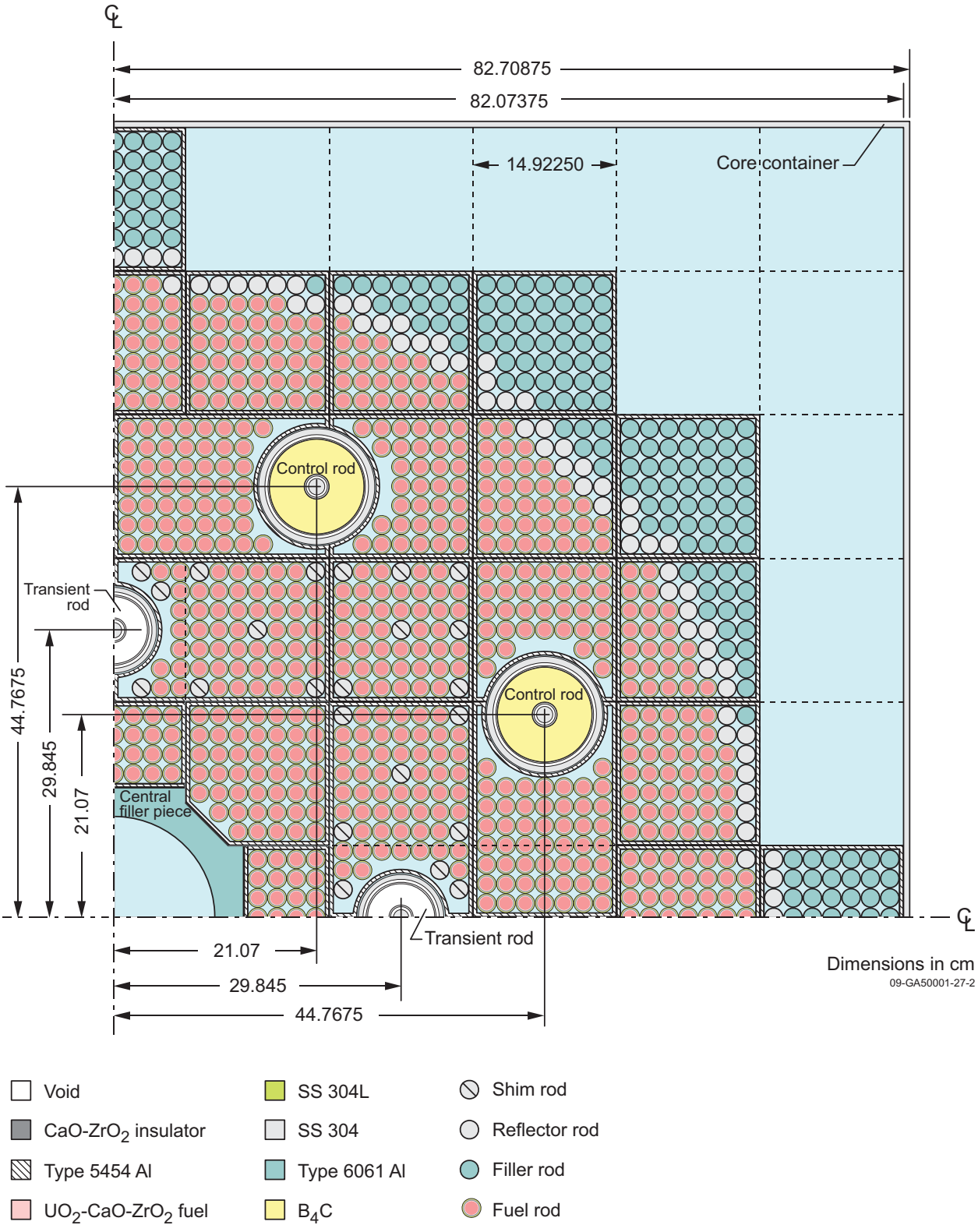

Figure 21. Positive Quadrant of Test 2 Model, Radial View, 15 cm Elevation.

The following simplifications were introduced to the model:

- IPT mockup has been removed, as described in Section 2.1.1, introducing a correction of 660 ± 35 pcm for Test 1, and 650 ± 35 pcm for Test 2.
- Helium and air are modeled as void.
- The reactor's 40 filler elements are modeled as water. Seven elements each contain one test instrument and 33 elements are empty. Instrumented elements are negligible for reasons previously described in Section 2.1.1. In addition to those reasons, an empty filler element is negligible because the space it occupies has more than 95 vol. % water and less than 5 vol. % Type 6061 aluminum. The empty element is indistinguishable from water given their relative densities and similar, low, thermal cross sections.
- Items with little mass and volume are neglected completely. The volume such an item occupies is either eliminated or filled with the material modeled around the neglected item. Such items include rod restraining bolts, captive strips, compression springs, and spacer blades in rods and assemblies, and much larger items outside the active core.
- The exact physical structure of perforated items, and of items outside the core container box, is neglected. Such structures are approximated with a homogeneous mixture of water and solid material, based on estimated relative volumes as described in Section 2.1.8. All such structures are outside the active core, except the mounting plate near the bottom of each in-pile rod assembly.
- The bearing spring and bearing spool are not completely defined in the references. The bearing spring is considered to have negligible effect on the multiplication factor and is removed from the model in this evaluation. The bearing spool is modeled as two components: a 0.79375-cm-thick, 1.42875-cm-diameter disc representing the cup shaped bearing spool base, and a 10.95375-cm-high, 1.19126-cm-inner-diameter, 1.42875-cm-outer-diameter cylindrical shell, representing the bearing spool wall. To take into account the central cavity in the cup shaped bearing spool base, the bearing spool base thickness was reduced from 0.79502 cm to 0.79375 cm, changing the inner length of the bearing spool from 10.95248 cm to 10.95375 cm.
- The upper end cap, insulator, springs and drive mechanisms of the control rods are above the core and are not included in the model. The bottom mechanical stop and other components inside the air shroud tube below the core are also not included in the model.

Aside from the IPT mockup removal, all these modifications are considered to have negligible effect in k_{eff}, compared to the experimental uncertainty.

3.2 Dimensions

3.2.1 Fuel Rods – Figure 22 and Figure 23 respectively show radial and axial views of the fuel rod modeled with dimensions and material identities. All components are modeled as concentric cylinders, neglecting the compression spring, mounting hardware, and geometry of handling components.

The active region of fuel rods is composed of a 91.44-cm-long, 0.70993-cm-radius UO_2-CaO-ZrO_2 ceramic fuel, surrounded by a 0.758825-cm-radius gap (modeled as void), a 97.79-cm-long, 0.880745-cm-radius CaO-ZrO2 ceramic insulator, a 0.88138-cm-outer-radius gap (modeled as void), and a 0.95377-cm-outer-radius Type 304L stainless steel clad.

Total fuel length is 120.65 cm. From the bottom the fuel pin includes a 2.936875-cm-long Type 304 L stainless steel bottom cap, the active region of the core, a Type 304 L stainless steel bearing spool composed of a 0.79375-cm-thick, 1.42875-cm-diameter disc representing the bearing spool base, and a 10.95375-cm-high, 1.19126-inner-diameter, 1.42875-outer-diameter cylindrical shell representing the bearing spool wall, and a 3.730625-cm-long Type 304 L stainless steel top end cap.

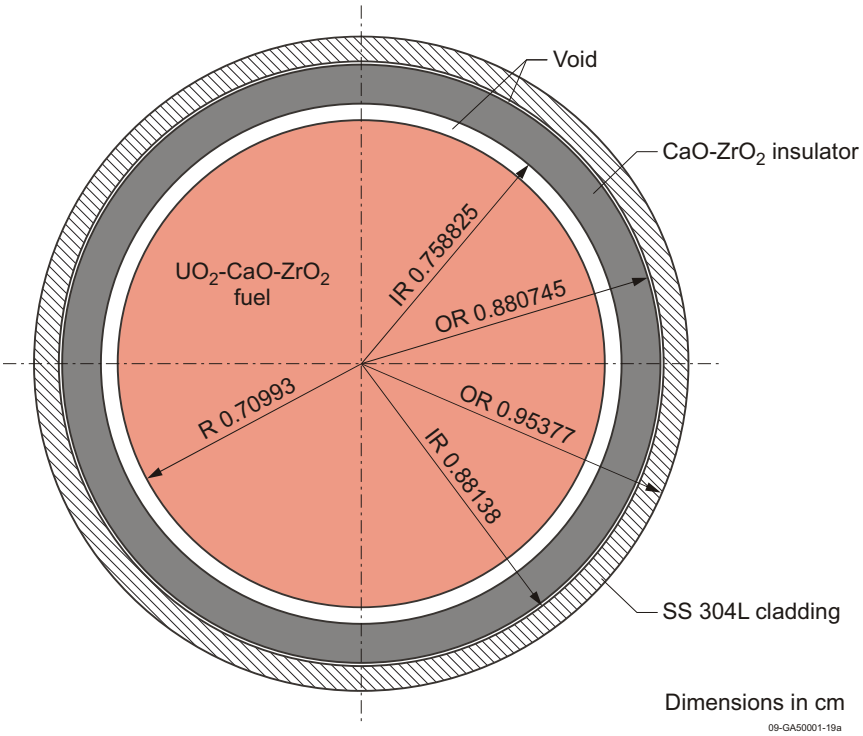

Figure 22. Fuel Rod Model, Radial View, 0 cm Elevation.

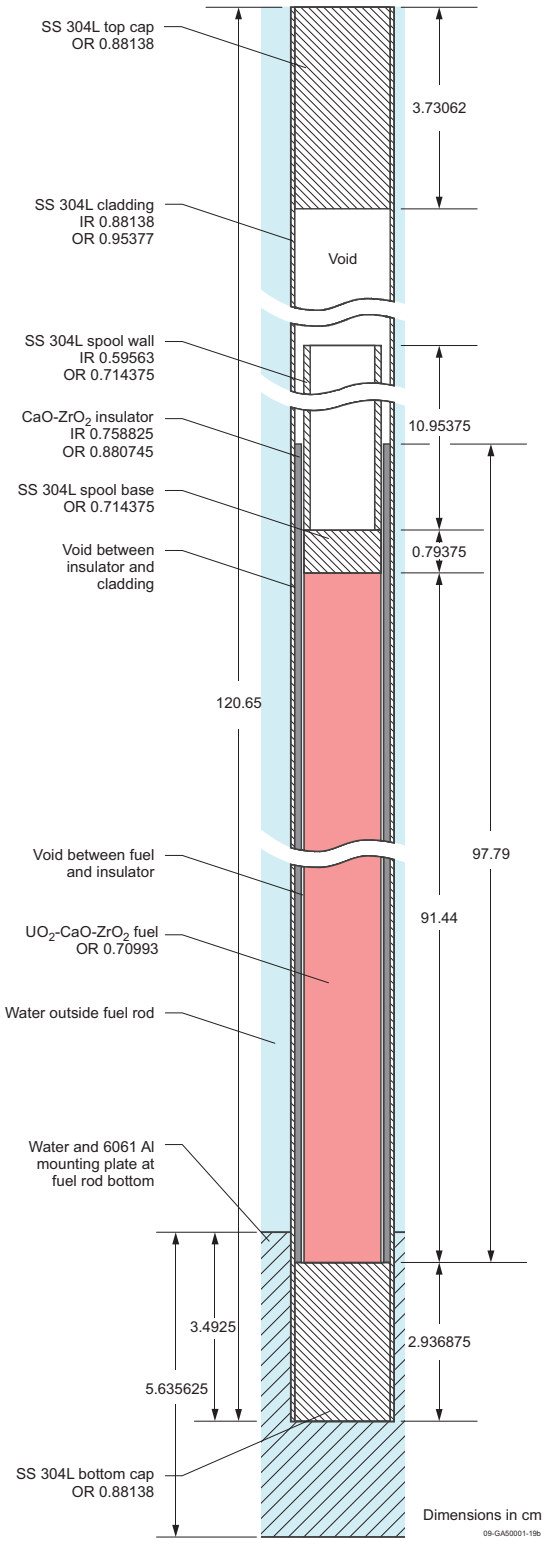

Figure 23. Fuel Rod Model, Axial View.

3.2.2 Shim, Reflector, and Filler Rods – Shim, reflector, and filler rods (Figure 24) are modeled as solid metal cylinders with a 0.95377 cm OR and 120.65 cm length. Shim and reflector rods are modeled as Type 304 stainless steel; filler rods are modeled as Type 6061 aluminum.

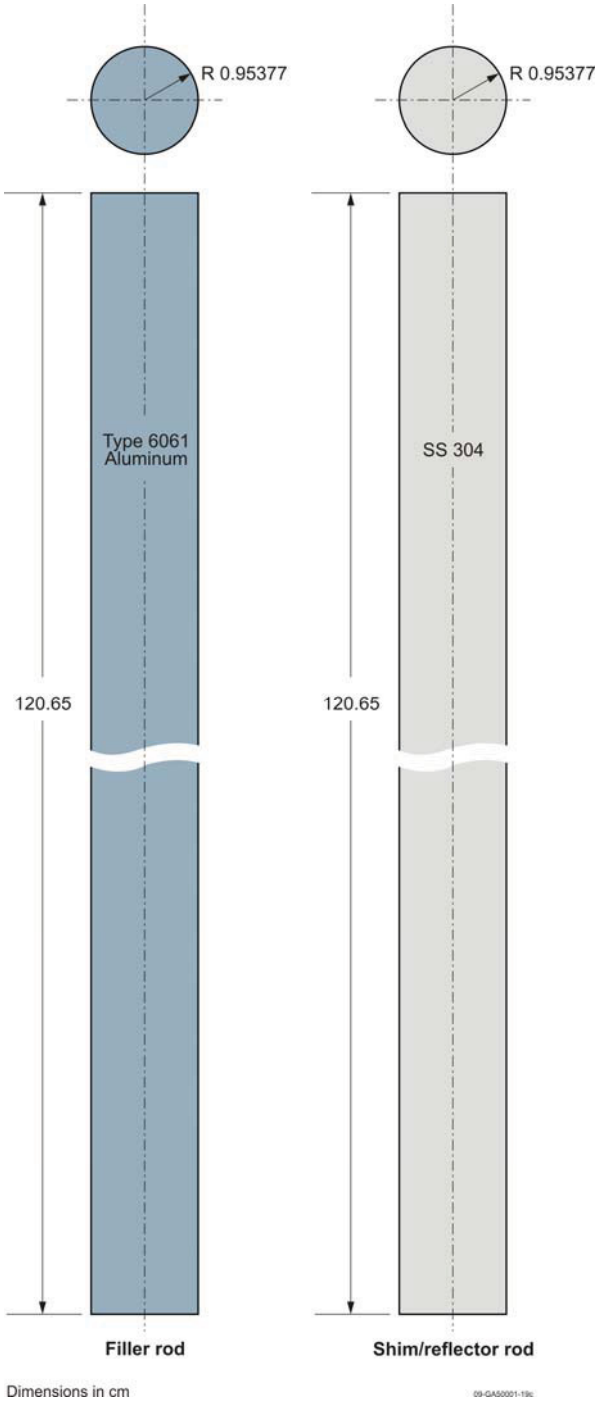

Figure 24. Fuel Rod Model, Axial View.

3.2.3 Assemblies – Six different types of assemblies are loaded into the reactor core, each one with different load patterns of fuel, shim, reflector and filler rods. All assemblies are 152.4 cm long, with the bottom edge at the -68.58 cm elevation (68.58 cm below the midplane of the active region of the core), contain 1.90754 cm OD rods with a 2.01168 cm square pitch and with their bottom edge at the -48.656875 cm elevation (19.923125 cm above the assembly bottom end), and contain a 5.635625 cm thick, water-and-6061 Al mounting plate with its bottom edge at the -50.80 cm elevation (17.78 cm above the assembly bottom end).

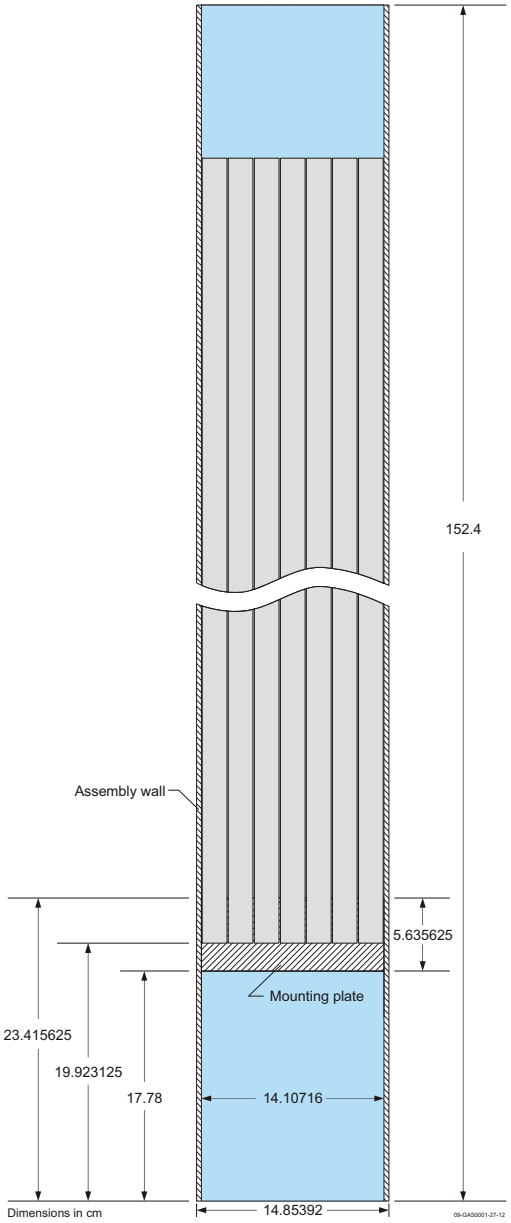

Figure 25. Assembly Axial Cross Section.

A description of each type of assembly follows.

49-rod assemblies: these assemblies (Figure 26) are composed of 49 rods in a 2.01168-cm-pitch, 7 x 7 pin array. The pin array is surrounded by 0.37338-cm-thick, Type 5454 aluminum walls, with an external dimension of 14.85392 cm. Center to center distance is 14.9225 cm, leaving a 0.06858 cm water gap between assembly walls. Loading pattern for specific 49-rod assemblies varies with position and some of them are different for Test 1 and Test 2.

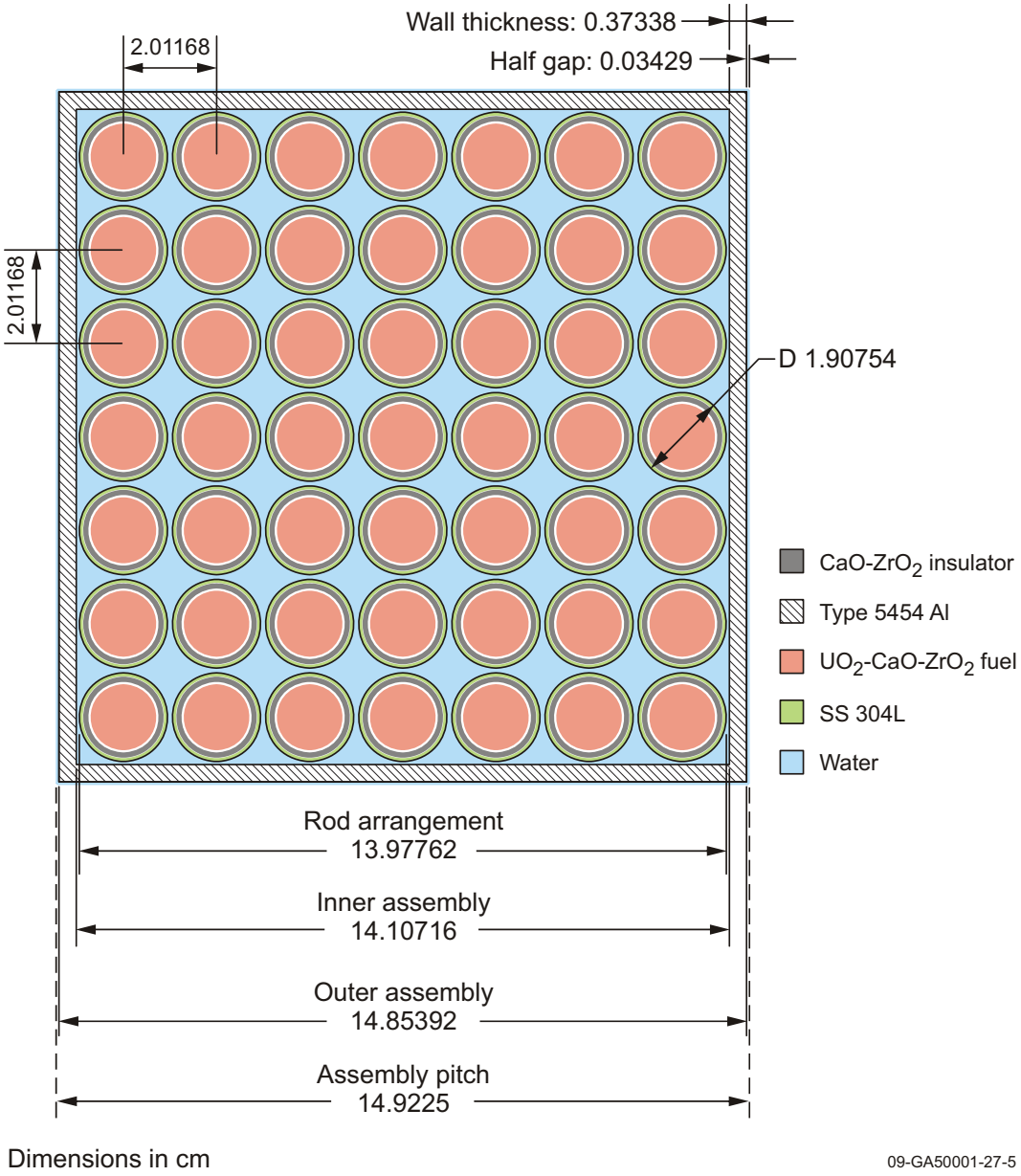

Figure 26. 49-rod Assembly at 0 cm Elevation.

28-rod assemblies: these assemblies (Figure 27) are located at 0°, 90°, 180° and 270° positions around the central test space. They have a 2.01168-cm-pitch, 4 x 7 pin array. The pin array is surrounded by 0.37338-cm-thick, Type 5454 aluminum walls, with an external dimension of 8.81888 x 14.85392 cm. A 0.06858 cm water gap separates these assemblies from neighboring assemblies, and from the central test space. All pins loaded in 28-rod assemblies are fuel rods in both Test 1 and Test 2.

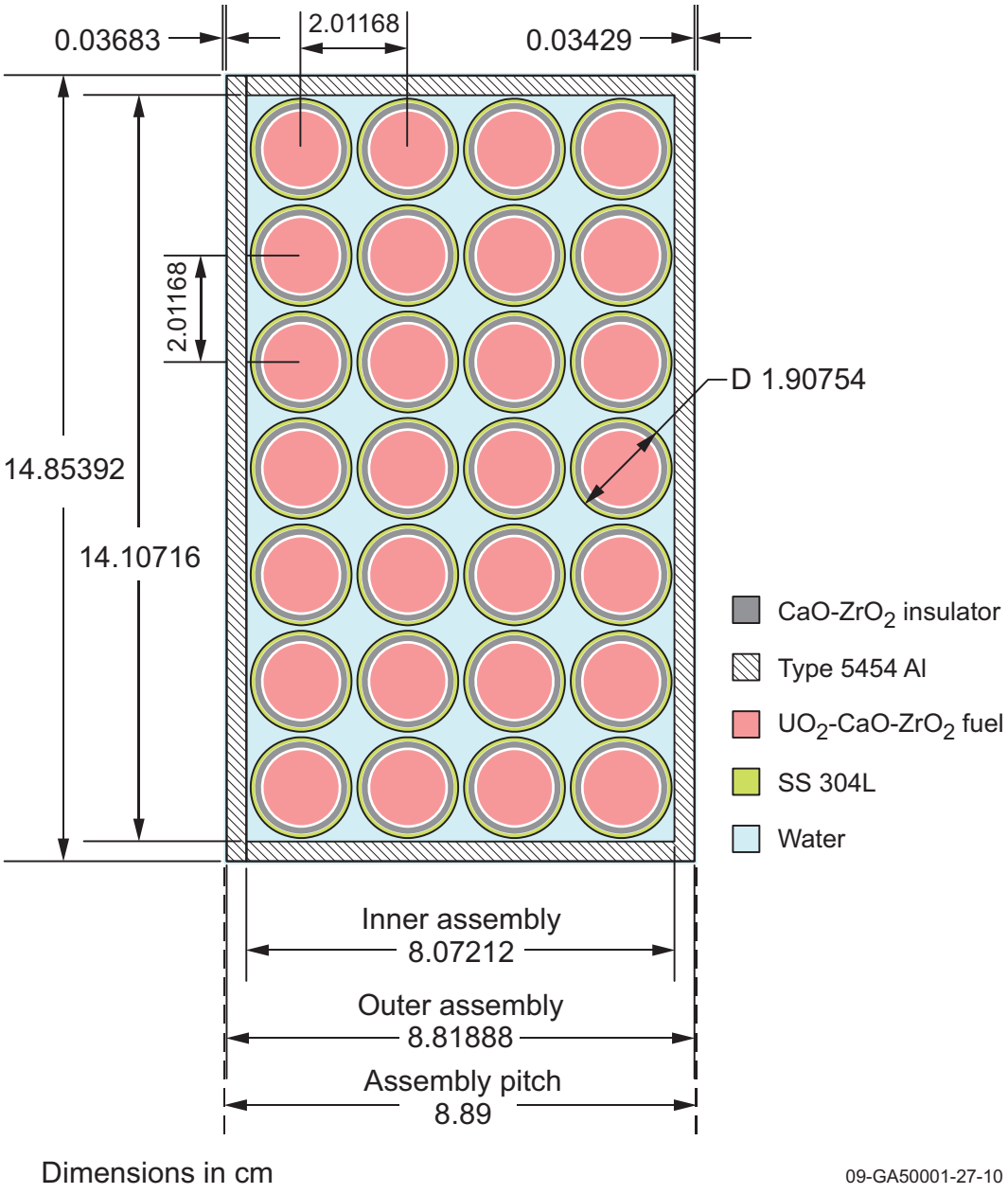

Figure 27. 28-rod Assembly at 0 cm Elevation.

46-rod assemblies: these assemblies (Figure 28) are located at 45°, 135°, 225° and 315° positions around the central test space. They are composed of 46 rods in a in a 2.01168-cm-pitch, 7 x 7 pin array where 3 rods were removed from one of its corners. The pin array is surrounded by 0.37338-cm-thick, Type 5454 aluminum walls, with an external dimension of 14.85392 cm along the 7-rod sides, 10.43792 cm along the 5-rod sides, and 6.24517 cm along the angled 3-rod side. All pins loaded in 46-rod assemblies are fuel rods in both Test 1 and Test 2.

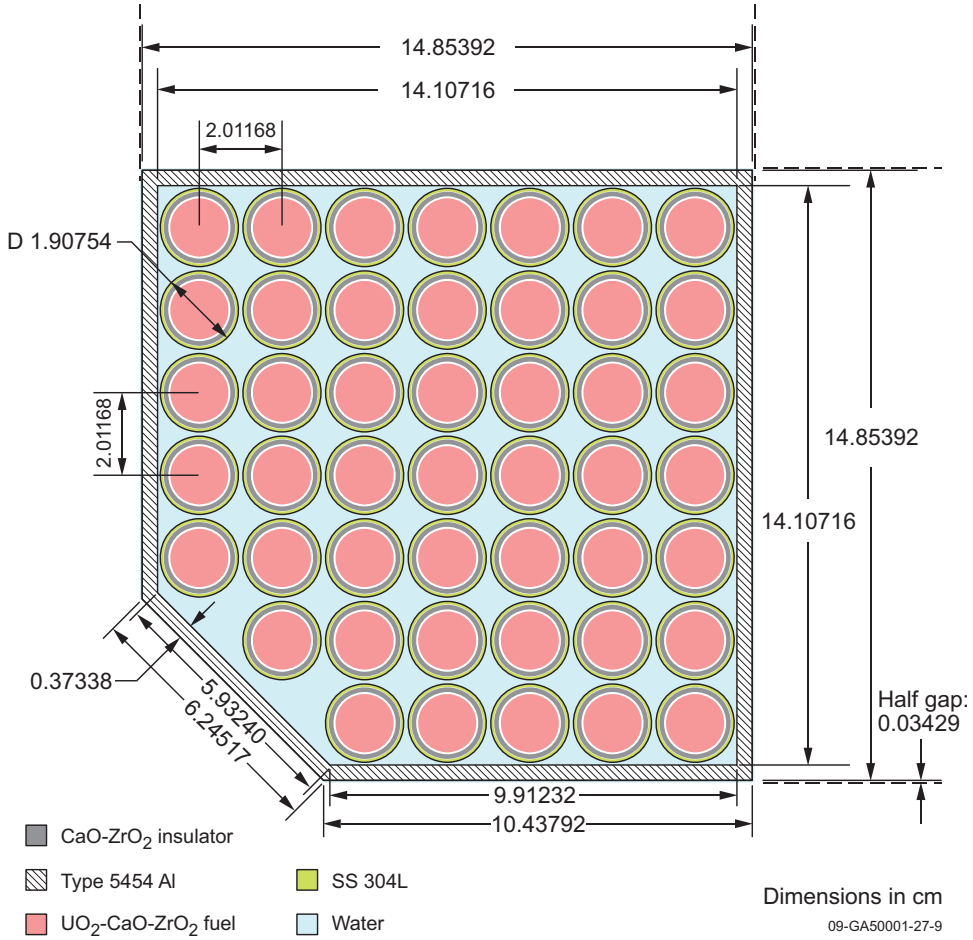

Figure 28. 46-rod Assembly at 0 cm Elevation.

62-rod assemblies: these assemblies (Figure 29) are composed of 62 rods in a 2.01168-cm-pitch, 7 x 10 pin array where 8 rods were removed to make space for one half of a transient rod shroud. The pin array is surrounded by 0.37338-cm-thick, Type 5454 aluminum walls, with an external dimension of 14.85392 cm along the 7-rod sides, 22.31517 cm along the 10-rod sides. The pin array is aligned to one of the 7-rod sides with a 1.39192 cm distance from the external side of the wall to the nearest pin center, the same distance than in the 49-rod assemblies. The other 7-rod side wall includes a concave, 0.37338-cm-thick, 4.6101-cm-inner-radius arc. This arched wall is centered along the midpoint of the 7-rod side at 0.03429 cm (half assembly gap) distance from the assembly wall. Some of the pin positions in the 62-rod assemblies are loaded with shim rods. Loading pattern varies from Test 1 to Test 2, but is the same for all 62-rod assemblies within each configuration.

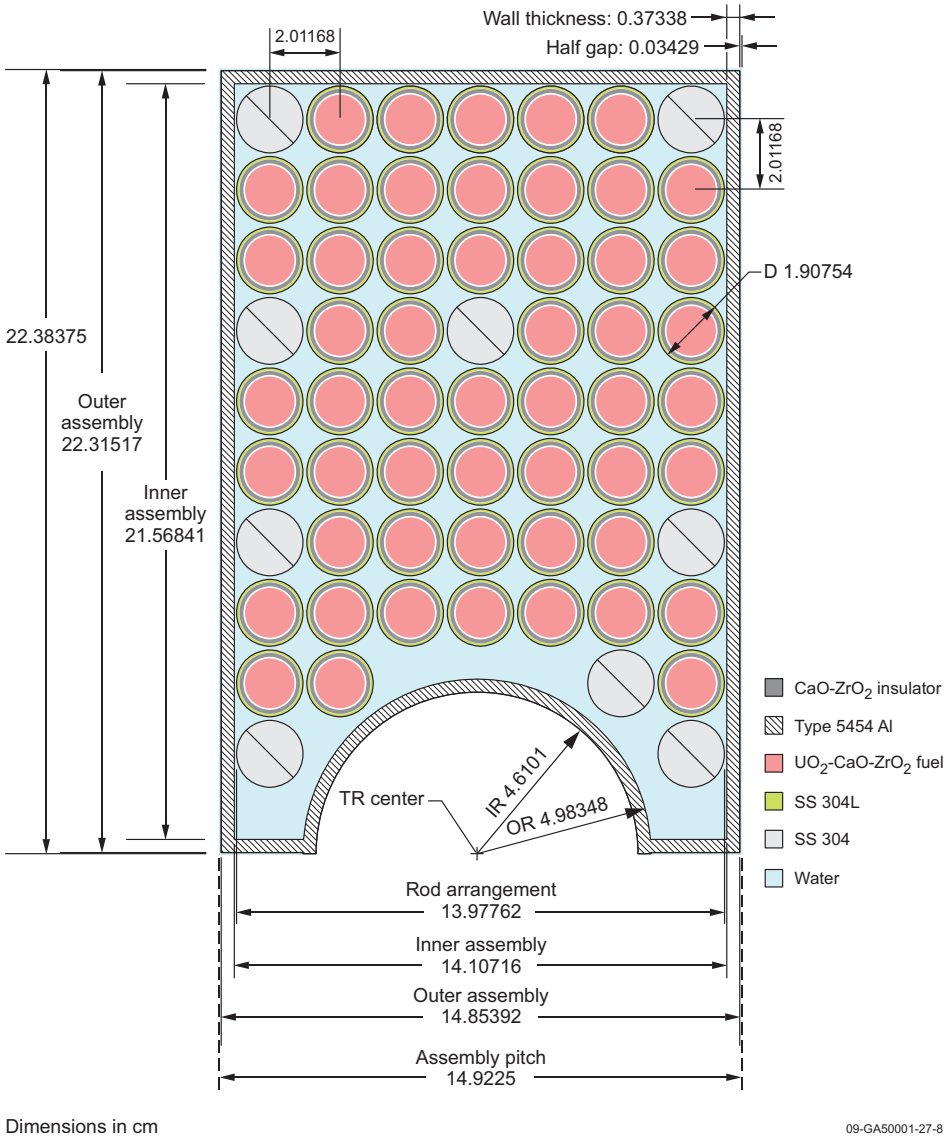

Figure 29. 62-rod Assembly at 0 cm Elevation, showing the Loading Pattern used in Test 1.

51-rod assemblies: these assemblies (Figure 30) are composed of 51 rods in a 2.01168-cm-pitch, 7 x 8 pin array where 5 rods were removed to make space for part of a control rod shroud. The pin array is surrounded by 0.37338-cm-thick, Type 5454 aluminum walls, with an external dimension of 14.85392 cm along the 7-rod sides, 22.31517 cm along the 8-rod sides. The pin array is aligned to one of the 7-rod sides with a 1.39192 cm distance from the external side of the wall to the nearest pin center, the same distance than in the 49-rod assemblies. The other 7-rod side wall includes a concave, 0.37338-cm-thick, 6.1595-cm-inner-radius arc. This arched wall is centered along the midpoint of the 7-rod side at 1.27946 cm distance from the assembly wall. All pins loaded in 51-rod assemblies are fuel rods in both Test 1 and Test 2.

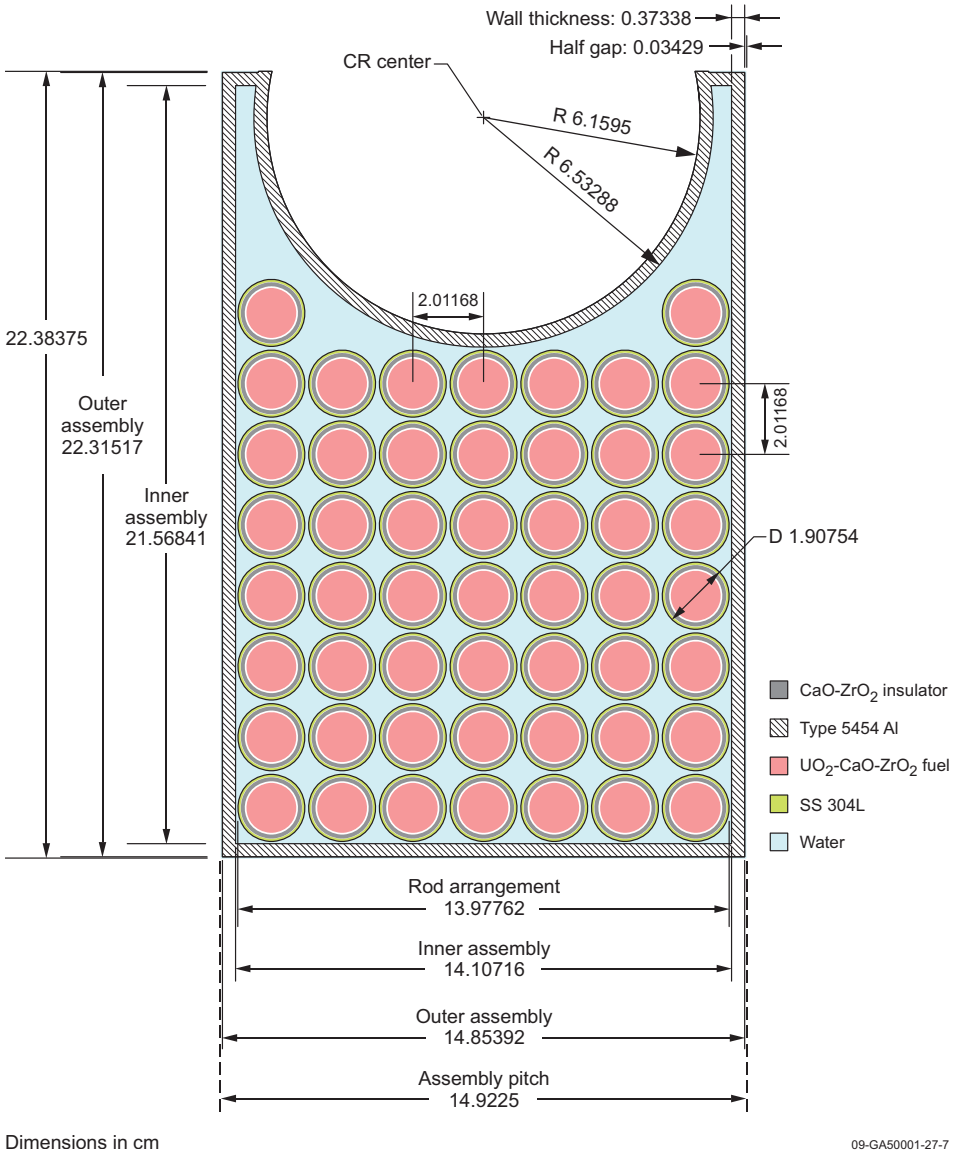

Figure 30. 51-rod Assembly at 0 cm Elevation.

34-rod assemblies: these assemblies (Figure 31) are composed of 34 rods in a 2.01168-cm-pitch, 7 x 6 pin array where 8 rods were removed to make space for part of a control rod shroud. The pin array is surrounded by 0.37338-cm-thick, Type 5454 aluminum walls, with an external dimension of 14.85392 cm along the 7-rod and the 6-rod sides. The pin array is aligned to one of the 7-rod sides with a 1.39192 cm distance from the external side of the wall to the nearest pin center, the same distance than in the 49-rod assemblies. The other 7-rod side wall includes a concave, 0.37338-cm-thick, 6.1595-cm-inner-radius arc. This arched wall is centered along the midpoint of the 7-rod side at 1.34804 cm distance from the assembly wall. All pins loaded in 34-rod assemblies are fuel rods in both Test 1 and Test 2.

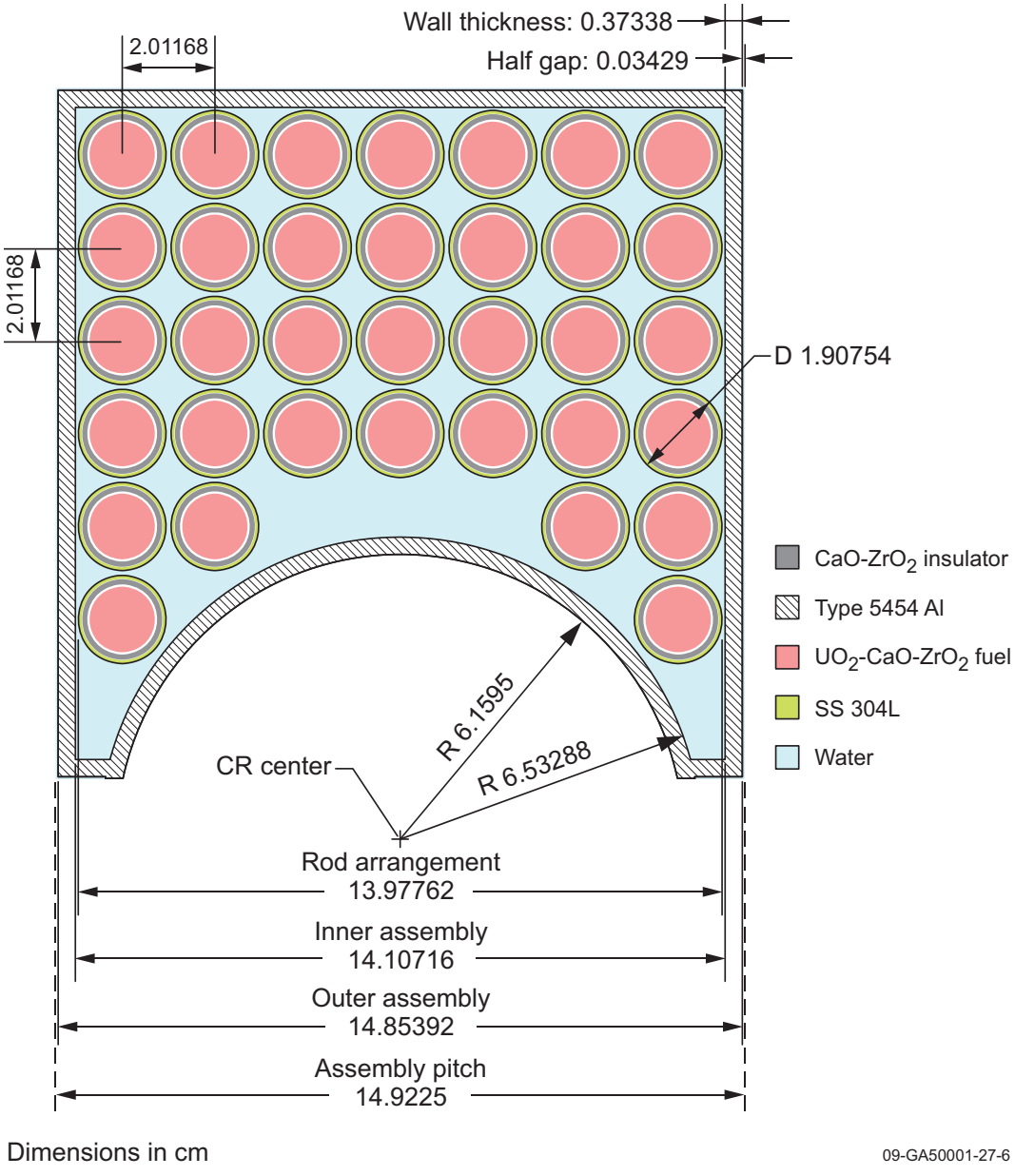

Figure 31. 34-rod Assembly at 0 cm Elevation.

3.2.4 Control and Transient Rods – Figures 32 and 33 respectively show control and transient rod models. Table 13 lists individual CR and TR coordinate positions with respect to the reactor model center, as described in Section 2.1.10.

From the inside out, the central region of the control rod model is composed by a Type 304 stainless steel tie rod, an annular inner air gap (modeled as void), a Type 304 stainless steel inner tube, an inner gap, an annular B_4C pellet, an outer gap, a Type 304 stainless steel outer tube, an annular outer air gap (modeled as void), a Type 6061 aluminum air-shroud tube, and a water gap. Outside this water gap is the Type 5054 aluminum assembly wall. Above the absorber region a 0.2667-cm-thick, 1.27-cm-inner-radius, 4.95554-cm-outer-radius, stainless steel plate represents the top closure plate, and a 1.27-cm-thick, 1.27-cm-inner-radius, 4.95554-outer-radius, supermica 620 plate represents the insulator. On the bottom of the absorber region a 0.9525-cm-thick, 5.08-cm-outer-radius plate represents the bottom end cap. The Type 6061 aluminum air shroud tube is modeled continuous from the bottom to the top of the reactor vessel. The tie rod starts at the bottom end cap and extends to the top of the reactor vessel.

Similarly, the transient rod model is composed of an inner Type 304 stainless steel tie rod, surrounded by an annular cooling air gap (modeled as void), a Type 304 stainless steel inner tube, an inner gap, an annular B_4C pellet, an outer gap, a Type 304 stainless steel outer tube, an outer cooling air gap, a Type 6061 aluminum air-shroud tube, and a water gap. Outside this gap is the Type 5054 aluminum assembly wall. Above the absorber region of the transient rod a 1.7145-cm-thick, 1.27-cm-inner-radius, 3.48615-cm-outer-radius supermica 620 plate represents the insulator, and a 0.635-cm-thick, 1.27-cm-inner-radius, 3.48615-cm-outer-radius Type 304 stainless steel plate represents the top closure plate and the spring retainer. Below the absorber region, a 0.9525-cm-thick, 3.65125-cm-outer-radius stainless steel plate represents the bottom closure plate. The tie rod starts at the bottom end cap and extends to the top of the reactor vessel.

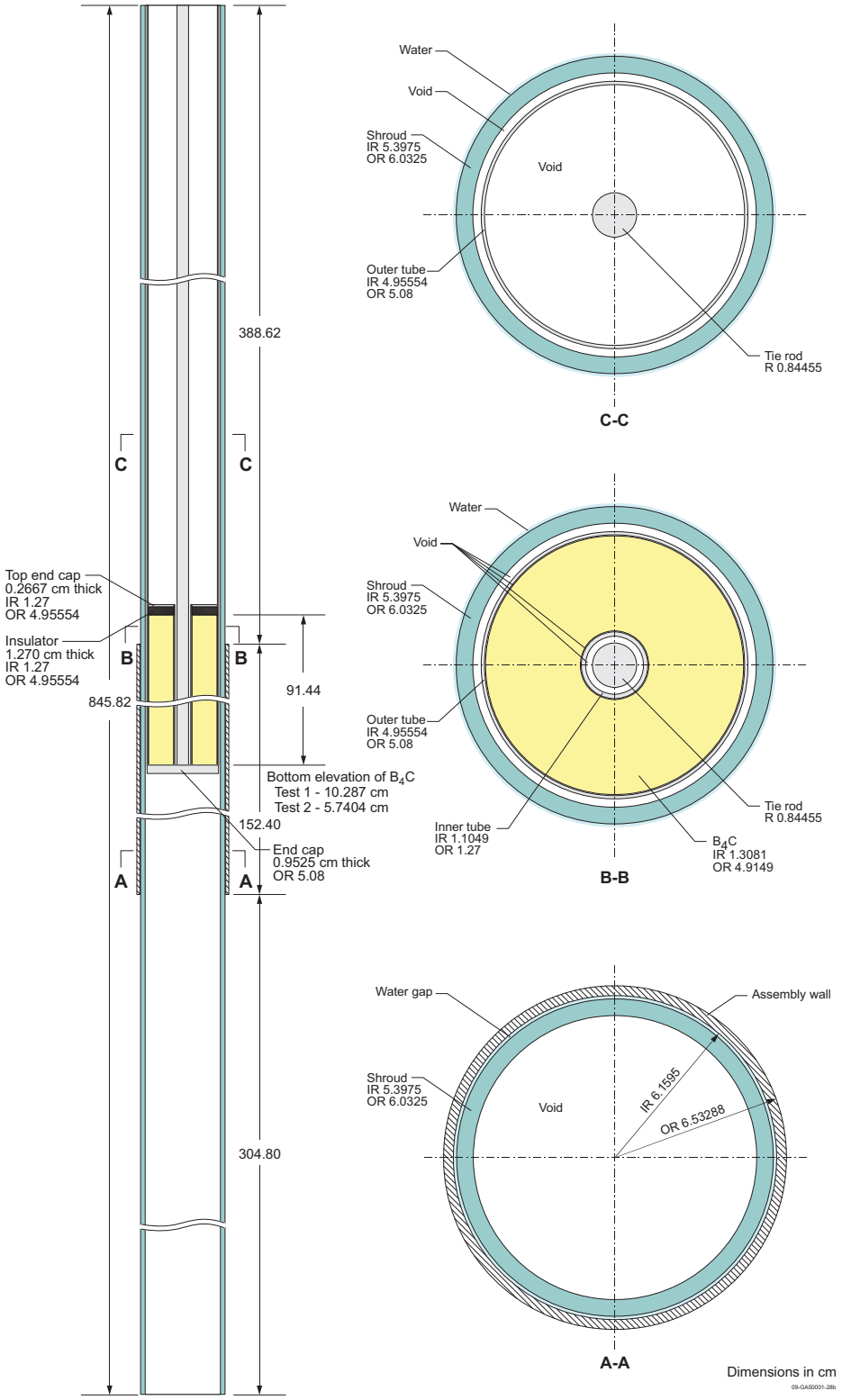

Figure 32. Control Rod Model, 15 cm Elevation.

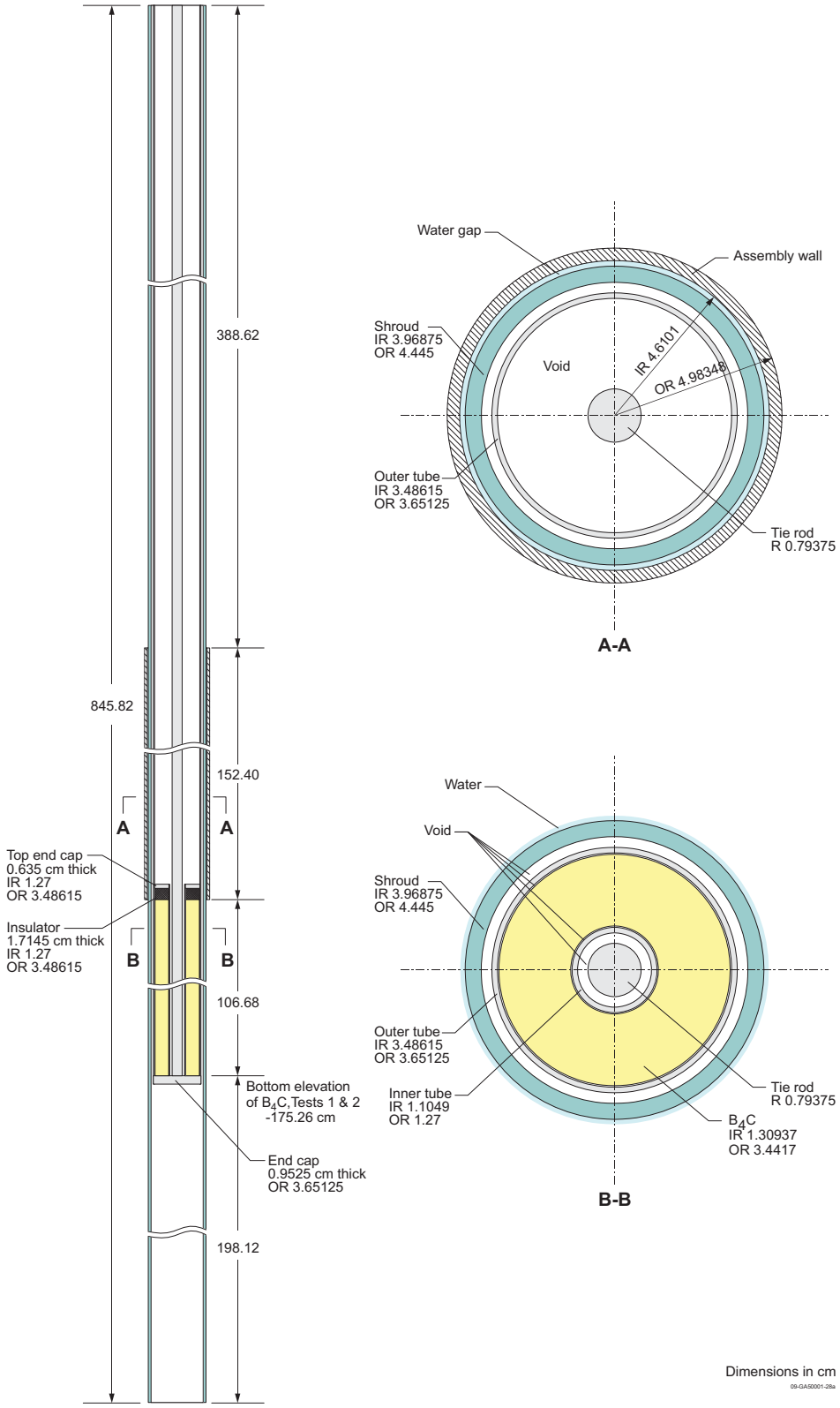

Figure 33. Transient Rod Model, -70 cm Elevation.

Table 13. Absorber Rod Model Coordinates.

Absorber Rod Identifier	Tie Rod Center Coord.		B_4C Elevation (Test 1)		B_4C Elevation (Test 2)	
	X	Y	Bottom	Top	Bottom	Top
CR1	21.07	44.7675	10.287	101.727	5.7404	97.1804
CR2	44.7675	21.07	10.287	101.727	5.7404	97.1804
CR3	44.7675	-21.07	10.287	101.727	5.7404	97.1804
CR4	21.07	-44.7675	10.287	101.727	5.7404	97.1804
CR5	-21.07	-44.7675	10.287	101.727	5.7404	97.1804
CR6	-44.7675	-21.07	10.287	101.727	5.7404	97.1804
CR7	-44.7675	21.07	10.287	101.727	5.7404	97.1804
CR8	-21.07	44.7675	10.287	101.727	5.7404	97.1804
TR1	0	29.845	-175.26	-68.58	-175.26	-68.58
TR2	29.845	0	-175.26	-68.58	-175.26	-68.58
TR3	0	-29.845	-175.26	-68.58	-175.26	-68.58
TR4	-29.845	0	-175.26	-68.58	-175.26	-68.58

3.2.5 Test Space Components – Figure 34 shows the test space model. Test space components include the Type 6061 aluminum central filler piece and water inside 10.4775 cm radius test space.

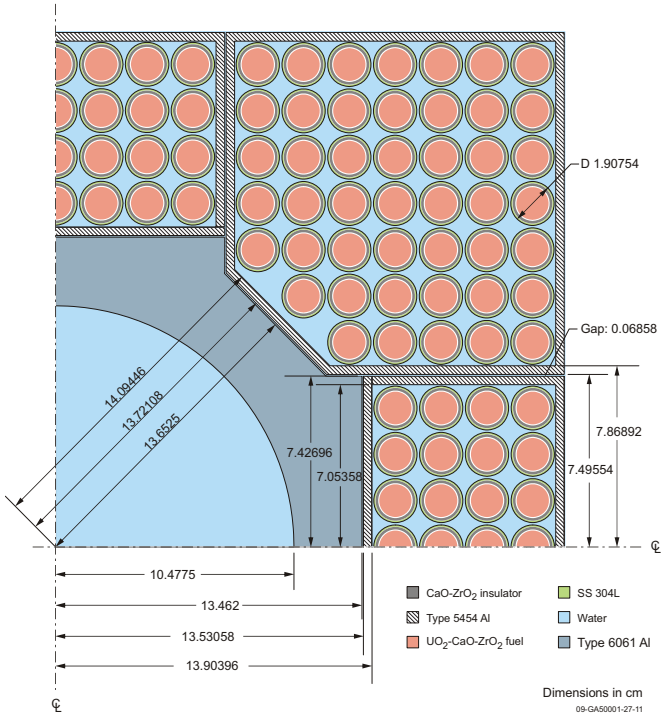

Figure 34. Model of Test Space Components.

3.2.6 Other Reactor Components – Already shown in Figure 17 and Figure 18, the PBF reactor model includes a simplified representation of items outside the PBF core. This representations is included because preliminary calculation results indicated some out-of-core items are not completely isolated from the core.[a]

The core support grid and orifice plates are represented by a 165.1475 cm wide square plate, 3.175 cm thick, with its bottom edge at the -71.755 cm elevation. Plate material is modeled as a homogenized mixture of 50 vol. % Type 7075 aluminum and 50 vol. % water to approximate water-flow holes in the metal plates and grid. The test space, four TRs, and eight CRs penetrate the modeled space, as implied in Figure 18. In the actual reactor the grid and plates are below the core container, but, for convenience, they are modeled as if they were the bottom of the core container, tightly fitting inside the core container walls. Below the core support grid, a 165.4175 cm square, 15.24-cm-thick plate represents the core support structure. Its material is a homogenized mixture of 25 vol. % SS 304 and 75 vol. % water to approximate the non-continuous nature of represented structures

The core container is represented by its stainless steel Type 304 box with outside dimensions of 165.4175 x 165.4175 x 156.5275 cm. The box's lower edge is modeled at the -71.755 cm elevation. The modeled box has 0.635 cm thick walls and top, but not bottom. With these dimensions, there is a 0.3175 cm water gap inside the box, between the box top and the top of assemblies. The test space, four TRs, and eight CRs penetrate the modeled box's top, as indicated in Figure 18. This model neglects the core container's exterior, radial ribs because they make up less than 5% of the volume they occupy.

An 165.4175 cm square plate, with its bottom edge at the 84.7725 cm elevation, represents the core hold down structure and other items above the core container. This plate is 15.24 cm thick. Its material is a homogenized mixture of 25 vol. % SS 304 and 75 vol. % water to approximate the non-continuous nature of represented structures. The test space, four TRs, and eight CRs penetrate the modeled plate, as implied in Figure 18.

The core support structure and other items below the core container are represented in the same manner as items above the core. However, this plate's bottom edge is modeled at the -86.995 cm elevation.

Water inside the reactor vessel is included in the reactor model. This water is contained in a 457.2-cm-diameter, 845.82-cm-height cylinder. The bottom edge of this cylinder is 373.38 cm below the midplane of the core.

[a] In the actual reactor, some out-of-core items are not isolated from the active core by at least 30 cm of water. This is partially because the active core design uses square pitch arrays and locates the core in a square-cross-section box. This design provided a close-enough approximation of a truly annular core.

3.3 Material Data

Table 14 through Table 20 list calculated nuclide densities used in final experiment models. These densities were calculated using nominal material descriptions from Sections 1.3 and 2.1.

All materials are assumed to be at full density and room temperature, with the exception of the homogenized materials described in Section 2.1.8.

Table 14. Fuel Matrix Composition [Density: 5.97 g/cm^3].

Element / Nuclide	Atom Density [atoms/cm barn]
^{234}U	6.2137 x10^{-06}
^{235}U	7.5524 x10^{-04}
^{238}U	3.3208 x10^{-03}
Zr	1.8031 x10^{-02}
O	4.9099 x10^{-02}
Ca	4.8725 x10^{-03}
^{10}B	1.1287 x10^{-06}
Total	7.6086 x10^{-02}

Table 15. Fuel Insulator Composition [Density: 4.70 g/cm^3].

Element	Atom Density [atoms/cm barn]
Zr	2.0443 x10^{-02}
O	4.6438 x10^{-02}
Ca	5.5520 x10^{-03}
Total	7.2433 x10^{-02}

Table 16. Aluminum Alloys and Mixtures Composition.

Element	Atom Density [atoms/cm barn]			
	Solid 5454 Al (2.69 g/cm^3)	**Solid 6061 Al (2.69 g/cm^3)**	**Perforated 6061 Al – Water Mixture (1.99 g/cm^3)**	**Perforated 7075 Al – Water Mixture (1.90 g/cm^3)**
H	-	-	2.7718 x10^{-02}	3.3283 x10^{-02}
O	-	-	1.3859 x10^{-02}	1.6641 x10^{-02}
Al	5.7532 x10^{-02}	5.8457 x10^{-02}	3.4116 x10^{-02}	2.7876 x10^{-02}
Mg	1.7996 x10^{-03}	6.6651 x10^{-04}	3.8897 x10^{-04}	8.6565 x10^{-04}
Ti	3.3833 x10^{-05}	1.1842 x10^{-05}	6.9108 x10^{-06}	1.7577 x10^{-05}
Cr	3.8944 x10^{-05}	6.2310 x10^{-05}	3.6364 x10^{-05}	3.7227 x10^{-05}
Mn	2.2115 x10^{-04}	2.2115 x10^{-05}	1.2906 x10^{-05}	2.2978 x10^{-05}
Fe	5.8014 x10^{-05}	1.0152 x10^{-04}	5.9249 x10^{-05}	3.7674 x10^{-05}
Cu	1.2746 x10^{-05}	6.3731 x10^{-05}	3.7194 x10^{-05}	2.1190 x10^{-04}
Zn	3.0967 x10^{-05}	3.0967 x10^{-05}	1.8072 x10^{-05}	7.2074 x10^{-04}
Si	7.2099 x10^{-05}	3.4607 x10^{-04}	2.0197 x10^{-04}	5.9930 x10^{-05}
Total	5.9800 x10^{-02}	5.9762 x10^{-02}	7.6454 x10^{-02}	7.9774 x10^{-02}

Table 17. Stainless Steel Composition.

Element	Atom Density [atoms/cm barn]		
	Solid SS 304L (8.00 g/cm^3)	**Solid SS 304 (8.00 g/cm^3)**	**SS 304 – Water Mixture (2.75 g/cm^3)**
H	-	-	4.9924 x10^{-02}
O	-	-	2.4962 x10^{-02}
Fe	5.9909 x10^{-02}	6.0535 x10^{-02}	1.5134 x10^{-02}
C	6.0166 x10^{-05}	1.6044 x10^{-04}	4.0111 x10^{-05}
Cr	1.7604 x10^{-02}	1.7604 x10^{-02}	4.4011 x10^{-03}
Mn	8.7693 x10^{-04}	8.7693 x10^{-04}	2.1923 x10^{-04}
Ni	8.2087 x10^{-03}	7.5930 x10^{-03}	1.8983 x10^{-03}
P	3.4997 x10^{-05}	3.4997 x10^{-05}	8.7492 x10^{-06}
Si	8.5768 x10^{-04}	8.5768 x10^{-04}	2.1442 x10^{-04}
S	2.2534 x10^{-05}	2.2534 x10^{-05}	5.6334 x10^{-06}
Total	8.7575 x10^{-02}	8.7685 x10^{-02}	9.6808 x10^{-02}

Table 18. Boron Carbide Composition[(a)] [Density: 2.505 g/cm^3].

Element / Nuclide	Atom Density [atoms/cm barn]
^{10}B	2.1732 x10^{-02}
^{11}B	8.7473 x10^{-02}
C	2.7301 x10^{-02}
Total	1.3651x10^{-01}

(a) Computed using a ^{10}B abundance of 19.9% (Section 2.2.4).

Table 19. Water Composition [Density: 0.99566 g/cm^3].

Element	Atom Density [atoms/cm barn]
H	6.6566 x10^{-02}
O	3.3283 x10^{-02}
Total	9.9848 x10^{-02}

Table 20. Mica Composition [Density: 2.83 g/cm^3].

Element	Atom Density [atoms/cm barn]
H	8.5519 x10^{-03}
Al	1.2837 x10^{-02}
Si	1.2838 x10^{-02}
O	5.1345 x10^{-02}
K	4.2771 x10^{-03}
Total	8.9849 x10^{-02}

3.4 Temperature Data

Temperature for all components in both cases is set to be 30 ºC.

3.5 Experimental and Benchmark Model k_{eff}

The number of rods for each experiment is a value extrapolated to critical. Therefore, the experimental value for the effective multiplication factor is 1.0000. Removal of IPT mockup requires the introduction of a correction of +0.89 $ in the multiplication of the model, which is equivalent in Test 1 to +0.00660 ± 0.00035 and in Test 2 to +0.00650 ± 0.00035.The experimental uncertainties lead to a combined benchmark model uncertainty of 0.0060 in k_{eff}, as explained in Section 2.

Therefore, the benchmark k_{eff} is 1.0066 ± 0.0060 for Test 1, and 1.0065 ± 0.0060 for Test 2.

4.0 RESULTS OF SAMPLE CALCULATIONS

Table 21 summarizes calculation results using the MCNP5 input listed in Appendix A.

Cases 1 and 2 are evaluations of two critical experiments performed at PBF. The experiments are very similar and differ only in the number of fuel rods and the position of the control rods. It can be assumed the information in both cases is highly correlated and are included here to allow analysis of the parameters changed between experiments, but they should not be used as independent points in validations.

Results are within 1% of the benchmark value.

Table 21. Sample Calculation Results..

Code → (Cross Section Set) → Experiment No. ↓	**Benchmark**	**MCNP 5 ENDF/B VI.6**	**MCNP 5 ENDF/B VII (John Bess – INL)**
Test 1	1.0066 ± 0.0060	1.0091 ± 0.0002	1.0151 ± 0.0002
Test 2	1.0065 ± 0.0060	1.0083 ± 0.0003	1.0139 ± 0.0002

5.0 REFERENCES

1. L. A. Stephan. “Nuclear Startup and Statics for PBF Reactor,” internal report CI-1282, Idaho Falls, Idaho: Aerojet Nuclear Company, July 1974.

2. V. L. Putman. “MCNP Validation with PBF Reactor Core,” report INEEL/EXT-99-00687 Rev. 1, November 2002.

3. Aerojet Nuclear Company, *Final Safety Analysis Report for the Power Burst Facility*, ANCR-1011, in 2 parts, Idaho Falls, Idaho: Aerojet Nuclear Company, July 1971.

4. S. D. Wahnschaffe, “The Power Burst Facility (PBF) Driver Core Fuel Summary Report,” internal report INEL-96/301, LMITCO, September 1996. Inventory information is based on an internal PBF report, “PBF Enriched Uranium Inventory Report”, December 7, 1994, which was confirmed by Gregory D. Gerber, electronic mail message to Kraig M. Wendt and Valerie L. Putman, March 17, 1999, 2:30pm.

APPENDIX A: TYPICAL INPUT LISTINGS

A.1 MCNP Input Listings

The MCNP 5 input file used to compute the results shown in Section 4 for Operational Test 1 is listed here. The geometry and material description is based on the data provided in Section 3. MCNP was run with ENDF/B VI.6 cross section libraries and thermal scattering kernels for hydrogen in water at 293 K from the same library. Zinc was replaced by copper due to unavailability of cross section sets in the library. The model was run with 820 cycles of 12500 particles, discarding the first 20 cycles to allow source convergence.

```
MCNP ENDF/B VI.6  Input Listings for Test 1 of Table 21.

PBF Operational Loading Test 1 model (Test 2 commented)
c  Alexis Weir - Ignacio Marquez - Valerie Putman - Jun 2009.
c
c  CELL CARDS
c  rods
1    4   8.7575E-02   -4    7  -9          u=1   imp:n=1  $ fuel rod bottom end cap
2    4   8.7575E-02   -4    5  -6          u=1   imp:n=1  $ fuel rod top end cap
3    1   7.6086E-02   -1   -8   9          u=1   imp:n=1  $ fuel stack
4    0     (202 -2 8 -15):(-203 13 -201)   u=1   imp:n=1  $ gap
5    0                 1   -2   9   -8     u=1   imp:n=1  $ gap
6    3   7.2433E-02    2   -3   9  -15     u=1   imp:n=1  $ insulator
7    4   8.7575E-02 -202    8 -13          u=1   imp:n=1  $ bearing spool bottom
8    4   8.7575E-02 -202  203  13 -201     u=1   imp:n=1  $ bearing spool wall
10   0              -202  201 -5           u=1   imp:n=1  $ void above bearing spool
11   0              -200  202  -5  15      u=1   imp:n=1  $ gap above insulator (neglect spring)
12   0                 3 -200   9 -15      u=1   imp:n=1  $ insulator-clad gap
13   4   8.7575E-02  200   -4  -5   9      u=1   imp:n=1  $ clad
14   5   9.9848E-02   -4   -7              u=1   imp:n=1  $ water directly below rod
15   5   9.9848E-02   -4    6              u=1   imp:n=1  $ water directly above rod
16  10   7.6454E-02    4  -16  17          u=1   imp:n=1  $ hold-down plate
17   5   9.9848E-02    4   16              u=1   imp:n=1  $ surrounding water above mounting plate
18   5   9.9848E-02    4  -17              u=1   imp:n=1  $ surrounding water above mounting plate
c
21  10   7.6454E-02  -999  -16  17         u=2   imp:n=1  $ hold-down plate side structure
22   5   9.9848E-02  -999   16             u=2   imp:n=1  $ water cell above mounting plate
23   5   9.9848E-02  -999  -17             u=2   imp:n=1  $ water cell below mounting plate
c
25   5   9.9848E-02  -999                  u=9   imp:n=1  $ all-water cell
c
31   6   5.9762E-02   -4   -6   7          u=3   imp:n=1  $ aluminum filler rod
32   5   9.9848E-02   -4   -7              u=3   imp:n=1  $ water directly below rod
33   5   9.9848E-02   -4    6              u=3   imp:n=1  $ water directly above rod
34  10   7.6454E-02    4  -16  17          u=3   imp:n=1  $ hold-down plate
35   5   9.9848E-02    4   16              u=3   imp:n=1  $ surrounding water above mounting plate
36   5   9.9848E-02    4  -17              u=3   imp:n=1  $ surrounding water below mounting plate
c
41   7   8.7685E-02   -4   -6   7          u=4   imp:n=1  $ steel shim/reflector rod
42   5   9.9848E-02   -4   -7              u=4   imp:n=1  $ water directly below rod
43   5   9.9848E-02   -4    6              u=4   imp:n=1  $ water directly above rod
44  10   7.6454E-02    4  -16  17          u=4   imp:n=1  $ hold-down plate
45   5   9.9848E-02    4   16              u=4   imp:n=1  $ surrounding water above mounting plate
46   5   9.9848E-02    4  -17              u=4   imp:n=1  $ surrounding water below mounting plate
c
51   7   8.7685E-02  -21   32              u=6   imp:n=1  $ TR tie rod
52   0                21  -22   32         u=6   imp:n=1  $ TR innermost gap
53   7   8.7685E-02   22  -23  -35  32     u=6   imp:n=1  $ TR inner tube
54   0                23  -24  -31  32     u=6   imp:n=1  $ TR 2nd gap
55   9   1.3651E-01   24  -25  -31  32     u=6   imp:n=1  $ TR B4C
56   0                25  -26  -31  32     u=6   imp:n=1  $ TR 3rd gap
57   0                22  -26   35         u=6   imp:n=1  $ TR above meat
58   0               -27  -67              u=6   imp:n=1  $ TR below meat
59   7   8.7685E-02   26  -27   32         u=6   imp:n=1  $ TR outer tube and driver tube
60   0                27  -29              u=6   imp:n=1  $ TR gap to shroud
61   6   5.9762E-02   29  -30              u=6   imp:n=1  $ shroud tube
```

```
62   5   9.9848E-02   30  -33             u=6   imp:n=1  $ water gap around TR
63   8   5.9800E-02   33 -119  31         u=6   imp:n=1  $ assembly walls nearest to TR
64   5   9.9848E-02   33
                      (119 -929:935:-930) u=6   imp:n=1  $ water above and below assembly wall
65  13   8.9849E-02   31 -20 23 -26       u=6   imp:n=1  $ TR top supermica insulator
66   7   8.7685E-02   20 -35 23 -26       u=6   imp:n=1  $ TR top closure plate
67  11   7.9774E-02   33 930 -31          u=6   imp:n=1  $ core support plate below assembly wall
68   7   8.7685E-02   33 929 -935         u=6   imp:n=1  $ top core container above assembly wall
69   7   8.7685E-02   -32 67 -27          u=6   imp:n=1  $ TR bottom closure plate
c
71   7   8.7685E-02  -36   47            u=7   imp:n=1  $ CR tie rod
72   0                36  -37   47        u=7   imp:n=1  $ CR innermost gap
73   7   8.7685E-02   37  -38  -61  47    u=7   imp:n=1  $ CR inner tube
74   0                38  -39  -46  47    u=7   imp:n=1  $ CR 2nd gap
76   9   1.3651E-01   39  -40  -46  47    u=7   imp:n=1  $ CR B4C
77   0                40  -41  -46  47    u=7   imp:n=1  $ CR 3rd gap
78   0                37  -41   61        u=7   imp:n=1  $ CR above meat
79   0               -42  -48             u=7   imp:n=1  $ CR below meat
80   7   8.7685E-02   41  -42   47        u=7   imp:n=1  $ CR outer tube and driver tube
81   0                42  -44             u=7   imp:n=1  $ CR outer air gap
82   6   5.9762E-02   44  -45             u=7   imp:n=1  $ shroud tube
83   5   9.9848E-02   45  -50             u=7   imp:n=1  $ water gap around CR
84   8   5.9800E-02   50 -119  31         u=7   imp:n=1  $ assembly walls nearest CR
85   5   9.9848E-02   50
                      (119 -929:935:-930) u=7   imp:n=1  $ water above and below assembly wall
86   7   8.7685E-02   48  -47  -42        u=7   imp:n=1  $ CR bottom closure plate
87  11   7.9774E-02   50 930 -31          u=7   imp:n=1  $ core support plate below assembly wall
88   7   8.7685E-02   50 929 -935         u=7   imp:n=1  $ top core container above assembly wall
89  13   8.9849E-02   46 -60 -41  23      u=7   imp:n=1  $ CR top insulator
90   7   8.7685E-02   60 -61 -41  23      u=7   imp:n=1  $ CR top closure plate
c
c  test space
91   5   9.9848E-02        -804               u=10  imp:n=1  $ IPT mockup removed
92   6   5.9762E-02 ((-805 -807 -809):
                      (809 -805 -117):
                      (809 -807 -115)) 804    u=10  imp:n=1  $ TS central filler piece
93   8   5.9800E-02  ((816 -115):(814 -117):
                      (131  132 818))
                      -119   31               u=10  imp:n=1  $ walls of adjacent assemblies
94   5   9.9848E-02 ((-814 -816 -818):
                      (818 -814 -132):
                      (818 -816 -131))
                       804  #92 -119 31       u=10  imp:n=1  $ water gap
95   5   9.9848E-02  ((-826 115 -131 816):
                      (-824 -132 117 814))
                                 -119 31      u=10  imp:n=1  $ water gap
96   5   9.9848E-02  (936:-929 119:-937)
                     (805:(117 809 115):807)  u=10  imp:n=1 $ water near test space
97   7   8.7685E-02  (-935 929)
                      (805:(117 809 115):807) u=10  imp:n=1 $ core container next to test space
98  12   9.6808E-02  (-936 935)
                      (805:(117 809 115):807) u=10  imp:n=1 $ core hold down structure to test
space
99  11   7.9774E-02  (-31 930)
                      (805:(117 809 115):807) u=10  imp:n=1 $ support plate to test space
100 12   9.6808E-02  (-930 937)
                      (805:(117 809 115):807) u=10  imp:n=1 $ core support to test space
c
c  assemblies/elements
104  0            -101  102 -103  104  lat=1           u=13  imp:n=1  $ 28-rod array
                  fill=-4:4 -4:4 0:0
                  2 2 2 2 2 2 2 2 2
                  2 2 2 2 2 2 2 2 2
                  2 2 2 2 2 2 2 2 2
                  2 2 2 2 2 2 2 2 2
                  2 1 1 1 1 1 1 1 2
                  2 1 1 1 1 1 1 1 2
                  2 1 1 1 1 1 1 1 2
                  2 1 1 1 1 1 1 1 2
                  2 2 2 2 2 2 2 2 2
105  5   9.9848E-02  -111  112 -113  114       fill=13  u=14  imp:n=1  $ internals
```

```
106  8   5.9800E-02 (111:-112:113:-114)
                -115  116 -117  118                u=14  imp:n=1  $ walls
107  5   9.9848E-02  (115:-116:117:-118)           u=14  imp:n=1  $ surrounding water
c
108  0           -101 102 -103 104  lat=1           u=15  imp:n=1  $ 46-rod array
                 fill=-4:4 -4:4 0:0
                 2 2 2 2 2 2 2 2 2
                 2 2 2 1 1 1 1 1 2
                 2 2 1 1 1 1 1 1 2
                 2 1 1 1 1 1 1 1 2
                 2 1 1 1 1 1 1 1 2
                 2 1 1 1 1 1 1 1 2
                 2 1 1 1 1 1 1 1 2
                 2 1 1 1 1 1 1 1 2
                 2 2 2 2 2 2 2 2 2
109  5   9.9848E-02  -111  112 -113  114      fill=15  u=16  imp:n=1  $ internals
110  8   5.9800E-02 (111:-112:113:-114)
                -115  116 -117  118                u=16  imp:n=1  $ walls
111  5   9.9848E-02  (115:-116:117:-118)           u=16  imp:n=1  $ surrounding water
c
112  0           -101 102 -103 104  lat=1           u=17  imp:n=1  $ 28-rod array
                 fill=-4:4 -4:4 0:0
                 2 2 2 2 2 2 2 2 2
                 2 2 2 2 1 1 1 1 2
                 2 2 2 2 1 1 1 1 2
                 2 2 2 2 1 1 1 1 2
                 2 2 2 2 1 1 1 1 2
                 2 2 2 2 1 1 1 1 2
                 2 2 2 2 1 1 1 1 2
                 2 2 2 2 2 2 2 2 2
113  5   9.9848E-02  -111  112 -113  114      fill=17  u=18  imp:n=1  $ internals
114  8   5.9800E-02 (111:-112:113:-114)
                -115  116 -117  118                u=18  imp:n=1  $ walls
115  5   9.9848E-02  (115:-116:117:-118)           u=18  imp:n=1  $ surrounding water
c
201  0           -101 102 -103 104  lat=1           u=32  imp:n=1  $ 62-rod array (part 1)
                 fill=-5:4 -4:4 0:0
                 2 2 2 2 2 2 2 2 2 2
                 2 1 4 1 1 4 1 1 4 2                              $ Op Load Test 1
c                 2 1 4 1 1 1 1 1 4 2                                 $ Op Load Test 2
                 2 1 1 1 1 1 1 1 1 2
                 2 1 1 1 1 1 1 1 1 2
                 2 1 1 1 1 4 1 1 1 2
                 2 1 1 1 1 1 1 1 1 2
                 2 1 1 1 1 1 1 1 1 2
                 2 1 4 1 1 1 1 1 4 2
                 2 2 2 2 2 2 2 2 2 2
202  5    9.9848E-02  -111  -113  114          fill=32  u=33  imp:n=1  $ internals
203  8    5.9800E-02 (111:113:-114)
                -115  -117  118                    u=33  imp:n=1  $ walls
204  5    9.9848E-02  (115:117:-118)               u=33  imp:n=1  $ surrounding water
c
205  0           -101 102 -103 104  lat=1  lat=1
                 trcl=(0.84074 0.0 0.0)            u=30  imp:n=1  $ 62-rod array (part 2)
                 fill=-1:5 -4:4 0:0
                 2 2 2 2 2 2 2
                 2 2 4 1 1 1 2
                 2 2 2 1 1 1 2
                 2 2 2 2 1 1 2
                 2 2 2 2 1 1 2
                 2 2 2 2 1 1 2
                 2 2 2 4 1 1 2
                 2 2 4 1 1 1 2
                 2 2 2 2 2 2 2
206  5    9.9848E-02  -113  114 162           fill=30  u=31  imp:n=1  $ internals
207  8    5.9800E-02 (113:-114:-162)
                -117  118 161                      u=31  imp:n=1  $ walls
208  5    9.9848E-02  (117:-118:-161)              u=31  imp:n=1  $ surrounding water
c
209  0           -101 102 -103 104  lat=1           u=34  imp:n=1  $ 49-rod array
```

```
                  fill=-4:4 -4:4 0:0
                  2 2 2 2 2 2 2 2 2
                  2 4 1 1 1 1 1 4 2
                  2 1 1 1 1 1 1 1 2
                  2 1 1 1 1 1 1 1 2
                  2 1 1 1 4 1 1 4 2
                  2 1 1 1 1 1 1 1 2
                  2 1 1 1 1 1 1 4 1 2                                  $ Op Load Test 1
c                  2 1 1 1 1 1 1 1 2                                    $ Op Load Test 2
                  2 4 1 1 4 1 1 4 2
                  2 2 2 2 2 2 2 2 2
210  5   9.9848E-02  -111  112 -113  114       fill=34  u=35  imp:n=1  $ internals
211  8   5.9800E-02 (111:-112:113:-114)
                 -115  116 -117  118                    u=35  imp:n=1  $ walls
212  5   9.9848E-02  (115:-116:117:-118)                u=35  imp:n=1  $ surrounding water
c
213  0            -101 102 -103 104  lat=1              u=36  imp:n=1  $ 62-rod array (part 1)
                  fill=-4:4 -5:4 0:0
                  2 2 2 2 2 2 2 2 2
                  2 1 1 1 1 1 1 1 2
                  2 4 1 1 1 1 1 4 2
                  2 1 1 1 1 1 1 1 2
                  2 1 1 1 1 1 1 1 2
                  2 4 1 1 4 1 1 1 2                                    $ Op Load Test 1
c                  2 1 1 1 4 1 1 1 2                                    $ Op Load Test 2
                  2 1 1 1 1 1 1 1 2
                  2 1 1 1 1 1 1 1 2
                  2 4 1 1 1 1 1 4 2
                  2 2 2 2 2 2 2 2 2
214  5   9.9848E-02  -111  112 -113            fill=36  u=37  imp:n=1  $ internals
215  8   5.9800E-02 (111:-112:113)
                 -115  116 -117                         u=37  imp:n=1  $ walls
216  5   9.9848E-02  (115:-116:117)                     u=37  imp:n=1  $ surrounding water
c
217  0            -101 102 -103 104  lat=1
                  trcl=(0.0 0.84074 0.0)                 u=38  imp:n=1  $ 62-rod array (part 2)
                  fill=-4:4 -1:5 0:0
                  2 2 2 2 2 2 2 2 2
                  2 2 2 2 2 2 2 2 2
                  2 4 2 2 2 2 2 4 2
                  2 1 1 2 2 2 4 1 2
                  2 1 1 1 1 1 1 1 2
                  2 1 1 1 1 1 1 1 2
                  2 2 2 2 2 2 2 2 2
218  5   9.9848E-02  -111  112   152    fill=38         u=39  imp:n=1  $ internals
219  8   5.9800E-02 (111:-112:-152)
                 -115  116  151                         u=39  imp:n=1  $ walls
220  5   9.9848E-02  (115:-116:-151)                    u=39  imp:n=1  $ surrounding water
c
301  0            -101  102 -103  104  lat=1
                  trcl=(1.46050 0. 0.) fill=1           u=51  imp:n=1  $ 51-rod array (part 1)
302  5   9.9848E-02  -113  114  162     fill=51         u=52  imp:n=1  $ internals
303  8   5.9800E-02 (113:-114:-162)
                 -117  118 161                          u=52  imp:n=1  $ walls
304  5   9.9848E-02  (117:-118:-161)                    u=52  imp:n=1  $ surrounding water
c
305  0            -101  102 -103  104  lat=1            u=53  imp:n=1  $ 51-rod array (part 2)
                  trcl=(0.61976 0 0)
                  fill=-6:6 -6:6 0:0
                  2 2 2 2 2 2 2 2 2 2 2 2 2
                  2 2 2 2 2 2 2 2 2 2 2 2 2
                  2 2 2 2 2 2 2 2 2 2 2 2 2
                  2 2 1 1 1 1 1 2 2 2 2 2 2
                  2 2 1 1 1 1 2 2 2 2 2 2 2
                  2 2 1 1 1 1 2 2 2 2 2 2 2
                  2 2 1 1 1 1 2 2 2 2 2 2 2
                  2 2 1 1 1 1 2 2 2 2 2 2 2
                  2 2 1 1 1 1 2 2 2 2 2 2 2
                  2 2 1 1 1 1 1 2 2 2 2 2 2
                  2 2 2 2 2 2 2 2 2 2 2 2 2
                  2 2 2 2 2 2 2 2 2 2 2 2 2
```

```
                 2 2 2 2 2 2 2 2 2 2 2 2 2
306  5   9.9848E-02  -115  -113  114       fill=53      u=54  imp:n=1  $ internals
307  8   5.9800E-02 (115:113:-114)
                -115  -117  118                         u=54  imp:n=1  $ walls
308  5   9.9848E-02  (115:117:-118)                     u=54  imp:n=1  $ surrounding water
c
309  0            -101  102 -103  104  lat=1            u=55  imp:n=1  $ 34-rod array
                  fill=-6:6 -6:6 0:0
                  2 2 2 2 2 2 2 2 2 2 2 2 2
                  2 2 2 2 2 2 2 2 2 2 2 2 2
                  2 2 2 2 2 2 2 2 2 2 2 2 2
                  2 2 2 2 1 1 1 1 1 1 2 2 2
                  2 2 2 2 2 1 1 1 1 1 2 2 2
                  2 2 2 2 2 2 1 1 1 1 2 2 2
                  2 2 2 2 2 2 1 1 1 1 2 2 2
                  2 2 2 2 2 2 1 1 1 1 2 2 2
                  2 2 2 2 2 1 1 1 1 1 2 2 2
                  2 2 2 2 2 2 2 2 2 2 2 2 2
                  2 2 2 2 2 2 2 2 2 2 2 2 2
                  2 2 2 2 2 2 2 2 2 2 2 2 2
310  5   9.9848E-02  -111  112 -113  114       fill=55  u=56  imp:n=1  $ internals
311  8   5.9800E-02 (111:-112:113:-114)
                -115  116 -117  118                     u=56  imp:n=1  $ walls
312  5   9.9848E-02  (115:-116:117:-118)               u=56  imp:n=1  $ surrounding water
c
313  0            -101  102 -103  104  lat=1            u=57  imp:n=1  $ 49-rod array
                  fill=-4:4 -4:4 0:0
                  2 2 2 2 2 2 2 2 2
                  2 1 1 1 1 1 1 1 2
                  2 1 1 1 1 1 1 1 2
                  2 1 1 1 1 1 1 4 2
                  2 1 1 1 1 1 4 4 2
                  2 1 1 1 1 4 4 3 2
                  2 1 1 1 4 4 3 3 2
                  2 1 1 4 4 3 3 3 2
                  2 2 2 2 2 2 2 2 2
314  5   9.9848E-02  -111  112 -113  114       fill=57  u=58  imp:n=1  $ internals
315  8   5.9800E-02 (111:-112:113:-114)
                -115  116 -117  118                     u=58  imp:n=1  $ walls
316  5   9.9848E-02  (115:-116:117:-118)               u=58  imp:n=1  $ surrounding water
c
317  0            -101  102 -103  104  lat=1            u=59  imp:n=1  $ 34-rod array
                  fill=-6:6 -6:6 0:0
                  2 2 2 2 2 2 2 2 2 2 2 2 2
                  2 2 2 2 2 2 2 2 2 2 2 2 2
                  2 2 2 2 2 2 2 2 2 2 2 2 2
                  2 2 2 2 2 2 2 2 2 2 2 2 2
                  2 2 2 1 2 2 2 2 2 1 2 2 2
                  2 2 2 1 1 2 2 2 1 1 2 2 2
                  2 2 2 1 1 1 1 1 1 1 2 2 2
                  2 2 2 1 1 1 1 1 1 1 2 2 2
                  2 2 2 1 1 1 1 1 1 1 2 2 2
                  2 2 2 1 1 1 1 1 1 1 2 2 2
                  2 2 2 2 2 2 2 2 2 2 2 2 2
                  2 2 2 2 2 2 2 2 2 2 2 2 2
                  2 2 2 2 2 2 2 2 2 2 2 2 2
318  5   9.9848E-02  -111  112 -113  114       fill=59  u=60  imp:n=1  $ internals
319  8   5.9800E-02 (111:-112:113:-114)
                -115  116 -117  118                     u=60  imp:n=1  $ walls
320  5   9.9848E-02  (115:-116:117:-118)               u=60  imp:n=1  $ surrounding water
c
321  0            -101  102 -103  104  lat=1            u=61  imp:n=1  $ 51-rod array (part 1)
                  trcl=(0 0.61976 0)
                  fill=-6:6 -6:6 0:0
                  2 2 2 2 2 2 2 2 2 2 2 2 2
                  2 2 2 2 2 2 2 2 2 2 2 2 2
                  2 2 2 1 1 1 1 1 1 1 2 2 2
                  2 2 2 1 1 1 1 1 1 1 2 2 2
                  2 2 2 1 1 1 1 1 1 1 2 2 2
                  2 2 2 1 1 1 1 1 1 1 2 2 2
```

```
                 2 2 2 1 2 2 2 2 2 1 2 2 2
                 2 2 2 2 2 2 2 2 2 2 2 2 2
                 2 2 2 2 2 2 2 2 2 2 2 2 2
                 2 2 2 2 2 2 2 2 2 2 2 2 2
                 2 2 2 2 2 2 2 2 2 2 2 2 2
                 2 2 2 2 2 2 2 2 2 2 2 2 2
                 2 2 2 2 2 2 2 2 2 2 2 2 2
322  5   9.9848E-02  -111  112 -113           fill=61  u=62  imp:n=1  $ internals
323  8   5.9800E-02 (111:-112:113)
                -115  116 -117                        u=62  imp:n=1  $ walls
324  5   9.9848E-02  (115:-116:117)                   u=62  imp:n=1  $ surrounding water
c
325  0           -101  102 -103  104  lat=1
                 trcl=(0. 1.46050 0.)       fill=1   u=63  imp:n=1  $ 51-rod array (part 2)
326  5   9.9848E-02  -111  112   152          fill=63  u=64  imp:n=1  $ internals
327  8   5.9800E-02 (111:-112:-152)
                -115  116   151                      u=64  imp:n=1  $ walls
328  5   9.9848E-02  (115:-116:-151)                 u=64  imp:n=1  $ surrounding water
c
401  0           -101  102 -103  104  lat=1          u=71  imp:n=1  $ 49-rod array
                 fill=-4:4 -4:4 0:0
                 2 2 2 2 2 2 2 2 2
                 2 1 1 1 1 1 1 1 2
                 2 1 1 1 1 1 1 1 2
                 2 1 1 1 1 1 1 1 2
                 2 1 1 1 1 1 1 1 2
                 2 1 1 1 1 1 1 1 2
                 2 1 1 1 1 1 1 1 2
                 2 4 1 1 1 1 1 4 2
                 2 2 2 2 2 2 2 2 2
402  5   9.9848E-02  -111  112 -113  114      fill=71  u=72  imp:n=1  $ internals
403  8   5.9800E-02 (111:-112:113:-114)
                -115  116 -117  118                  u=72  imp:n=1  $ walls
404  5   9.9848E-02  (115:-116:117:-118)             u=72  imp:n=1  $ surrounding water
c
405  0           -101  102 -103  104  lat=1          u=73  imp:n=1  $ 49-rod array
                 fill=-4:4 -4:4 0:0
                 2 2 2 2 2 2 2 2 2
                 2 1 1 1 1 1 1 1 2
                 2 1 1 1 1 1 1 1 2
                 2 1 1 1 1 1 1 1 2
                 2 1 1 1 1 1 1 1 2
                 2 1 1 1 1 1 1 1 2
                 2 1 1 1 1 1 4 4 2
                 2 4 4 4 4 4 4 3 2
                 2 2 2 2 2 2 2 2 2
406  5   9.9848E-02  -111  112 -113  114      fill=73  u=74  imp:n=1  $ internals
407  8   5.9800E-02 (111:-112:113:-114)
                -115  116 -117  118                  u=74  imp:n=1  $ walls
408  5   9.9848E-02  (115:-116:117:-118)             u=74  imp:n=1  $ surrounding water
c
409  0           -101  102 -103  104  lat=1          u=75  imp:n=1  $ 49-rod array
                 fill=-4:4 -4:4 0:0
                 2 2 2 2 2 2 2 2 2
                 2 1 1 1 1 1 1 1 2
                 2 1 1 1 1 1 1 1 2
                 2 1 1 1 1 1 4 4 2
                 2 1 1 1 4 4 4 3 2
                 2 1 4 4 4 3 3 3 2
                 2 4 4 3 3 3 3 3 2
                 2 3 3 3 3 3 3 3 2
                 2 2 2 2 2 2 2 2 2
410  5   9.9848E-02  -111  112 -113  114      fill=75  u=76  imp:n=1  $ internals
411  8   5.9800E-02 (111:-112:113:-114)
                -115  116 -117  118                  u=76  imp:n=1  $ walls
412  5   9.9848E-02  (115:-116:117:-118)             u=76  imp:n=1  $ surrounding water
c
413  0           -101  102 -103  104  lat=1          u=77  imp:n=1  $ 49-rod array
                 fill=-4:4 -4:4 0:0
                 2 2 2 2 2 2 2 2 2
                 2 4 4 4 3 3 3 3 2
```

```
                  2 4 3 3 3 3 3 2
                  2 4 3 3 3 3 3 2
                  2 3 3 3 3 3 3 2
                  2 3 3 3 3 3 3 2
                  2 3 3 3 3 3 3 2
                  2 3 3 3 3 3 3 2
                  2 2 2 2 2 2 2 2
414  5   9.9848E-02  -111  112 -113  114       fill=77  u=78  imp:n=1  $ internals
415  8   5.9800E-02 (111:-112:113:-114)
                 -115  116 -117  118                    u=78  imp:n=1  $ walls
416  5   9.9848E-02  (115:-116:117:-118)               u=78  imp:n=1  $ surrounding water
c
417  0            -101  102 -103  104  lat=1           u=79  imp:n=1  $ 49-rod array
                  fill=-4:4 -4:4 0:0
                  2 2 2 2 2 2 2 2 2
                  2 1 1 1 1 1 4 3 2
                  2 1 1 1 1 4 4 3 2
                  2 1 1 1 1 4 3 3 2
                  2 1 1 1 4 4 3 3 2
                  2 1 1 1 4 3 3 3 2
                  2 1 1 4 4 3 3 3 2
                  2 1 1 4 3 3 3 3 2
                  2 2 2 2 2 2 2 2 2
418  5   9.9848E-02  -111  112 -113  114       fill=79  u=80  imp:n=1  $ internals
419  8   5.9800E-02 (111:-112:113:-114)
                 -115  116 -117  118                    u=80  imp:n=1  $ walls
420  5   9.9848E-02  (115:-116:117:-118)               u=80  imp:n=1  $ surrounding water
c
421  0            -101  102 -103  104  lat=1           u=81  imp:n=1  $ 49-rod array
                  fill=-4:4 -4:4 0:0
                  2 2 2 2 2 2 2 2 2
                  2 1 1 1 1 1 1 4 2
                  2 1 1 1 1 1 1 4 2
                  2 1 1 1 1 1 1 4 2
                  2 1 1 1 1 1 1 4 2
                  2 1 1 1 1 1 1 4 2
                  2 1 1 1 1 1 4 4 2
                  2 1 1 1 1 1 4 3 2
                  2 2 2 2 2 2 2 2 2
422  5   9.9848E-02  -111  112 -113  114       fill=81  u=82  imp:n=1  $ internals
423  8   5.9800E-02 (111:-112:113:-114)
                 -115  116 -117  118                    u=82  imp:n=1  $ walls
424  5   9.9848E-02  (115:-116:117:-118)               u=82  imp:n=1  $ surrounding water
c
425  0            -101  102 -103  104  lat=1           u=83  imp:n=1  $ 49-rod array
                  fill=-4:4 -4:4 0:0
                  2 2 2 2 2 2 2 2 2
                  2 1 1 1 1 1 1 4 2
                  2 1 1 1 1 1 1 1 2
                  2 1 1 1 1 1 1 1 2
                  2 1 1 1 1 1 1 1 2
                  2 1 1 1 1 1 1 1 2
                  2 1 1 1 1 1 1 1 2
                  2 1 1 1 1 1 1 4 2
                  2 2 2 2 2 2 2 2 2
426  5   9.9848E-02  -111  112 -113  114       fill=83  u=84  imp:n=1  $ internals
427  8   5.9800E-02 (111:-112:113:-114)
                 -115  116 -117  118                    u=84  imp:n=1  $ walls
428  5   9.9848E-02  (115:-116:117:-118)               u=84  imp:n=1  $ surrounding water
c
501  0            -101  102 -103  104  lat=1           u=91  imp:n=1  $ 49-rod array
                  fill=-4:4 -4:4 0:0
                  2 2 2 2 2 2 2 2 2
                  2 4 4 4 4 4 4 4 2
                  2 3 3 3 3 3 3 3 2
                  2 3 3 3 3 3 3 3 2
                  2 3 3 3 3 3 3 3 2
                  2 3 3 3 3 3 3 3 2
                  2 3 3 3 3 3 3 3 2
                  2 3 3 3 3 3 3 3 2
                  2 2 2 2 2 2 2 2 2
```

```
502  5   9.9848E-02  -111  112 -113  114       fill=91  u=92  imp:n=1  $ internals
503  8   5.9800E-02 (111:-112:113:-114)
                  -115  116 -117  118                   u=92  imp:n=1  $ walls
504  5   9.9848E-02  (115:-116:117:-118)               u=92  imp:n=1  $ surrounding water
c
505  0            -101  102 -103  104  lat=1            u=93  imp:n=1  $ 49-rod array
                   fill=-4:4 -4:4 0:0
                   2 2 2 2 2 2 2 2 2
                   2 4 3 3 3 3 3 3 2
                   2 4 3 3 3 3 3 3 2
                   2 4 3 3 3 3 3 3 2
                   2 4 3 3 3 3 3 3 2
                   2 4 3 3 3 3 3 3 2
                   2 4 3 3 3 3 3 3 2
                   2 4 3 3 3 3 3 3 2
                   2 2 2 2 2 2 2 2 2
506  5   9.9848E-02  -111  112 -113  114       fill=93  u=94  imp:n=1  $ internals
507  8   5.9800E-02 (111:-112:113:-114)
                  -115  116 -117  118                   u=94  imp:n=1  $ walls
508  5   9.9848E-02  (115:-116:117:-118)               u=94  imp:n=1  $ surrounding water
c
c  core
801  5   9.9848E-02  -121  122 -123  124   lat=1        u=800 imp:n=1  $ loading pattern
                  fill=0:5 0:5 0:0
               800   18   39   64   84   94
                14   16   37   62   82  800
                31   33   35   60   80  800
                52   54   56   58   78  800
                72   74   76   78  800  800
                92  800  800  800  800  800
802  5   9.9848E-02  -925  915 -927  916 -119  120
                                  fill=800            u=801  imp:n=1
c  water inside core container
803  5   9.9848E-02  -925  -927 -929  119              u=801  imp:n=1
c flow orifice + core support plate
804 11   7.9774E-02  -925  -927 -120  930              u=801  imp:n=1
c core container sides
805  7   8.7685E-02 (925:927) -931 -933 -929  930
                                                      u=801  imp:n=1
c core container top
806  7   8.7685E-02  929 -935                          u=801  imp:n=1
c core hold-down and core support structures
807 12   9.6808E-02  (935:-930) -936  937              u=801  imp:n=1
c water above and below core container, etc
808  5   9.9848E-02   936:-937                         u=801  imp:n=1
c
901  0             ((-824 -826 -828 917 918):
                     (828 -824 -132):(828 -826 -131))
                     -992  993                        fill=10   imp:n=1  $ TS
902  0                -34 -992  993 917
                      trcl=(0. 29.845 0.)             fill=6    imp:n=1  $ TR 1
903  0                -34 -992  993 918
                      trcl=(29.845 0. 0.)             fill=6    imp:n=1  $ TR 2
911  0                -51 -992  993
                      trcl=(21.07 44.7675 0.)         fill=7    imp:n=1  $ CR 1
912  0                -51 -992  993
                      trcl=(44.7675  21.07  0.)       fill=7    imp:n=1  $ CR 2
951  0      -931  917 -933  918 -992  993
              #901 #902 #903 #911 #912                fill=801  imp:n=1  $ core
998  5   9.9848E-02  (931:933:992:-993)
                  -991 -992  993 917 918
                #901 #902 #903 #911 #912                        imp:n=1
c water inside reactor vessel
999  0            (991:992:-993:-917:-918)                      imp:n=0  $ outside world

c  SURFACE CARDS
c  relative to core axial and radial centerline
1   cz     0.70993                    $ fuel pellet OR, nom OD=0.559in=1,41986 cm
2   cz     0.758825                   $ insulator IR
3   cz     0.880745                   $ insulator OR
200 cz     0.88138                    $ clad IR
```

```
4   cz     0.95377                  $ clad OR
5   pz    68.2625                   $ rod cap bottom
6   pz    71.993125                 $ rod top
7   pz   -48.656875                 $ rod bottom
8   pz    45.72                     $ fuel meat top (36in active fuel length)
9   pz   -45.72                     $ fuel meat bottom
13  pz    46.51375                  $ bearing spool base top
15  pz    52.07                     $ insulator top
16  pz   -45.164375                 $ hold-down plate top
17  pz   -50.80                     $ hold-down plate bottom
201 pz    57.4675                   $ bearing spool wall top
202 cz     0.714375                 $ bearing spool wall OR
203 cz     0.59563                  $ bearing spool wall IR
c
21  cz     0.79375                  $ TR tie rod radius
22  cz     1.1049                   $ TR & CR inner tube IR
23  cz     1.27                     $ TR & CR inner tube OR
24  cz     1.30937                  $ TR B4C IR
25  cz     3.4417                   $ TR B4C OR
26  cz     3.48615                  $ TR outer tube IR
27  cz     3.65125                  $ TR outer tube OR
29  cz     3.96875                  $ TR shroud IR
30  cz     4.445                    $ TR shroud OR
31  pz   -68.58                     $ TR meat top
32  pz  -175.26                     $ TR bottom
33  cz     4.6101                   $ water around TR shroud
34  cz     4.98348                  $ assembly wall next to TR shroud
20  pz   -66.8655                   $ TR top supermica insulator
35  pz   -66.2305                   $ TR top spring retainer
67  pz  -176.2125                   $ TR bottom closure plate thickness=0.375 in.
c
36  cz     0.84455                  $ CR tie rod R
37  cz     1.1049                   $ TR & CR inner tube IR
38  cz     1.27                     $ TR & CR inner tube OR
39  cz     1.3081                   $ CR B4C IR
40  cz     4.9149                   $ CR B4C OR
41  cz     4.95554                   $ CR outer tube IR
42  cz     5.08000                  $ CR outer tube OR
44  cz     5.39755                  $ CR shroud IR
45  cz     6.0325                   $ CR shroud OR
46  pz   101.727                    $ Op Test 1 CR meat top
47  pz    10.287                    $ Op Test 1 CR bottom
c 46  pz    97.1804                   $ Op Test 2 CR meat top based on below
c 47  pz     5.7404                  $ Op Test 2 CR bottom
48  pz     9.3345                   $ bottom closure plate
c 48  pz     4.7884                   $ bottom closure plate test 2
50  cz     6.1595                   $ water around CR shroud
51  cz     6.53288                  $ assembly wall next to CR shroud
60  pz   102.997                    $ CR insulator top thickness = 0.5 in.
61  pz   103.2637                   $ CR top closure plate thickness= 0.105 in.
c
c assemblies/elements
101 px     1.00584                  $ fuel rod window
102 px    -1.00584
103 py     1.00584
104 py    -1.00584
111 px     7.05358                  $ most assemblies, inner walls (7-rod direction)
112 px    -7.05358
113 py     7.05358
114 py    -7.05358
115 px     7.42696                  $ most assemblies, outer wall thickness
116 px    -7.42696
117 py     7.42696
118 py    -7.42696
119 pz    83.82                     $ assembly top
120 pz   -68.58                     $ assembly bottom 9in. below fuel meat bottom
121 px     7.46125                  $ 49-rod assembly window
122 px    -7.46125
123 py     7.46125
124 py    -7.46125
131 px     7.49554
```

```
132 py     7.49554
150 py     0.0                          $ 62 rods assembly plane across TR
151 py     0.03429                      $ half water gap assembly
152 py     0.40767                      $ 62 rod assembly wall
160 px     0.0                          $ 62 rods assembly plane across TR
161 px     0.03429                      $ half water gap assembly
162 px     0.40767                      $ 62 rod assembly wall
c
804 cz    10.4775                       $ Test Space IR
805 px    13.462                        $ central filler piece boundary
807 py    13.462                        $
809 p 0.707106781  0.707106781 0  13.6525  $
814 px    13.53058                      $ water gap around TS
816 py    13.53058
818 p 0.707106781  0.707106781 0  13.72108
824 px    13.90396                      $ adjacent assembly walls
826 py    13.90396
828 p 0.707106781  0.707106781 0  14.09446
c
915 px 0.0
916 py 0.0
*917 px 0.0001
*918 py 0.0001
c
925 px    82.07375                      $ core x-y window
927 py    82.07375
929 pz    84.1375                       $ inside core container top
c
c rest of Rx
930 pz   -71.755                        $ core support structure top
931 px    82.70875                      $ core container exterior
933 py    82.70875
935 pz    84.7725
936 pz   100.0125                       $ top of core hold-down structure
937 pz   -86.995                        $ bottom of core support structure
991 cz   228.6                          $ reactor vessel IR
992 pz   472.44                         $ water level
993 pz  -373.38                         $ reactor vessel base
999 cz   300

c  DATA CARDS
c  calculation mode
mode n
c  nom materials
m1   $ fuel matrix UO2-CaO-ZrO2, Ntot=7.6085E-02
        92234.66c  6.2137E-06 $ U234
        92235.66c  7.5524E-04 $ U235 from 30.6 wt% U(18.31)02
        92238.66c  3.3208E-03 $ U238
        40000.66c  1.8031E-02 $ Zr from 61.8 wt% ZrO2
        8016.66c   4.9099E-02 $ O
        20000.66c  4.8725E-03 $ Ca from 7.6wt% CaO
         5010.66c  1.1287E-06 $ B 10 equivalent to 5e-4 1/cm
m3   $ CaO-ZrO2 ceramic insulator, 4.7g/cc, Ntot=7.2433E-02
        40000.66c  2.0443E-02 $ Zr  89wt% ZrO2 in feed
        8016.66c   4.6438E-02 $ O   O from CaO and ZrO2
        20000.66c  5.5520E-03 $ Ca  11wt% CaO in feed
m4   $ SST 304L clad, 8.0 g/cc,     Ntot= 8.7575E-02  at/b cm
        6000.66c        6.0166E-05          $  C
       25055.66c        8.7693E-04          $  Mn
       15031.66c        3.4997E-05          $  P
       16000.66c        2.2534E-05          $  S
       14028.66c        7.9104E-04          $  Si28
       14029.66c        4.0165E-05          $  Si29
       14030.66c        2.6477E-05          $  Si30
       24050.66c        7.6491E-04          $  Cr50
       24052.66c        1.4751E-02          $  Cr52
       24053.66c        1.6726E-03          $  Cr53
       24054.66c        4.1634E-04          $  Cr54
       26054.66c        3.5017E-03          $  Fe54
       26056.66c        5.4969E-02          $  Fe56
       26057.66c        1.2695E-03          $  Fe57
```

```
       26058.66c        1.6894E-04          $  Fe58
       28058.66c        5.5882E-03          $  Ni58
       28060.66c        2.1526E-03          $  Ni60
       28061.66c        9.3579E-05          $  Ni61
       28062.66c        2.9830E-04          $  Ni62
       28064.66c        7.6012E-05          $  Ni64
m5   $ water, 0.99566 g/cc, 30degC, Ntot=9.9848E-02
        1001.66c  6.6566E-02 $ H
        8016.66c  3.3283E-02 $ O
mt5  lwtr.60t
m6   $ 6061-T6 Al filler/structure, 2.69g/cc, Ntot=5.9762E-02 atoms/b-cm
       13027.66c        5.8457E-02    $  Al
       12000.66c        6.6651E-04    $  Mg
       22000.66c        1.1842E-05    $  Ti
       25055.66c        2.2115E-05    $  Mn
       14028.66c        3.1918E-04    $  Si28
       14029.66c        1.6207E-05    $  Si29
       14030.66c        1.0683E-05    $  Si30
       24050.66c        2.7074E-06    $  Cr50
       24052.66c        5.2209E-05    $  Cr52
       24053.66c        5.9201E-06    $  Cr53
       24054.66c        1.4736E-06    $  Cr54
       26054.66c        5.9341E-06    $  Fe54
       26056.66c        9.3152E-05    $  Fe56
       26057.66c        2.1513E-06    $  Fe57
       26058.66c        2.8630E-07    $  Fe58
       29063.66c        6.5503E-05    $  Cu63
       29065.66c        2.9195E-05    $  Cu65
m7   $ 304 SST shim/reflector/structure, 8.0 g/cc,      Ntot= 8.7685E-02  at/b cm
        6000.66c        1.6044E-04    $  C
       25055.66c        8.7693E-04    $  Mn
       15031.66c        3.4997E-05    $  P
       16000.66c        2.2534E-05    $  S
       14028.66c        7.9104E-04    $  Si28
       14029.66c        4.0165E-05    $  Si29
       14030.66c        2.6477E-05    $  Si30
       24050.66c        7.6491E-04    $  Cr50
       24052.66c        1.4751E-02    $  Cr52
       24053.66c        1.6726E-03    $  Cr53
       24054.66c        4.1634E-04    $  Cr54
       26054.66c        3.5383E-03    $  Fe54
       26056.66c        5.5543E-02    $  Fe56
       26057.66c        1.2827E-03    $  Fe57
       26058.66c        1.7071E-04    $  Fe58
       28058.66c        5.1691E-03    $  Ni58
       28060.66c        1.9911E-03    $  Ni60
       28061.66c        8.6561E-05    $  Ni61
       28062.66c        2.7593E-04    $  Ni62
       28064.66c        7.0312E-05    $  Ni64
m8   $ 5454-O Al asse walls, 2.69g/cc, Ntot=5.9800E-02 atoms/b-cm
       13027.66c        5.7532E-02    $  Al
       12000.66c        1.7996E-03    $  Mg
       22000.66c        3.3833E-05    $  Ti
       25055.66c        2.2115E-04    $  Mn
       14028.66c        6.6497E-05    $  Si28
       14029.66c        3.3764E-06    $  Si29
       14030.66c        2.2257E-06    $  Si30
       24050.66c        1.6921E-06    $  Cr50
       24052.66c        3.2631E-05    $  Cr52
       24053.66c        3.7001E-06    $  Cr53
       24054.66c        9.2103E-07    $  Cr54
       26054.66c        3.3909E-06    $  Fe54
       26056.66c        5.3230E-05    $  Fe56
       26057.66c        1.2293E-06    $  Fe57
       26058.66c        1.6360E-07    $  Fe58
       29063.66c        3.0236E-05    $  Cu63
       29065.66c        1.3477E-05    $  Cu65
m9   $ B4C neutron absorber, 2.505 g/cc, Ntot=1.3651E-01 atoms/b-cm
        5010.66c  2.1732E-02 $ B-10  19.90a% of 78.26wt% B
        5011.66c  8.7473E-02 $ B-11  80.10a% of 78.26wt% B
        6000.66c  2.7301E-02 $ C     21.74wt% balance
```

```
m10  $ 6061-T6 Al hold-down plate with flow holes, 1.9855g/cc,      Ntot= 7.6454E-02  at/b cm
c      reduce Al density (mult m6 nuclide dens by 58.36%)
c      add water (mult m5 nulide dens by 100-58.36=41.64%)
       13027.66c        3.4116E-02    $  Al
       12000.66c        3.8897E-04    $  Mg
       22000.66c        6.9108E-06    $  Ti
       25055.66c        1.2906E-05    $  Mn
        1001.66c        2.7718E-02    $  H
        8016.66c        1.3859E-02    $  O
       14028.66c        1.8628E-04    $  Si28
       14029.66c        9.4582E-06    $  Si29
       14030.66c        6.2348E-06    $  Si30
       24050.66c        1.5800E-06    $  Cr50
       24052.66c        3.0469E-05    $  Cr52
       24053.66c        3.4550E-06    $  Cr53
       24054.66c        8.6002E-07    $  Cr54
       26054.66c        3.4631E-06    $  Fe54
       26056.66c        5.4364E-05    $  Fe56
       26057.66c        1.2555E-06    $  Fe57
       26058.66c        1.6708E-07    $  Fe58
       29063.66c        3.8227E-05    $  Cu63
       29065.66c        1.7038E-05    $  Cu65
mt10  lwtr.60t
m11  $ 7075-T6 Al orifice/support plate homog w/ flow holes, 1.8966g/cc,       Ntot= 7.9774E-02
at/b cm
       13027.66c        2.7876E-02    $  Al
       12000.66c        8.6565E-04    $  Mg
       22000.66c        1.7577E-05    $  Ti
       25055.66c        2.2978E-05    $  Mn
        1001.66c        3.3283E-02    $  H
        8016.66c        1.6641E-02    $  O
       14028.66c        5.5274E-05    $  Si28
       14029.66c        2.8065E-06    $  Si29
       14030.66c        1.8501E-06    $  Si30
       24050.66c        1.6175E-06    $  Cr50
       24052.66c        3.1192E-05    $  Cr52
       24053.66c        3.5369E-06    $  Cr53
       24054.66c        8.8042E-07    $  Cr54
       26054.66c        2.2020E-06    $  Fe54
       26056.66c        3.4567E-05    $  Fe56
       26057.66c        7.9831E-07    $  Fe57
       26058.66c        1.0624E-07    $  Fe58
       29063.66c        6.4510E-04    $  Cu63
       29065.66c        2.8753E-04    $  Cu65
mt11  lwtr.60t
m12  $ 304 SST core support& hold-down structures homog w/ openings, 2.7287g/cc,  Ntot= 9.6808E-
02  at/b cm
        6000.66c        4.0111E-05    $  C
       25055.66c        2.1923E-04    $  Mn
       15031.66c        8.7492E-06    $  P
       16000.66c        5.6334E-06    $  S
        1001.66c        4.9924E-02    $  H
        8016.66c        2.4962E-02    $  O
       14028.66c        1.9776E-04    $  Si28
       14029.66c        1.0041E-05    $  Si29
       14030.66c        6.6192E-06    $  Si30
       24050.66c        1.9123E-04    $  Cr50
       24052.66c        3.6876E-03    $  Cr52
       24053.66c        4.1815E-04    $  Cr53
       24054.66c        1.0409E-04    $  Cr54
       26054.66c        8.8456E-04    $  Fe54
       26056.66c        1.3886E-02    $  Fe56
       26057.66c        3.2068E-04    $  Fe57
       26058.66c        4.2677E-05    $  Fe58
       28058.66c        1.2923E-03    $  Ni58
       28060.66c        4.9778E-04    $  Ni60
       28061.66c        2.1640E-05    $  Ni61
       28062.66c        6.8983E-05    $  Ni62
       28064.66c        1.7578E-05    $  Ni64
mt12  lwtr.60t
m13  $ mica dens= 2.83 g/cm3 Ntot= 8.9849E-02
```

```
       14028.66c        1.1840E-02    $  Si28
       14029.66c        6.0119E-04    $  Si29
       14030.66c        3.9630E-04    $  Si30
       13027.66c        1.2837E-02    $  Al
       19000.66c        4.2771E-03    $  K
        1001.66c        8.5519E-03    $  H
        8016.66c        5.1345E-02    $  O
mt13  lwtr.60t
c  k-eff calculation
kcode 12500 1 20 820
c  starting source, start w/ 1 pt/assembly
c     A-1 thru A-3     B-1 thru B-3     C-1 thru C-5     D-1 thru D-9
ksrc   0.1 19    0     13   30    0      5   45    0      0.1 60    0
      19   19    0     26   30    0     32   45    0     15   60    0
      19    0.1  0     28   13    0     45   45    0     30   58    0
       6   15    0     30    6    0     45   32    0     58   30    0
       6   21    0      6   30    0     45    6    0     60   15    0
      15    6    0     34   34    0      1   39    0     60    0.1  0
      21    6    0     30    6    0     39    1    0     54    9    0
      15   15    0                     1   51    0      9   54    0
      21   21    0                    51    1    0      0.1 67    0
                                      41   51    0     67    0.1  0
                                      51   41    0     17   64    0
                                      30   51    0     64   17    0
                                      51   30    0      6   64    0
                                                       64    6    0
print
```

APPENDIX B: ADDITIONAL MEASUREMENTS[a]

The measurements from the Loading and Statics Experiments are summarized in this section. The data included represent primarily maximum, minimum, average, and endpoint results.

B.1 Loading

B.1.1 Critical Experiment – The loading experiment consisted of introducing poison shim wires, adequate to render the fully loaded core a subcritical configuration, into the fueled assemblies prior to loading, and then loading all assemblies to form the complete core. The poison shims consisted of 1064 aluminum boron wires, which were inserted into the coolant channels between fuel rods extending along the full length of the fuel column. The poison shim wires were then removed in discrete steps until a critical configuration was obtained. Criticality was obtained with 264 wires remaining in the core.

B.1.2 Operational Loading and Control Rod Calibration – Starting with the just-critical configuration (264 wires remaining in the core), shim wires were removed in discrete increments. At each step in the removal of the wires, the differential reactivity worth of the control rods was measured, thus generating the control rod worth over the region. For the core configuration of all poison shims removed, the critical position of the control rods was determined to be 22.05 in withdrawn, at which position the differential reactivity worth of the controls rods was determined to be 0.456 $/in. The excess reactivity for this configuration was determined to be 3.50 $.

In order to carry out the PBF long range program adequately, an excess reactivity of greater than 4.00$ is required. For adjusting the excess reactivity, 104 stainless steel shim rods distributed in 12 fuel assemblies were included in the design. To accomplish an increase in excess reactivity above 3.50 $ level, 12 stainless steel shim rods were replaced with standard fuel rods. The replacement increased the excess reactivity to 4.25 $.

B.1.3 In-Pile Tube Reactivity Worth – The IPT was determined to have a negative reactivity worth of 0.93 $.

B.1.4 Shutdown Reactivity – The shutdown reactivity for the core after the excess reactivity had been adjusted to 4.25 $ was determined to be 7.52 $. The total worth of the control rods (4.25 $ excess plus 7.52 $ shutdown) was determined to be 11.77 $.

B.2 Statics

B.2.1 Fuel Assembly Reactivity Worths – The reactivity changes generated by removal from the core of individual and combinations of fuel assemblies are shown in Table B.1. The removal of individual and combinations of fuel assemblies in all cases resulted in a decrease in the reactivity worth of the core. Evaluated on the bases of the number of fuel rods per assembly, the fuel assemblies have the highest worth in the A-ring, and the worth per assembly decreases as the radial distance from the center of the core increases. The reactivity worths resulting from the removal of two fuel assemblies were less than the sum of the worths of the individual assemblies.

[a] Adapted from Reference 1, pages 72 to 74.

Table B.1. Fuel Assembly Worth.

Core Position	Measured Worth [$]
A-4	-2.10
A-5	-1.56
B-5	-1.32
B-6	-2.00
C-8	-0.29
C-9	-0.61
C-10	-1.38
D-15	-0.17
D-16	-0.43
D-17	-0.54
A-4 and B-5	-2.62
A-4 and B-4	-3.03
B-4 and B-5	-2.55
C-10 and D-16	-1.55

B.2.2 Shim Rod Worth – The reactivity changes generated by replacing stainless steel shim rods are shown in Table B.2. An increase in reactivity of 0.84 $ resulted from replacing 12 stainless steel shim rods in the core with standard PBF fuel rods. On the basis of the reactivity worth of the shim rods measured, it was determined that the full complement of shim rods was worth -7.05 $ and the shim rods remaining in the core are -6.12 $.

Table B.2. Reactivity Effect of Replacing Shim Rods with Fuel Rods.

Core Position	Number of Rods Removed	Reactivity Worth ($)	Reactivity Worth/Rod ($)
B-5	1	0.04	0.04
B-8, B-11, and B-2	3	0.13	0.04
B-6	1	0.08	0.08
B-7, B-9, B-10, B-12, B-1, B-3, and B-4	7	0.59	0.0866

B.2.3 Core Void Coefficients of Reactivity – Axial void coefficient for assembly B-5 was determined to be -0.019 ¢/cm^3 (maximum) and -0.0116 ¢/cm^3 (average). Axial void coefficient for assembly B-6 was determined to be -0.0234 ¢/cm^3 (maximum) and -0.0146 ¢/cm^3 (average). Radial void coefficient was determined to be 0.0234 ¢/cm^3 (maximum) and -0.0127 ¢/cm^3 (average).

B.2.4 In-Pile Tube Void Coefficient – A cylindrical void volume 3.0 in. OD by 36 in. long located at the center of the IPT was determined to be worth +0.20 $ (+0.0048 ¢/cm^3). The void simulates the volume that will be occupied by an average test train.

A cylindrical shell 3.0 in. ID by 5.0 in. OD by 36 in. long located at the center of the IPT was determined to be worth +0.55 $ (0.0074 $/cm^3). This void simulates the volume between the flow skirt and the volume occupied by an average test train.

Totally voiding the IPT was determined to be worth +3.08 $. This reactivity worth for the total IPT void is applicable for the configuration whereby the reactor would be critical at a control rod position of 20 in. with the IPT water-filled. The control rod worth data obtained with the voided IPT were decreased approximately 7%. A measure of the excess reactivity available to the system is the integration of the differential control rod worth curve. Integration of this curve from the critical position to the upper limit of the control rod withdrawal showed that the total available excess reactivity of the core was increased by approximately 2.7 $ due to IPT voiding, which is in excellent agreement with the calculations.

B.2.5 Transient Rod Reactivity Worths – The total reactivity worth of the transient rods was determined to be 7.6 $. Flooding one withdrawn transient rod was determined to be worth -0.40 $. Flooding all four withdrawn transient rods was determined to be worth -1.60 $.

B.2.6 Coolant Temperature Coefficient of Reactivity – The coolant temperature coefficient was determined to be negative over the range of temperatures tested.

Temperature: 69 ^{o}F, Coefficient: -0.47 ¢/^{o}F.
Temperature: 100 ^{o}F, Coefficient: -1.00 ¢/^{o}F.
Average over temperature range: -0.78 ¢/^{o}F.

B.2.7 Flow Effect – Reactivity change for coolant flow (15,000 gpm) to no flow:

Temperature: 69 ^{o}F. Effect: -1.43 ¢.
Temperature: 85 ^{o}F. Effect: -1.20 ¢.
Temperature: 100 ^{o}F. Effect: -0.95 ¢.

B.2.8 Ion Chamber Calibration – The chamber calibration constant for Supplemental Linear No. 1 was determined to be 0.056 mA/MW.